

Effect of Thermal-Hydraulic Parameters on CaCO_3 Scaling on Heat Exchangers

by

Mohammad Sultan Khan

A Thesis Presented to the

FACULTY OF THE COLLEGE OF GRADUATE STUDIES

KING FAHD UNIVERSITY OF PETROLEUM & MINERALS

DHAHRAN, SAUDI ARABIA

In Partial Fulfillment of the
Requirements for the Degree of

MASTER OF SCIENCE

In

MECHANICAL ENGINEERING

May, 1996

INFORMATION TO USERS

This manuscript has been reproduced from the microfilm master. UMI films the text directly from the original or copy submitted. Thus, some thesis and dissertation copies are in typewriter face, while others may be from any type of computer printer.

The quality of this reproduction is dependent upon the quality of the copy submitted. Broken or indistinct print, colored or poor quality illustrations and photographs, print bleedthrough, substandard margins, and improper alignment can adversely affect reproduction.

In the unlikely event that the author did not send UMI a complete manuscript and there are missing pages, these will be noted. Also, if unauthorized copyright material had to be removed, a note will indicate the deletion.

Oversize materials (e.g., maps, drawings, charts) are reproduced by sectioning the original, beginning at the upper left-hand corner and continuing from left to right in equal sections with small overlaps. Each original is also photographed in one exposure and is included in reduced form at the back of the book.

Photographs included in the original manuscript have been reproduced xerographically in this copy. Higher quality 6" x 9" black and white photographic prints are available for any photographs or illustrations appearing in this copy for an additional charge. Contact UMI directly to order.

UMI

A Bell & Howell Information Company
300 North Zeeb Road, Ann Arbor MI 48106-1346 USA
313/761-4700 800/521-0600

Effect of Thermal-Hydraulic Parameters on CaCO₃ Scaling in Heat Exchangers

BY

Mohammad Sultan Khan

A Thesis Presented to the

FACULTY OF THE COLLEGE OF GRADUATE STUDIES

KING FAHD UNIVERSITY OF PETROLEUM & MINERALS

DHAHRAN, SAUDI ARABIA

In Partial Fulfillment of the
Requirements for the Degree of

MASTER OF SCIENCE

In

Mechanical Engineering

May 1996

UMI Number: 1379996

UMI Microform 1379996
Copyright 1996, by UMI Company. All rights reserved.
This microform edition is protected against unauthorized
copying under Title 17, United States Code.

UMI
300 North Zeeb Road
Ann Arbor, MI 48103

KING FAHD UNIVERSITY OF PETROLEUM AND MINERALS
DHAHRAN, SAUDI ARABIA
COLLEGE OF GRADUATE STUDIES

This thesis, written by

Mohammad Sultan Khan

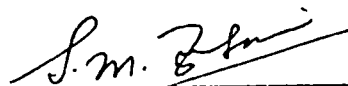
*under the direction of his Thesis Advisor, and approved by his Thesis committee, has
been presented to and accepted by the Dean, College of Graduate Studies, in partial
fulfillment of the requirements for the degree of*

**MASTER OF SCIENCE IN MECHANICAL
ENGINEERING**

Thesis Committee :



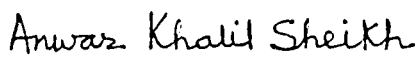
Dr. Mohammad O. Budair (Chairman)



Dr. Syed M. Zubair (Co-Chairman)



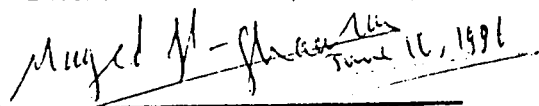
*Dr. Mohammad O. Budair
Department Chairman*



Dr. Anwar K. Sheikh (Member)



*Dr. Ala H. Rabeh
Dean, College of Graduate Studies*



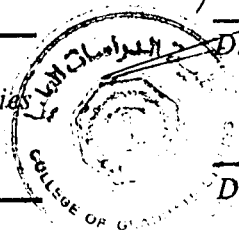
June 16, 1996

Dr. M.A.I. El-Shaarawi (Member)



Dr. O. A. Ashiru (Member)

Date: 17. 6 '96



Effect of Thermal-Hydraulic Parameters on CaCO₃ Scaling in Heat Exchangers

By

Mohammad Sultan Khan

Mechanical Engineering Department

May 1996

Dedicated to

my Parents

&

Sisters

Acknowledgment

In the name of Allah, Most Gracious, Most Merciful. Knowest thou not that it is Allah unto whom belongeth the sovereignty of the heavens and the earth; and ye have not , beside Allah, any friend or helper.

(The Holy Quran, The cow-107)

All praise to Almighty Allah, who bestowed me strength and patience to accomplish my goals.

Acknowledgement is due to King Fahd University of Petroleum & Minerals and Research Institute for providing support to this research work.

I am thankful to Dr. M.O. Budair both as my thesis committee chairman and chairman of the Mechanical Engineering Department for his help and am grateful for the time he spared, out of his busy schedule, for this work. I appreciate his valuable guidance during the research.

I am indebted to my thesis co-chairman, Dr. S.M. Zubair for the guidance, expert advice and cooperation. He always had answers to all my questions and presented

a solution to every confronted problem. His encouragement was a great support. I am obliged to Dr. A.K. Sheikh and Dr. M.A. El-Shaarawi for their valuable advice and suggestions. Thanks are due to Dr. O.A. Ashiru, whose interest and cooperation made the experimental study possible. I am obliged to Mr. A. Quddus for his guidance from the very first stage of this work. His encouragement and experience was a great help. Thanks are due to Mr. T.A. Abbasi whose help during the initial setup of the test apparatus, which is a critical stage of any experimental study, is much appreciated.

I am thankful to all my friends and colleagues, especially Mr. Johar Farooqi, whose amicable and understanding attitude made my stay as a graduate student a pleasant experience.

Last but not the least, thanks are due to my parents and sisters for their prayers, guidance and moral support throughout my academic career. This work is dedicated to my parents and sisters for their hard work and taking pains to fulfill my academic pursuits. My parents advice, to strive for excellence, has made all this work possible.

Contents

Acknowledgement	i
List of Tables	viii
List of Figures	ix
Nomenclature	xiii
Abstract (English)	xv
Abstract (Arabic)	xvi
1 Introduction	1
2 History and Importance of Fouling Research	7
2.1 Historical Background	7
2.2 Importance of Fouling Research	9
2.3 Economic Impact of Fouling	12

2.3.1	Capital expenditures	12
2.3.2	Additional energy costs	14
2.3.3	Maintenance costs	16
2.3.4	Costs due to loss in production	16
2.3.5	Safety	17
2.4	Status of Present Research	18
2.5	Precipitation Fouling	25
3	Experimental Setup and Procedure	30
3.1	Test Equipment Design	30
3.2	Thermal and Hydraulic Parameters	35
3.3	Experimental Procedure	36
3.4	Assumptions	38
3.5	Design of Experiments	39
4	Results and Discussion	41
4.1	Calculation of Induction Time	43
4.2	Effect of thermal-hydraulic parameters on the growth rate of Fouling	
	Resistance	50
4.2.1	Effect of Reynolds Number (Re)	51
4.2.2	Effect of Tube Diameter (D)	51
4.2.3	Effect of Tube Outer Surface Temperature (T_s)	55

	v
4.2.4 Effect of Tube Length	55
4.2.5 Effect of $CaCO_3$ concentration	57
4.3 Fouling Resistance Models	60
4.3.1 Model Adequacy	65
4.4 Application	88
5 Concluding Remarks	90
5.1 Recommendations for Future Research	92
Bibliography	93
Appendices	103
A Heat Exchanger Drawings	104
B Uncertainty analysis	113
C Results of Chemical Solution Analysis	114
D Data Obtained from the Experiments	116
E Data in Graphical Form	127
F Sample Calculation	157
G Results of tube inner Surface Analysis	159

H Sensitivity Analysis	160
I Results of SEM and EDX Analysis	161
Vita	163

List of Tables

3.1	Experimental parameters	36
3.2	Design of experiments	40
4.1	Schedule of experiments	42
4.2	Results of induction time calculations	45
4.3	Estimated range of induction time (obtained by linear extrapolation of first two data points)	49
4.4	Coefficients of A and B of the R_f models	62
C.1	Results of chemical solution analysis	115
D.1	Data of Experiments 1, 2 and 3	117
D.2	Data of experiments 4, 5 and 6	118
D.3	Data of experiments 7, 8 and 9	119
D.4	Data of experiments 10, 11 and 12	120
D.5	Data of experiments 13, 14 and 15	121
D.6	Data of experiments 16, 17 and 18	122

D.7	Data of experiments 19, 20 and 21	123
D.8	Data of experiments 22, 23 and 24	124
D.9	Data of experiments 25, 26 and 27	125
D.10	Data of experiments 28 and 29	126
G.1	Results of surface analysis	159
H.1	Results of sensitivity analysis showing percentage increase in R_f^* . . .	160

List of Figures

1.1	Change in deposit thickness with time [1]	4
2.1	Behavior of normal and inverse solubility salt solutions [1]	27
3.1	Schematic of the double tube heat exchanger	31
3.2	Schematic of a scale deposition equipment	34
4.1	A sample curve of R_f vs time showing increase of slope	44
4.2	Induction time determined for the experimental study	46
4.3	Effect of Reynolds No. on R_f	52
4.4	Effect of tube diameter on R_f	53
4.5	Effect of tube surface temperature on R_f	56
4.6	Variation of R_f along the test sections	58
4.7	Effect of $CaCO_3$ concentration on R_f	59
4.8	Observed R_f versus predicted R_f for model of test section 1	66
4.9	Observed R_f versus predicted R_f for model of test section 2	67
4.10	Observed R_f versus predicted R_f for model of test section 3	68

4.11 Observed R_f versus predicted R_f for model of test section 4	69
4.12 Observed R_f versus predicted R_f for model of test section 5	70
4.13 Observed R_f versus predicted R_f for model of test section 6	71
4.14 Observed R_f versus predicted R_f for average R_f model	72
4.15 Normal probability plot for model of test section 1	73
4.16 Normal probability plot for model of test section 2	74
4.17 Normal probability plot for model of test section 3	75
4.18 Normal probability plot for model of test section 4	76
4.19 Normal probability plot for model of test section 5	77
4.20 Normal probability plot for model of test section 6	78
4.21 Normal probability plot for model of average R_f	79
4.22 Predicted fouling resistance versus residuals for model of section 1 . .	81
4.23 Predicted fouling resistance versus residuals for model of section 2 . .	82
4.24 Predicted fouling resistance versus residuals for model of section 3 . .	83
4.25 Predicted fouling resistance versus residuals for model of section 4 . .	84
4.26 Predicted fouling resistance versus residuals for model of section 5 . .	85
4.27 Predicted fouling resistance versus residuals for model of section 6 . .	86
4.28 Predicted fouling resistance versus residuals for model of average R_f .	87
A.1 Assembly drawing of the heat exchanger	105
A.2 Schematic of the heat exchanger shell	106

A.3	Drawing of plate A of 1/2 inch tube heat exchanger	107
A.4	Drawing of plate B of 1/2 inch tube heat exchanger	108
A.5	Drawing of plate A of 3/8 inch tube heat exchanger	109
A.6	Drawing of plate B of 3/8 inch tube heat exchanger	110
A.7	Drawing of plate A of 1/4 inch tube heat exchanger	111
A.8	Drawing of plate B of 1/4 inch tube heat exchanger	112
E.1	R_f vs time of experiment No.1	128
E.2	R_f vs time of experiment No.2	129
E.3	R_f vs time of experiment No.3	130
E.4	R_f vs time of experiment No.4	131
E.5	R_f vs time of experiment No.5	132
E.6	R_f vs time of experiment No.6	133
E.7	R_f vs time of experiment No.7	134
E.8	R_f vs time of experiment No.8	135
E.9	R_f vs time of experiment No.9	136
E.10	R_f vs time of experiment No.10	137
E.11	R_f vs time of experiment No.11	138
E.12	R_f vs time of experiment No.12	139
E.13	R_f vs time of experiment No.13	140
E.14	R_f vs time of experiment No.14	141

E.15 R_f vs time of experiment No.15	142
E.16 R_f vs time of experiment No.16	143
E.17 R_f vs time of experiment No.17	144
E.18 R_f vs time of experiment No.18	145
E.19 R_f vs time of experiment No.19	146
E.20 R_f vs time of experiment No.20	147
E.21 R_f vs time of experiment No.21	148
E.22 R_f vs time of experiment No.22	149
E.23 R_f vs time of experiment No.23	150
E.24 R_f vs time of experiment No.24	151
E.25 R_f vs time of experiment No.25	152
E.26 R_f vs time of experiment No.26	153
E.27 R_f vs time of experiment No.27	154
E.28 R_f vs time of experiment No.28	155
E.29 R_f vs time of experiment No.29	156
I.1 Results of SEM analysis	162
I.2 Corresponding EDX plot	162

Nomenclature

A	surface area (m^2)
A_o	outer surface area of the scale (m^2)
A_i	inner surface area of the scale (m^2)
bpd	Barrels Per Day
BPR	Back Pressure Regulator
C_{min}/C_{max}	capacitance ratio
$CTWCB$	constant temperature water circulating bath
D	tube diameter (m)
D_{max}	maximum tube diameter ($= 0.0127$ m)
D^*	D/D_{max}
GNP	Gross National Product
k	thermal conductivity of $CaCO_3$ (W/m.K)
l	length of the test section (m)
ν	kinematic viscosity of water (m^2/sec)
R^2	coefficient of determination (ratio of sum of squares of regression and total sum of squares)
R_f	fouling resistance ($m^2.K/W$)
$R_{f,max}$	maximum fouling resistance ($= 244 * 10^{-7} m^2.K/W$)

R_f^*	$R_f/R_{f,max}$
Re	Reynolds number
Re_{max}	maximum Reynolds number (= 1700)
Re^*	Re/Re_{max}
r_1	average radius of the deposit (m)
r_2	inside radius of the tube (m)
ρ	mass density of $CaCO_3$ (kg/m^3)
t	time (hour)
t_i	induction time (hour)
t_{max}	maximum time (10 hours)
t^*	t/t_{max} (ranging from 0.2 to 1)
T_s	inner tube outer surface temperature (K)
$T_{s,max}$	maximum inner tube outer surface temperature (= 358.15 K)
T^*	$T/T_{s,max}$
U	Overall heat transfer coefficient (W/K)
U_c	Overall heat transfer coefficient under clean conditions (W/K)

Abstract

Name: Mohammad Sultan Khan
Title: Effect of Thermal-Hydraulic Parameters on
 CaCO_3 Scaling in Heat Exchangers.
Major Field: Mechanical Engineering

Date of Degree: May, 1996

The term fouling is generally used to describe the deposition of unwanted (initially fluid) particles, which increases both resistance to heat transfer and pressure drop through the heat exchanger. CaCO_3 which is predominantly present in the cooling water, has inverse solubility characteristics i.e., it is less soluble in warm water, resulting in deposition of scales on heat transfer surfaces. An experimental study is carried out to determine the effect of tube surface temperature, Reynolds number, tube diameter and scaling salt concentration on the induction time of CaCO_3 scaling. It was observed that tube surface temperature, Reynolds number and tube diameter have no effect on the onset time of the scaling whereas salt concentration and tube surface roughness have a profound influence on the induction period. The effect of tube surface temperature, Reynolds number, tube diameter and salt concentration on the growth rate of fouling has also been studied. It was concluded that for the range of parameters studied Reynolds number does not influence the fouling resistance substantially. However, the tube surface temperature, tube diameter and salt concentration have profound effect on the growth rate of scaling. The data collected from the experiments are used to develop dimensionless fouling resistance models for estimation and prediction purpose.

Master of Science Degree
Department of Mechanical Engineering
King Fahd University of Petroleum and Minerals
Dhahran, Saudi Arabia
May, 1996

ملخص

اسم الباحث : محمد سلطان خان
 عنوان الرسالة : تأثير المعاملات الهيدروليكية - الحرارية على
 ترسب قشور كربونات الكالسيوم في المبادلات
 الحرارية .
 التخصص الرئيسي : الهندسة الميكانيكية
 تاريخ الرسالة : مايو ١٩٩٦م

إن مصطلح " ترسب " يستخدم بشكل عام لوصف ترسب جزيئات غير مرغوب فيها (تكون بداية ذائبة في المائع) مما يتسبب في زيادة كل من مقاومة انتقال الحرارة وانخفاض الضغط داخل المبادل الحراري . إن كربونات الكالسيوم والتي توجد بنسبة كبيرة في مياه التبريد لها خصائص ذوبان انعكاسية بمعنى انها اقل ذوبانا في الماء الدافئ مما ينتج عنه ترسبها في شكل قشور على أسطح انتقال الحرارة . لقد اجريت دراسة عملية في هذا البحث لتحديد تأثير درجة حرارة سطح الأنابيب ، رقم رينولدز ، قطر الأنابيب وتركيز الملح المترسب على وقت ترسب قشور كربونات الكالسيوم . وقد لوحظ أن درجة حرارة السطح ، رقم رينولدز وقطر الأنابيب ليس لها تأثير على الفترة اللازمة لبداية الترسيب بينما لوحظ أن تركيز الأملاح ودرجة خشونة سطح الأنابيب لها تأثير على وقت بداية الترسيب . كما تمت دراسة تأثير درجة حرارة سطح الأنابيب ، رقم رينولدز ، قطر الأنابيب وتركيز الملح المترسب على معدل نمو الطبقة المترسبة . وتم التوصيل الى أن رقم رينولدز ليس له تأثير جوهري على مقاومة الترسيب في مدى المعاملات التي تم دراستها وبالرغم من ذلك فإن درجة حرارة سطح الأنابيب ، قطر الأنابيب وتركيز الملح المترسب لها تأثير ملموس على معدل نمو القشور . ولقد تم استخدام النتائج المجمعة من التجارب للحصول على نموذج لابعدي بغرض التنبؤ بمقاومة الطبقة المترسبة .

درجة الماجستير في العلوم

قسم الهندسة الميكانيكية

جامعة الملك فهد للبترول والمعادن

الظهران / المملكة العربية السعودية

مايو ١٩٩٦م

Chapter 1

Introduction

The deposition of unwanted particles on the surfaces of heat exchangers is defined as fouling. The presence of these deposits represents an additional thermal resistance to heat transfer which reduces the thermal-hydraulic performance of heat transfer equipment. The deposition may be crystalline, biological material, products of chemical reactions including corrosion, or particulate matter [1]. The fluid (liquid or gas) flowing through the heat transfer equipment determines the characteristics of the fouling deposit. Temperature conditions in the heat exchanger may decompose the organic fluid and cause fouling deposition. The deposits can also be due to the presence of some form of containment in the flowing fluid. Examples of such containment, often at low concentration are solid particles and micro-organisms [1].

The problems associated with heat exchanger fouling have been known since

the first heat exchanger was invented. Steam played a major role to bring about the industrial revolution. Coal was used to generate steam. The accumulation of unwanted deposits on the heat transfer surfaces of the boilers resulted in serious consequences. The presence of these deposits, usually crystalline in character originating from the dissolved salts in the feed water, caused the surface temperature of the boiler tube to reach dangerous levels allowing failure to occur [1].

In majority of the industrial processes, it is required to transfer heat from one fluid to another. As a consequence, designers of heat transfer equipment have focussed their attention on efficient heat exchanger design by studying various mechanisms involved in heat transfer. On the other hand, relatively little consideration had been given to the problem of surface fouling in heat exchangers. Getting more aware of the consequences of fouling, concern has developed among heat transfer engineers. It has now become more necessary than ever before to understand its nature, to formulate methods for its elimination, (or at least its control), and to take it into account in the design of heat transfer equipment. Improved understanding of the mechanisms that lead to the accumulation of deposits on surfaces will provide opportunities to reduce or even eliminate, the problem in certain situations. In this regard, three basic processes may be visualized in relation to deposition on surfaces from a moving fluid. They are [1]:

- (a) The diffusional transport of the foulant or its precursors across the boundary

layers adjacent to the solid surface within the flowing fluid.

- (b) The adhesion of the deposit to the surface and to itself.
- (c) The transport of material away from the surface.

The amalgamation of above three processes results in the growth of deposits on heat transfer surfaces. The difference between the deposition rate and removal rate is the rate with which the deposits grow on the heat transfer surface [1].

There are generally three types of fouling growth curves [2]. The growth may be linear with time or it can follow a power law. The third type is asymptotic growth. Fig. 1.1 shows an asymptotic graph of the fouling growth rate on a heat transfer surface. It takes some time for the adhesion to start. Region A represents the conditioning (or induction) period t_i . Depending upon the application, this induction time may be of the order of seconds or it may even take several weeks for the onset of fouling [1]. After the induction period, steady growth of deposit takes place which is represented by region B. The processes of deposition and removal occur simultaneously during this stage. The rate of deposition gradually falls while the rate of removal of deposit gradually increases. Finally the rate of removal and the rate of deposition may become equal so that a steady state or asymptote is reached (as shown in Region C) when the deposit thickness remains virtually constant [1].

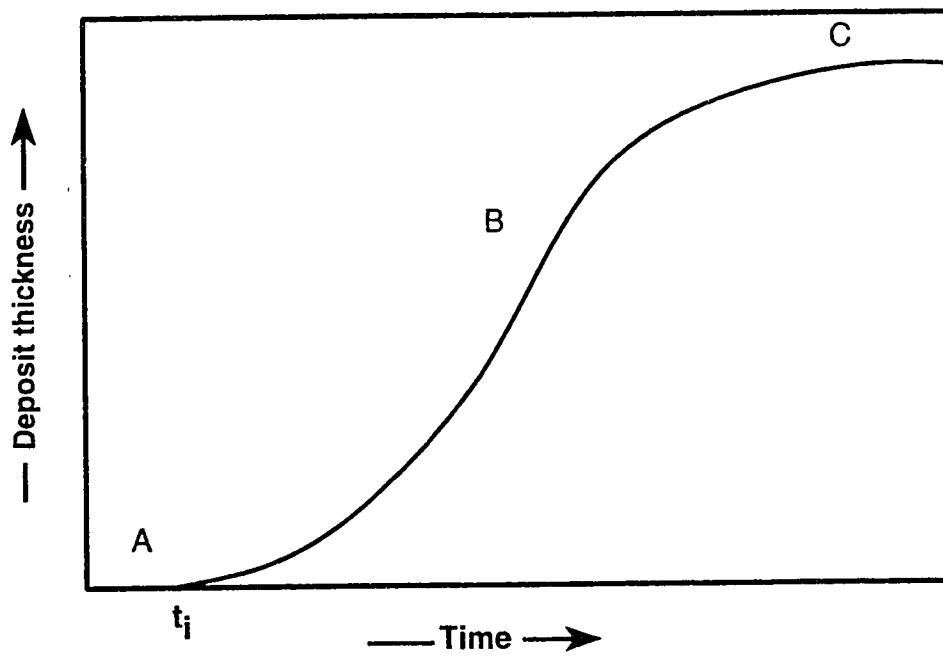


Figure 1.1: Change in deposit thickness with time [1]

The objective of the present study is to determine the influence of thermal-hydraulic parameters on the initiation and growth rate of $CaCO_3$ scaling in heat exchangers. The following Chapter discusses the history of fouling alongwith importance of fouling related research with emphasis on precipitation fouling. Chapter 2 also covers the aftermath of fouling and its impact on economics of heat exchangers operation and maintenance. The costs associated with the impact of fouling make us realize the significance and need of research in this field. In this regard, a literature survey was carried out to gather information regarding present status of fouling related research.

Chapter 3 covers the Experimental Setup which includes various components of the apparatus used to simulate conditions encountered in the operation of cooling water industrial heat exchangers. The thermal-hydraulic parameters considered in this study are also mentioned alongwith the procedure followed to obtain fouling resistance data.

The data thus obtained from the experiments are analyzed in Chapter 4. Influence of thermal-hydraulic parameters on the induction period and later growth of the scaling is also studied in detail. This Chapter also includes dimensionless fouling resistance models that were developed for prediction and estimation purpose. Results of several techniques used to verify model adequacy have also been presented.

Finally Chapter 5 summarizes the conclusions of the study and recommendations for future research in this field.

Chapter 2

History and Importance of Fouling Research

2.1 Historical Background

The phenomenon of fouling has been with us since fire was discovered. Reviewing the history of fouling, Somerscales [3] states “It is not difficult to imagine the annoyance of the early ancestors who first burnt the porridge, or who noted with exasperation the increasing time it took to boil water as a consequence of “furring” of the kettle. Clearly fouling has had a long history, and it is equally clear that it has had, and still has, an important effect on the efficiency of heat-transfer equipment, on the selection of material used in the construction of heat-transfer devices, and on the operation of many industrial processes”.

This review by Somerscales traces the history of heat exchanger fouling. It suggests four epochs in the development of an understanding of fouling-related problems. In the first period upto about 1920, concern was directed towards observing the phenomenon and devising methods for reducing the problem with less emphasis on the scientific understanding of the mechanisms involved. The second period from 1920 - 1935 covered development in the measurement of fouling. The following ten years from 1935 - 1945 witnessed the extended use of the so-called "fouling factor". From 1945 to the present time, a more scientific approach to the problem of fouling has been introduced with detailed investigations into the mechanisms that underline the problem of heat exchanger fouling.

In 1965, Gilmour [4] described fouling as often a result of unintelligent application of the laws of fluid dynamics and that the mere use of a high fouling factor will generally cause a high degree of fouling. Taborek et al. [5] carried out a major investigation on fouling, based on Heat Transfer Research Incorporated (HTRI's) research work which was probably the first systematic investigation of fouling applied to process industry. Different aspects of the deposition process and its characteristics are discussed in this pioneering paper of Taborek et al. They have classified fouling as a major unresolved problem in heat transfer applications. Ganapathy [6] described fouling as a silent heat transfer thief which slowly steals heat duty by reducing the

overall heat transfer coefficient. Garret-Price et al. [7] has mentioned the work of Epstein who presented an overview of fouling in which he proposed six basic types of fouling mechanisms. Knudsen [8] discussed how to minimize fouling during the design and operation of tubular heat exchangers. It is thus important to emphasize that fouling cannot be overlooked during the design stages and can also be controlled during the operation of the heat exchange equipment in case proper awareness is available to the concerned personnel.

2.2 Importance of Fouling Research

Economics of a process depends crucially on the amount of energy consumed. Energy conservation is an important factor and therefore fouling problem can be considered as a challenge to designers, technologists and scientists involved in research regarding heat transfer equipment. There are innumerable sources of energy utilization and large amount of energy is thus consumed. In majority of the power plants, fossil fuels are being used to generate steam which in turn produces electricity. During the process of electricity generation a lot of heat exchangers are employed to transfer heat into a coolant, generally water. Efficiencies of such heat transfer equipment are reduced, due to the presence of fouling, and thus more energy is consumed to overcome the fouling resistance. In other processes the primary fuels, coal, oil or natural gas are used for process heating. Reduced efficiency of the heat exchangers

due to fouling, represents an increase in fuel consumption with repercussions not only in cost but also in the conservation of the world's energy resources. The use of additional fossil fuels to recover the shortfall in energy due to fouling, will also have an impact on the environment.

The increased carbon dioxide produced during combustion will add to the "global warming" effect [1]. Although reduced heat transfer efficiency is of prime importance, there may also be pressure drop problems. The presence of the foulant will restrict flow that results in increased pressure drop, and in severe cases of fouling, the exchanger may become inoperable. Pressure drop problems may have a more pronounced effect than the loss of thermal efficiency [1].

Chemical additives are usually used to overcome the problem of fouling. For instance, a whole industry has built up to produce chemicals that are used for the treatment of water for cooling purpose and the various chemicals added to the water fall into three categories, i.e. control of biological growth, prevention of scale formation and corrosion inhibition. Careful choice of treatment program will do much to reduce the accumulation of deposits on heat exchange surfaces.

The presence of fouling deposits hinders the flow of fluid. Therefore to achieve certain output, velocity has to be increased. This requires more pumping energy

which results in increase of costs. Many pumps are electrical and so the increased energy requirement is in terms of the more expensive secondary energy. Other operating costs can accrue from the presence of the deposits such as increased maintenance requirements or reduced output [1]. Emergency shutdown as a direct result of heat exchanger fouling can be particularly expensive. It is not necessary that the deposit cleaning schedule may coincide with the planned maintenance shutdown of the plant. Thus it becomes necessary to install standby heat exchangers to replace the primary heat exchangers when their cleaning is deemed necessary [1].

There is also a human dimension linked to the problem of fouling. Frequent cleaning of the heat exchangers affects the employee morale also [9]. The repeated and persistent need to shut down the plant to clean heat exchangers, or difficulties in maintaining the desired output due to the accumulation of deposits will inevitably lead to frustration on the part of those employees whose duty is to maintain production and product quality [1]. The fouling of heat exchangers is a wide ranging topic covering many aspects of technology. It plays a vital role in the product cost and is also linked to conservation of precious sources of energy and world environment. Adequate solution of the fouling problem would also lead to better industrial working conditions [1].

2.3 Economic Impact of Fouling

An understanding of the economic penalties associated with fouling is one of the primary reasons for greater interest in the fouling research. Pritchard [10] presented cost estimates associated with fouling in Britain. Thackery [11] estimated the overall annual cost of surface fouling in U.K of about 0.3% of GNP for the year 1978 (approximately \$1 billion). The order of magnitudes of these estimates is confirmed by Van Nostrand et al. [12] while investigating the fouling related costs for the U.S specific refinery units. Steinhagen et al. [13] indicated the fouling-related costs for New Zealand at about \$30 to \$46 million which is about 0.1 % to 0.17 % of the annual GNP for the year 1988. The costs associated with fouling can be classified under four main headings: Capital Expenditures, Fuel Costs, Maintenance Costs and Loss of Production [2].

2.3.1 Capital expenditures

This section covers increased cost of heat exchangers due to fouling. The costs can be subdivided into a number of components. These include costs of increased heat transfer surface area to be provided due to fouling and associated extra civil works required for installing larger heat transfer equipment [2]. A detailed discussion on the effects of fouling on the condenser design for power plants, including heat exchanger size, flow velocity (and thus pumping power) and pressure and temperature drop

was presented by Curlett and Impagliazzo [14]. They concluded that an increase of 50% could be expected in the capital cost of a \$10M condenser for a hypothetical 600 MW coal fired power plant depending upon the fouling resistance chosen.

Provision of extra heat transfer surface

Heat exchangers are usually designed for a fixed heat-transfer duty that can be described in terms of the overall heat-transfer coefficient U and the surface area A

$$1/UA = 1/U_cA + R_f. \quad (2.1)$$

It is obvious from this relation that fouling resistance, R_f , can result in providing more surface area 'A'. The designer of a heat exchanger should therefore be able to decide what values of R_f to use before he can decide on the surface area. A value of 30-40% excess was found in a survey of heat exchanger manufacturers in the United States in 1982, leading to an extra cost of \$320M [7]. Cases are known in which the excess area has been up to an order of magnitude larger than was subsequently found to be necessary, and this suggests that about half of the extra surface area currently being built into heat exchangers may be unnecessary [2].

The cost of installation

In order to make up the heat lost due to fouling, usually more heat transfer area is provided which results in heavier heat exchangers. The cost of extra-surface area must therefore be added to the cost of the civil engineering work required, involving

the provision of extra space, stronger foundations, and increased transport and installation charges. On readily accessible sites, this may do little more than double the cost of heat exchanger itself, but in remote sites (e.g., on offshore oil platforms) a factor of ten may be reasonable as recommended by [2].

Capital costs of antifouling equipment

Penner et al. [15] estimated that the capital cost in 1981 of gas clean-up systems was about 10% of the capital cost of \$1000/kW(e) for a coal-fired power-station and suggested that the percentage of the cost might rise as much as 45% for a station designed to meet 1985 standards. The provision of anti-biofouling equipment for a proposed 300MW(e) Ocean Thermal Energy Conversion plant, the capital costs (reported in 1977) ranged from \$1-2M to \$10M depending upon the choice of chemical treatment or balls/brushes [16]. One of the major techniques for controlling biofouling in cooling waters is dosing with chlorine gas or hypochlorite solution. Being a widely used technique in power industry, it was estimated that the total capital cost of chlorination facilities in the U.S.A., calculated on a fixed charge rate of 20% related to the value of chlorine consumed, was \$267M [17].

2.3.2 Additional energy costs

Heat exchangers are employed to transfer energy from one fluid to another. Due to fouling, efficiency of the heat exchanger is reduced and thus additional fuel is

consumed. In one of the most detailed assessments made to date, Van Nostrand et al. [12] calculated the fouling related expenses attributable to extra fuel burnt, lost output and maintenance and cleaning in various refinery units in the U.S.A. They estimated total cost due to extra fuel burnt at \$427.7M per year, based on a process fuel cost at \$2.80/MBtu [12]. Extension of these calculations to the non-communist world suggested a cost of over \$1,500M per year, though of course the individual costs will depend upon the local cost of process fuel. The calculations for the U.S.A. is reasonably consistent with the estimate of Garrett-Price et al. [7], of \$700-3500M for the fuel burnt to overcome fouling problems, though this estimate included natural gas and coal as well as petroleum products.

The loss of heat transfer due to scale formation on boilers has been calculated [18] to lead to losses of output of 2-7% for a scale thickness of 0.8 mm, the loss depending upon the methodology and composition of the scale. Significant fuel savings could be made if some or all of the dissolved salts were removed from the feedwater beforehand, thus allowing a higher concentration factor without scaling, and a smaller loss of heat through the reduced rate of blowdown. A figure of 0.8-1.0% of fuel costs for 2% blowdown has been suggested [19], together with costs of water treatment ranging from 15% of the raw water cost for sodium zeolite ion exchange treatment to 100-400% for complete demineralization. Examples of increased pumping costs due to fouling are hard to mention, but Terrel [20] stated that in a 250 m^3 reciprocating

system with a 10-inch (254 mm) main, a 10% decrease in diameter would double the pressure drop and thus the pumping power.

2.3.3 Maintenance costs

The annual sales in 1982 of companies supplying heat exchanger on-line and off-line cleaning equipment, chemicals and cleaning services in the U.S.A. were quoted as \$2,000M [7]. Substantial use is made of antifoulant chemicals in oil refineries, and Van Nostrand et al. [12] suggested that antifoulant costs \$155,000/year for a crude unit processing 100,000 barrels per day (bpd), and \$40,000/year on a hydrotreater processing 25,000 bpd. Steinhagen et al. [13] have indicated that maintenance costs constitute 72.4% of the total heat-exchangers fouling costs for New Zealand. Maintenance costs can be divided into two main classes [2], i.e., the costs of removing fouling deposits during planned or unplanned maintenance, and the costs of chemicals or other operating costs of antifouling devices.

2.3.4 Costs due to loss in production

Unwanted plant shut-downs result in loss of production. Major costs are associated to plants shut-down due to fouling either because of contamination of product or due to low efficiency of the heat transfer equipment. With experience, scheduled shut-downs can be arranged to return the exchanger to normal operation before problem gets out of hand, thereby minimizing costs in terms of lost production [2].

Van Nostrand et al. [12] estimated an annual cost of \$872M due to loss of throughput caused by fouling in United States refineries, the largest part is found to be associated with crude-distillation units.

A survey of 27 ammonia plants in the U.S.A. in 1973 showed that a waste heat boiler failure could be expected every three years, leading to 5 days loss of output [21]. It does not seem unreasonable to expect that these failures were mainly associated with deposit formation, giving an annual loss of 100,000 pounds of product in 1973 [2]. Collier [22] stated that the loss of electricity generation attributable to steam generator unreliability in pressurized water reactors (mainly caused by corrosion associated with deposit formation) averaged 10-11 days/year. He stated that the mean duration of an outage for repairs was 20 days, and for a 1000 MW(e) plant this caused an economic loss of 4M pounds.

2.3.5 Safety

Fouling is not normally associated with safety problems, and this is probably one reason why it has not received as much attention as corrosion etc. It is worth mentioning that fouling can be considered as a safety hazard. Scaling effects the thermal-hydraulic performance of the heat transfer equipment and reduces the heat transfer coefficient. This results in overheating of the metal tubes which contributes to boiler explosion [2].

2.4 Status of Present Research

As is evident from the above mentioned discussion, the unwanted deposition of material, originally suspended or dissolved in the fluids onto the heat transfer surfaces has to be taken seriously and must be given due consideration. Despite the enormous costs associated with it only very limited research has been done to determine accurately the economic penalties due to fouling and to attribute these costs to the various aspects of the heat exchanger design and operation [2].

The designer generally provides an additional heat transfer area to compensate for the fouling. This oversizing results in several system related problems, in addition to extra capital investment. An important part of the specifications for the heat exchanger is the assignment of fouling resistance to provide added heat transfer area so as to permit satisfactory performance after some fouling has occurred. The challenge was to provide reasonable values of fouling resistance and to identify the consequences of this selection. The standards of TEMA (Tubular Exchanger Manufacturers Association) [23] have influenced profoundly the mechanical design practice of shell and tube exchangers. The TEMA tables of fouling resistances are quoted world wide as a unique reference. These standards are critically reviewed by Taborek et al. [24]. A joint committee of HTRI (Heat Transfer Research Incorporated)/TEMA has reviewed the fouling sections of TEMA standards [25].

It is now becoming clear that fouling is a factor of increasing importance in the design and operation of heat exchangers [26]. Pilvachi et al. [27] presented information of the research activities aimed at controlling fouling behavior of heat exchangers in industry. A lot of experimental and analytical work has been carried out by many engineers and scientists. Pritchard [26] discussed results of an investigation of fouling in a number of industrial organizations in the U.K. Parry et al. [26] studied problems faced in the midlands region of U.K. in power station condensers due to fouling. A critical survey of reported work on fouling of heat exchange surfaces is presented by Epstein [26]. Various types of fouling and a review of current theories of fouling are described by Collier [28]. Fouling of heat exchangers is reviewed with special emphasis on basic fouling mechanisms and heat transfer equipment design aspects by O'Callaghan [28].

Fryer [29] conducted experimental research to investigate similarities between two types of temperature dependent fouling from geothermal fluids and food. Chan et al. [30] presented fouling data from geothermal brines with different pH values, chemical compositions and thermal-hydraulic conditions. The effects of supersaturation, pH, Reynolds number and concentration of ions in the brine solution on the formation of silica scale in the heat exchanger tubes were discussed. A systematic study of scaling characteristics of cooling tower was conducted by Morse and Knud-

sen [31]. The study discussed influence of alkalinity on the scaling of simulated cooling tower water. Effect of surface temperature on the scaling behavior was discussed by Story and Knudsen [32]. Lee and Knudsen [33] designed an experimental apparatus so as to simulate the operating conditions of a cooling tower. This is a somewhat extensive investigation to determine the effect of flow velocity, surface temperature and water quality on scaling on the outer surfaces of tubes in cooling towers. Automatic data acquisition system recorded the data. The test section consisted of a heater to provide constant heat flux. Thermocouples were embedded in the wall of the test section to measure the wall temperature. In addition, flow rate and power input to heater were also monitored. Difference of wall temperature at fouled and clean conditions was calculated and dividing it by the heat flux, fouling resistance was determined. Coates and Knudsen [34] discussed results of their experiments conducted for obtaining data for $CaCO_3$ scaling. Watkinson and Martinez [35] studied scaling due to $CaCO_3$ in copper heat exchanger tubes under conditions that promote rapid and severe scaling. Artificially hardened water of high dissolved and suspended solids was circulated through a heated test section. Effects of flow velocity, tube diameter and bulk temperature on asymptotic fouling resistance have been determined.

Manzoor [36], conducted fouling related experiments and statistical analysis of the fouling data. In this regard, experiments were conducted for $CaCO_3$ scaling.

The objective of the experimental study was to demonstrate that fouling resistance varies from point to point along a horizontal tube and also for the same point it varies from replicate to replicate. The operating parameters were temperature, pressure, solution concentration and velocity. These parameters were kept constant during the experimental study. Scaling data were gathered using a 4.6 mm (I.D.) stainless steel tube and fouling resistance was determined at different sections of the tube at about two hours time interval. The replicate data for a given test section were fitted with a probability distribution also known as α -distribution. Konings [37] on the basis of experimental work with cooling water, treated by different methods in a test rig, presented a table of guide values for the fouling resistance. An experimental study of tube side fouling resistance in water chilled evaporator was carried out by Haider et al. [38] in which 12.6 foot long evaporator tubes were used and fouling data were taken for four tube geometries. No data were taken at different sections of the tube. The fouling characteristics of cooling water for precipitation and particulate fouling were also discussed by Knudsen [39] where he emphasized serious problems encountered when heat exchangers are overdesigned due to the use of incorrect design fouling allowance. To make continuous operation of the heat exchanger possible, appropriate chemical treatments were recommended. The study shows that fouling may be reduced by low surface temperature and high velocities.

In another study, effect of *NaCl* and *KCl* salts in aqueous solutions on silica

fouling of heat exchangers was studied experimentally by Chan et al. [40] over a range of pH values, velocities and concentration levels. The test equipment consisted of double-pipe heat exchanger with brine in tube side and distilled water in shell side. Scale was formed on the inner surface of titanium tube (2.82m long, 2.54cm diameter and 0.165 cm thick). Crittenden and Khater [41] obtained data for fouling rate by passing kerosene at a low flow rate through a small horizontal tube furnace. Crittenden et al. [42] conducted fouling experiments with light Arabian oil flowing inside a 3/4 inch O.D. 14 BWG (British Wire Gauge) tube with constant heat flux and velocity. In an other experimental study, recommendations for the use of fouling resistance is given by Watkinson [43] for augmented tube in terms of plain tube fouling resistance. Kim and Webb [44] reported the results of their fouling experiments performed on two enhanced tubes used in water chiller condensers. A stochastic model for the induction step on particulate fouling was developed by Vatisstas [2]. It was reported that smoothness of the fouling surface is an important contributory factor that effects the induction period. Various mechanisms involved in particulate fouling have been discussed and effect of friction velocity on the induction time has been studied. Crittenden et al. [45] discussed results of experiments on chemical reaction fouling and in [46] fouling of crude oil preheat exchanger. Crittenden et al. [47] conducted experiments using wire matrix inserts to control hydrocarbon fouling. Inserts were used in a pilot scale research using light Arabian crude oil containing a waxy residue. Yang et al. [48] investigated use of heat transfer augments

as a fouling cleaner. A spiral wire was used to augment heat transfer in tubes of condensers.

In order to design efficient heat exchanger accurately, a better understanding is required regarding the foulants that are deposited on the heat transfer surfaces. As fouling received attention many techniques and devices were developed for its measurement. Manohar [49] described design and fabrication of gas side fouling measuring device and its testing in an industrial environment. Owens [50] discussed a simple device to monitor the thermal resistance of fouling from sea water. For the use of petroleum industry, Dickakien [51] presented another fouling analyzer. Thompson and Bridgewater [52] discussed use of another device to measure fouling resistance on the tube side of the heat exchanger. Several other techniques are also discussed by Knudsen [53] for the measurement of fouling on heat exchange surfaces.

An investigation was carried out by Zhang et al. [54], to reduce deposition on the gas side of extended surface heat exchanger. Short and long term experiments were conducted by Panchal and Sasscer [55] for bio and corrosion fouling in rectangular flow channels tested in an experimental research program of Natural Energy Laboratory in Hawaii. Practical and fundamental aspects of precipitation fouling ($CaCO_3$ scaling) were reviewed by Hasson [56]. He considered the problem of defining precipitation fouling tendency by reviewing principles of solution equilibria and

precipitation kinetics for salt systems frequently encountered in heat exchanger applications. Branch and Muller-Steinhagen [57] developed a model for fouling in shell and tube heat exchangers by modifying Hasson's ionic diffusion model for $CaCO_3$ scaling. Hesselgreaves [58] discussed the effect of system parameters on the fouling performance of heat exchangers subject to fouling. Experiments were conducted by Yiantsios and Karabelas [59] for examination of fouling behavior of tube surfaces due to flowing solutions and suspensions. A mathematical model was then developed for the macroscopic fouling behavior based on the technique of population balance.

Brown [60] investigated that sometimes cost of maintenance of heat exchangers outweighs the energy savings related to cleaning of fouling. He emphasized that fouling should be a design concern and should not be considered as an inevitable side effect of the process. A relatively new approach to cleaning fouled surfaces is described by [61]. Uses of spiral turbulators for enhancement as well as a fouling cleaning tool have been discussed. Hughes [62] discussed use of additives to inhibit or reduce fouling. An interesting model was presented by Bejan et al. [63] for the removal of fouling from heat exchangers. They have demonstrated that a strategy similar to defrosting of refrigerators can be employed for cleaning of heat exchangers. A model for $CaCO_3$ scale formation which gives reliable prediction of the rate fouling process was developed by Tretyakov et al. [64]. Duffua and Budair [65] deduced a schedule for scale removal in a brine heat exchanger of a desalination plant

using energy utilization function. Panchal and Watkinson [66] developed a chemical reaction fouling model for single phase heat transfer. The objective of their study was to evaluate a fouling model to identify the governing mechanisms of the fouling process. Another model was developed by Oufer and Knudsen [67] to predict fouling due to deposition of unwanted material on a heat transfer surface under local boiling conditions. Fouling due to organic fluid was considered by Panchal et al. [68] and a model was developed. Silica fouling was studied and a semi-analytical model was presented by Neusen [69].

From the above discussion it is clear that fouling has many dimensions which must be considered by the designers and operators of heat exchangers. However, for the analysis purpose, we shall restrict ourselves to studies of calcium carbonate scaling under precipitation fouling. A brief description of such a fouling process is given below.

2.5 Precipitation Fouling

Precipitation fouling may be defined as the phenomenon of a solid layer deposition on a heat-transfer surface, arising primarily from the presence of dissolved inorganic salts in the flowing solution which exhibit supersaturation under the process conditions [39]. The problem of precipitation fouling is encountered in industrial

operations and processes with natural water or aqueous solutions containing dissolved scaling salts. Some of these salts or their combinations have inverse solubility properties, so that they are less soluble in the hot fluid adjacent to the heat transfer surface. This hot layer can become supersaturated causing the salts to precipitate on the surface and adhere to it. The deposit thus formed is called "scale". Figure 2.1 shows the behavior of normal and inverse solubility salt solutions. For normal solubility salt solution, at point A, solution is under saturated but on cooling to point B it becomes just saturated. On further cooling, the solution becomes supersaturated and crystal nucleation occurs at point C. As crystallization and cooling proceeds solution concentration falls and moves in the direction of D. Now for an inverse solubility salt solution it is undersaturated at point A, as it is heated it reaches the solubility limit at point B at temperature T_1 where it becomes just saturated. Upon further heating the solution becomes supersaturated reaching point C at temperature T_2 where precipitation starts. For pure salts, the deposit is often quite hard and adherent. On the other hand, if a mixture of salts and suspended solids deposit on the heated surface, the deposit is often quite soft and does not adhere strongly to the surface [70]. The term scaling is generally used to describe a dense crystalline deposit, well bounded to the heat transfer surface. It is often associated with the crystallization of salts, e.g., inverse solubility characteristics of CaCO_3 when it encounters a heat-transfer surface at a relatively high temperature.

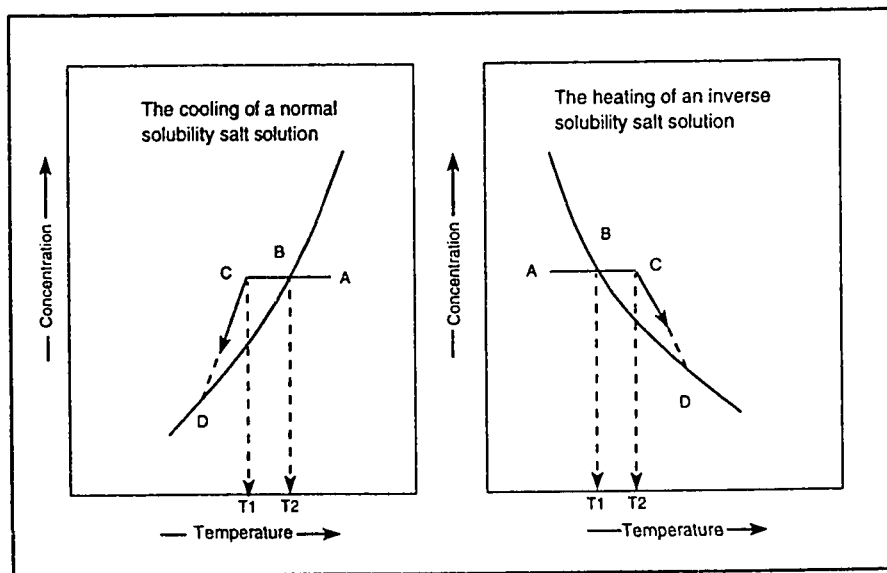


Figure 2.1: Behavior of normal and inverse solubility salt solutions [1]

The formation of scale on heat transfer surfaces is a common phenomenon where aqueous solutions are involved, e.g., the use of natural waters for cooling purposes or evaporative desalination. Unless suitable measures are taken the problem can give rise to serious consequences. In steam boilers, for instance, the presence of scale on water side can give rise to high metal temperatures that may result in mechanical failure of heat-transfer equipment [1]. When scale causes a rapid rise in tube wall temperature a violent rupture occurs as plastic conditions are reached at temperature in the region of 975-1100K [71]. The prevention of scale formation and other forms of deposit in boilers is essential for safe operation.

Hanlon et al. [1] commented on the potential of scale formation in industrial equipment as very high. As an example he observed that for a 1 million gallon/day desalination plant under normal concentration conditions, a maximum of about 1400 kg of $CaCO_3$ or 800 kg $Mg(OH)_2$ could precipitate each day. In terms of scale thickness it would represent a build up of 0.1 mm per day on the total heat exchanger surface within a typical plant. Although this may be regarded as an extreme example, it does illustrate the extent of the seriousness of fouling in industrial plants.

The present investigation considers the effect of thermal-hydraulic parameters (Reynolds number, tube diameter, tube outer surface temperature and salt concentration) on the induction time of $CaCO_3$ scaling. The influence of these parameters

on the later growth rate of $CaCO_3$ scaling has also been considered. The experimental study carried out in this regard is followed in the next Chapter.

Chapter 3

Experimental Setup and Procedure

3.1 Test Equipment Design

The test equipment was a double-pipe counter-flow heat exchanger as shown in Fig.

3.1. The scaling fluid was passed through the inner tube which consisted of six test sections, each 0.1524 m long. Three heat exchangers were fabricated with inner tube sizes of 1/4 inch (0.00635m), 3/8 inch (0.00952m) and 1/2 inch (0.0127m). During the design stage special emphasis was given to the fact that the heat exchanger was to be assembled and dismantled quite frequently during the course of the experimental study. The inner tube was fixed with one of the end plates and it could slide into the other end plate using a neoprene O-ring for sealing. Four studs were used

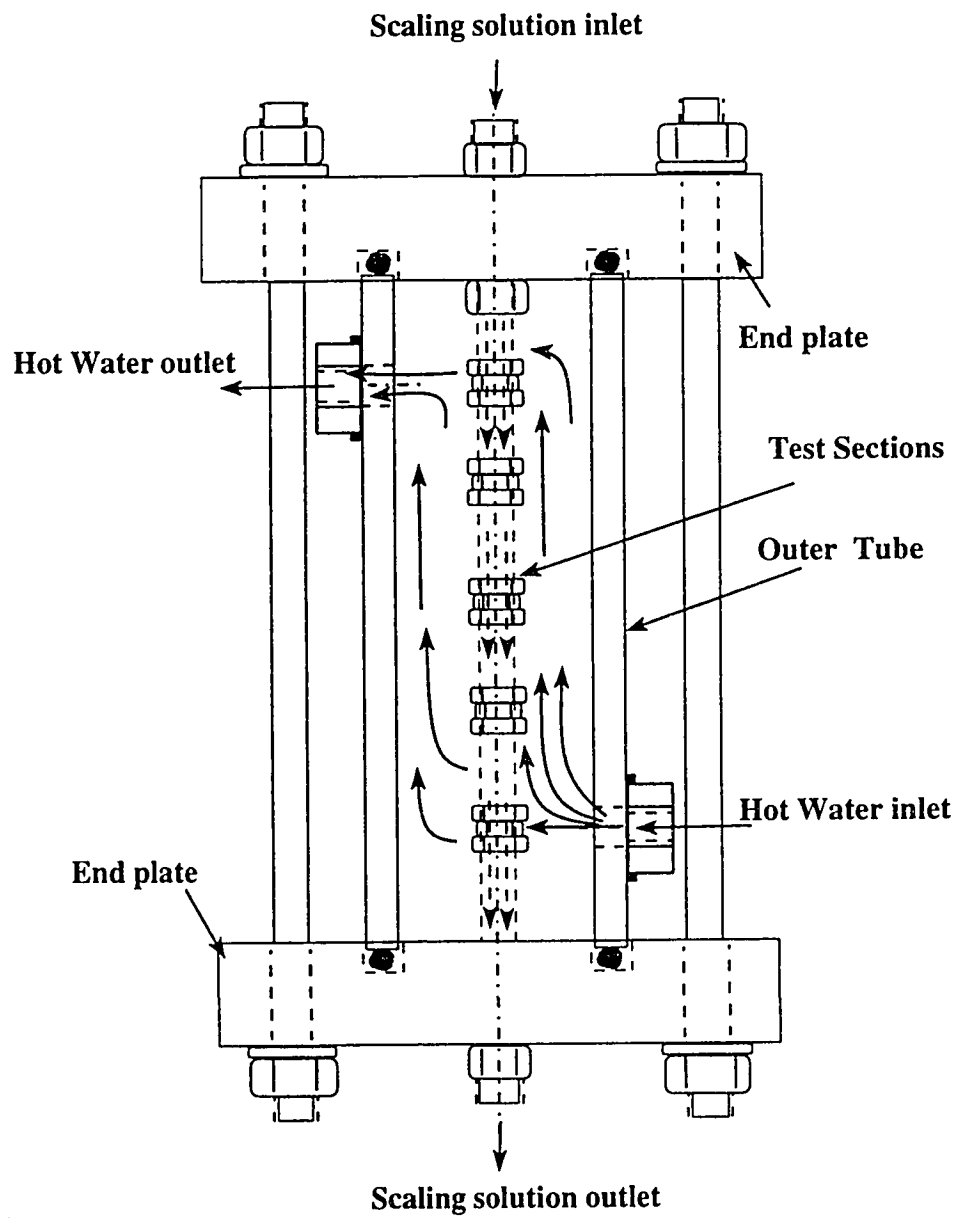
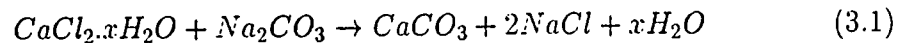


Figure 3.1: Schematic of the double tube heat exchanger

to assemble the heat exchanger. Detailed drawings of the three heat exchangers are presented in Appendix A. The outer to inner radii ratio of the tubes was set at four for all the three heat exchangers. All test sections and fittings were made of SS 316. The ends of the test sections were deburred and ground. They were numbered for identification purpose and to keep them in the same order for the next test run. The orientation of the tubes was also kept same for all the test runs for each set of experiments. The tubes were connected together with the help of unions. Nuts were fitted on the tubes using ferrules so that they could be attached to the unions.

The inner tube was heated by circulating hot water in the outer tube using a Constant-Temperature Water-Circulator Bath (CTWCB), which had a provision of variable temperature settings. To simulate the conditions encountered in cooling water systems, Na_2CO_3 and $CaCl_2$, solutions prepared in demineralized (distilled) water were used to produce $CaCO_3$ as a product of chemical reaction. The product solution, when passed through the inner tube, resulted in the deposition of $CaCO_3$ scale on the inner side of the tube. The chemical reaction to produce $CaCO_3$ scale is given by [72]



The chemical solutions were pre-heated, separately, using pre-heaters and heating tapes (wrapped around the tubes carrying fluids from the tanks into the mixing chamber) to achieve a temperature of 50°C before the solution entered the heat exchanger. The system was once-through type and a Back Pressure Regulator (BPR) was used to maintain a pressure of 100 psi (689 kPa) at the end of the heat exchanger. Two high pressure diaphragm type pumps were used to pump the two solutions into the mixing chamber. Due to the limitations of the pumping capacity of the pumps the flow was restricted to the Laminar regime and the maximum Reynolds number attained was 1700. Two storage tanks with a capacity of 40 liters each were used. Filters of 15 microns were fitted at the outlet of the storage tanks. Heating bands that were used had a total capacity of 3 kW. Four thermocouples were used to measure the temperature at the inlet and outlet of the inner and outer tubes of the heat exchanger. In order to maintain a constant fluid temperature at the inlet of the inner tube an electric relay was used to cut off the power to the heaters when the desired temperature was achieved. Figure 3.2 shows the scaling apparatus which consisted of two high pressure variable stroke pumps, storage tanks for the chemical solutions, pre-heaters, heating tapes, CTWCB, thermocouples, temperature controllers and a BPR.

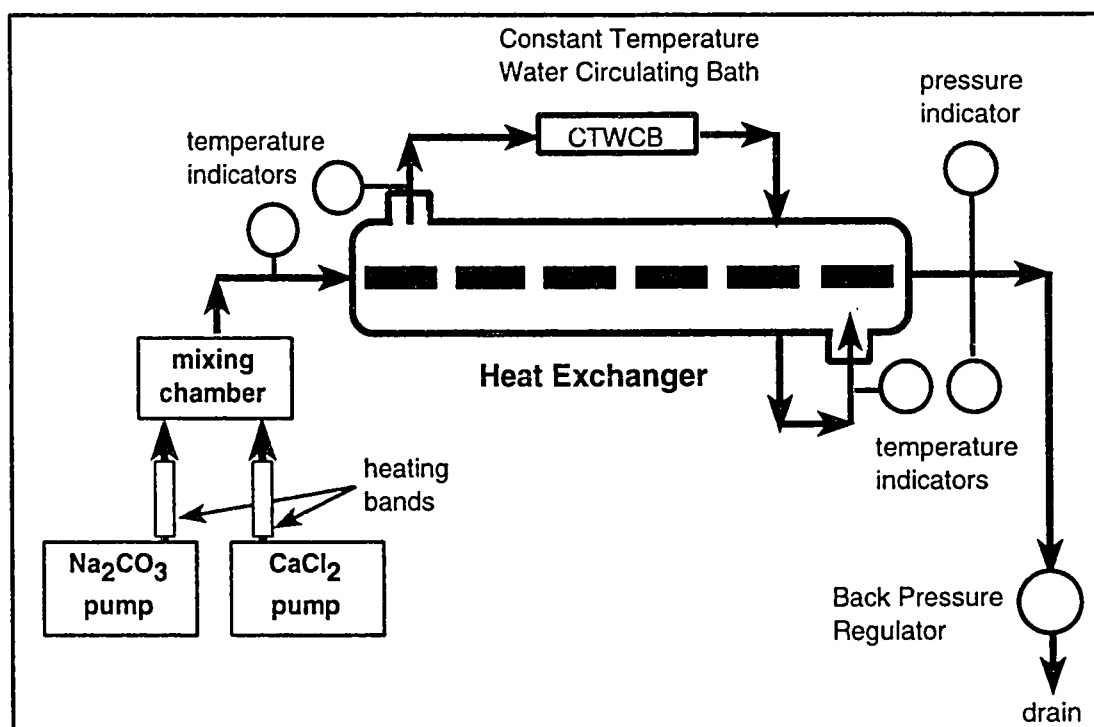


Figure 3.2: Schematic of a scale deposition equipment

3.2 Thermal and Hydraulic Parameters

Three parameters that were varied are Reynolds number, tube outer surface temperature and diameter of the inner tube. The experiments were conducted for all possible combinations of the parameter values shown in Table 3.1 in which the Reynolds number is based on the inner diameter of the test section. The concentration of the product solution was kept constant at 0.0006 moles/liter. This required 2.543 and 3.528 grams of Na_2CO_3 and $CaCl_2$ respectively to be mixed in 40 liters of water. The solutions were prepared in distilled water. Solution concentration was then changed to 0.0012 moles/liter and one experiment was conducted keeping Re , T_s and D constant. Similarly for the same values of Re , T_s and D an experiment was conducted for 0.0003 moles/liter salt concentration.

During the course of experiments, the scaling fluid temperature at the inlet of the inner tube of the heat exchanger was maintained at 50°C. Back pressure at the exit of the heat exchanger was also fixed at 689 kPa. In order to ensure that the outer surface of all the test sections were at the same temperature, a CTWCB was used and hot water was circulated in the outer tube at 22 l/min. The temperature at the outlet and inlet of the outer tube were thus found to be same with an accuracy of $\pm 1^\circ F$ ($\pm 0.56^\circ C$). It is therefore important to mention that the fluid capacitance rate at the shell side of the heat exchanger was very large and thus the

Table 3.1: Experimental parameters

Reynolds No., $Re=VD/\nu$	900	1300	1700
Surface Temperature, T_s (K)	338.15	348.15	358.15
Tube diameter, D (inch, m)	1/4(0.0063)	3/8(0.0095)	1/2(0.0127)

fluids capacitance ratio (C_{min}/C_{max}) was approaching zero.

3.3 Experimental Procedure

The experiments were conducted in controlled laboratory environment. As mentioned earlier three heat exchangers were designed and fabricated for the three tube sizes. For a particular size, Reynolds number was fixed and various experiments were conducted by varying the surface temperatures of the inner tube with the help of the CTWCB. To ensure equal volumes of the two solutions were being mixed, calibration of the two pumps was carried out by adjusting stroke lengths of the pumps. In the start, the test pieces were cleaned with acetone and washed with distilled water and their mass was measured. Each experiment consisted of five-two hour runs for a particular set of parameters. First the desired temperature of the CTWCB was achieved and then flow was started in the inner tube. Heating bands

were used to heat the chemical solutions before they entered the mixing chamber. Only 2-3 minutes were required to attain 50°C at the inlet of the inner tube for the maximum flow rate. It required less time to achieve 50°C temperature condition for the lower flow rates. Temperature controllers were used to ensure that the temperature at the inlet was kept constant, with an accuracy of $\pm 1^\circ\text{F}$, throughout the run. Each run consisted of two hours. At the end of each run, the heat exchanger was dismantled and the six test pieces were dried in an oven. Mass gain of the test pieces due to scaling was then measured using an analytical weighing scale which had an accuracy of ± 1 mg resulting in an experimental uncertainty of fouling resistance by $\pm 0.3\%$ (refer to Appendix B). The heat exchanger was then re-assembled for the next experimental run. It was observed that 0.25 inch (0.0127 m) tube blocked due to scaling after 10 hours of operation thus restricting the duration of the experiments to a maximum of 10 hours. Periodic measurements of the flow rates were carried out to maintain a constant Reynolds number during the experiment. For the next set of experiment, new set of tubes were used.

Using the mass gain method, Fouling Resistance (R_f) was determined as follows

$$R_f = \frac{r_2 - r_1}{k}, \quad (3.2)$$

where r_2 is the inside radius of the tube. The three inner radii considered for the study are 0.004699, 0.003111 and 0.00226 m. r_1 is the average value of radius due

to the deposit for a particular test section which can be calculated by using the relation

$$r_1 = \sqrt{r_2^2 - \frac{\text{mass gain}}{\pi \rho l}}. \quad (3.3)$$

3.4 Assumptions

- (1) It was assumed that scale deposition is uniform over the entire (six inch) length of a test section.
- (2) Water analysis of solution samples taken at the inlet and outlet of the heat exchanger showed that there was almost no difference in the pH values of the two samples. It was thus assumed that the pH value of the solution passing through the inner tube of the heat exchanger remained constant. Results of water solution analysis are presented in Appendix C.
- (3) Reynolds number was considered based on the clean tube dimensions.
- (4) Results of water analysis also indicated that the density of solution in the heat exchanger was almost the same as that of pure distilled water. Also, due to the lack of data available regarding the kinematic viscosity of $CaCO_3$ solution, kinematic viscosity of water was used in the calculations of the Reynolds number.

3.5 Design of Experiments

3^k factorial design was used for the experiments in which $k = 3$, which is the number of parameters considered for the experimentation. Each parameter had three levels. The design thus obtained is shown in Table 3.2.

Experiments were thus conducted accordingly and data collected. Data analysis was carried out and the results are discussed in the next chapter.

Table 3.2: Design of experiments

Expt. #	Tube diameter	Re = VD/ν	Tube Surface Temperature
1	level 1	level 1	level 1
2	level 1	level 1	level 2
3	level 1	level 1	level 3
4	level 1	level 2	level 1
5	level 1	level 2	level 3
6	level 1	level 2	level 2
7	level 1	level 3	level 1
8	level 1	level 3	level 2
9	level 1	level 3	level 3
10	level 2	level 1	level 1
11	level 2	level 1	level 2
12	level 2	level 1	level 3
13	level 2	level 2	level 1
14	level 2	level 2	level 2
15	level 2	level 2	level 3
16	level 2	level 3	level 1
17	level 2	level 3	level 2
18	level 2	level 3	level 3
19	level 3	level 1	level 1
20	level 3	level 1	level 2
21	level 3	level 1	level 3
22	level 3	level 2	level 1
23	level 3	level 2	level 2
24	level 3	level 2	level 3
25	level 3	level 3	level 1
26	level 3	level 3	level 2
27	level 3	level 3	level 3

Chapter 4

Results and Discussion

Experiments were conducted by varying three parameters i.e., Re , D and T_s . Each parameter had three levels, hence all possible combinations required 27 experiments to be performed. The schedule of experiments showing the values of parameters for which the experiments were performed is presented in Table 4.1. For all experiments, first reading for the fouling resistance was measured after two hours of operation. After that data were collected every two hours and one experiment was conducted for ten hours, in total consisting of five test runs of two hours each. Therefore, in total, 135 runs were performed to gather data for $CaCO_3$ scaling at six test sections of the heat exchanger. The data thus obtained are shown in tabular and graphical forms in the Appendices D and E respectively.

Table 4.1: Schedule of experiments

EXPT NO.	Tube diameter	Re = VD/ ν	Tube surface temperature
	m		K
1	0.0127	1700	338.15
2	0.0127	1700	348.15
3	0.0127	1700	358.15
4	0.0127	1300	338.15
5	0.0127	1300	358.15
6	0.0127	1300	348.15
7	0.0127	900	338.15
8	0.0127	900	348.15
9	0.0127	900	358.15
10	0.0095	1700	338.15
11	0.0095	1700	348.15
12	0.0095	1700	358.15
13	0.0095	1300	338.15
14	0.0095	1300	348.15
15	0.0095	1300	358.15
16	0.0095	900	338.15
17	0.0095	900	348.15
18	0.0095	900	358.15
19	0.0064	1700	338.15
20	0.0064	1700	348.15
21	0.0064	1700	358.15
22	0.0064	1300	338.15
23	0.0064	1300	348.15
24	0.0064	1300	358.15
25	0.0064	900	338.15
26	0.0064	900	348.15
27	0.0064	900	358.15

4.1 Calculation of Induction Time

Regression technique was used to determine the induction time of the scaling. Fouling resistance was plotted with respect to time (in hours) for the six test sections of the heat exchanger. The plots showed that the slope of all curves was continuously changing with time. To illustrate this behavior a representative figure (Fig. 4.1) is selected. The curve shown in this figure is of test section number 3 of tube diameter of 0.0095 m at surface temperature of 338.15 K with Reynolds number 900. The slope is seen to change and its value varies between 4.701 to 12.496. Similar trend was observed in all the curves for the six test sections. From the shape of the curves a power law model i.e., $R_f = A(t)^B$ was chosen with different values of A and B. In order to check the suitability of the model, coefficient of determination (R^2) was calculated for all the experiments. Fouling resistance curves were plotted as R_f vs $(t - t_i)$ in which t_i is the induction time. Different values of t_i were chosen and their respective effect on the R^2 value of the model was determined. The value of induction time representing the highest R^2 was considered as the induction time of that curve. This procedure was repeated for every test section curve and for all the experiments. It is worth noting that the values of R^2 varied from 0.96 to 1.0. The values of induction time, for six test sections in each experiment, thus obtained are shown in Table 4.2 and in the form of bar chart in Fig. 4.2.

From the data it can be observed that the induction time calculated for the tube

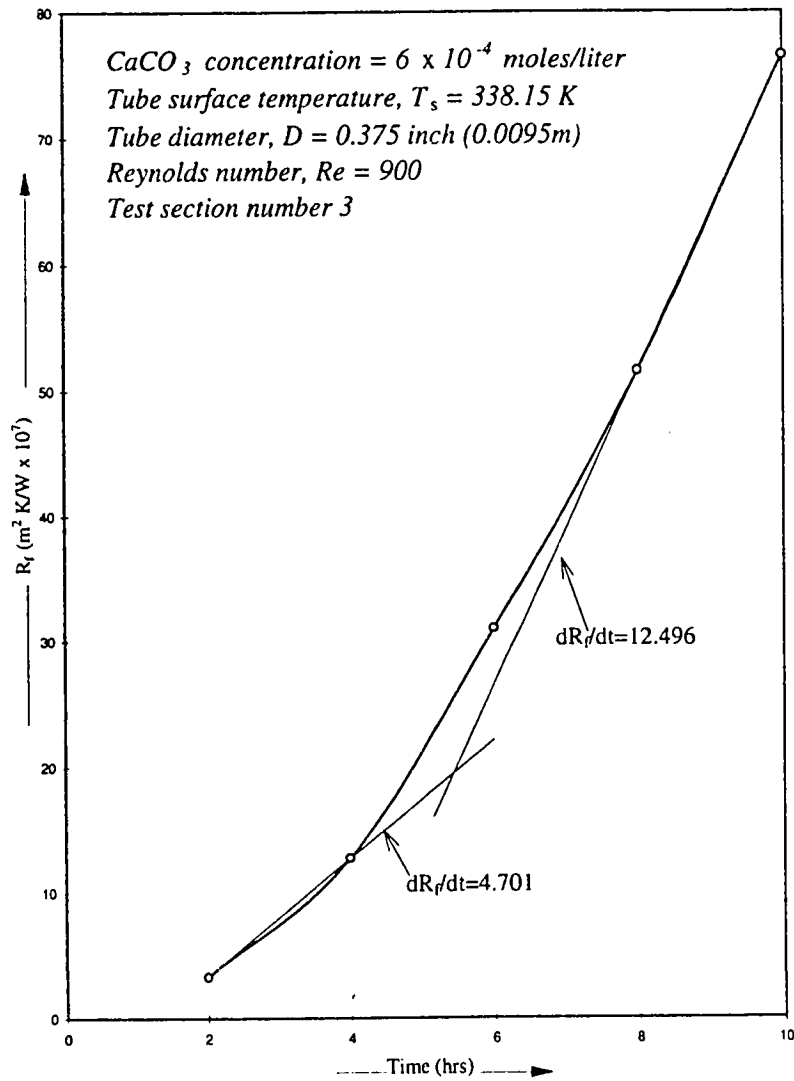


Figure 4.1: A sample curve of R_f vs time showing increase of slope

Table 4.2: Results of induction time calculations

EXPT NO.	Tube	Re =	Tube surface	INDUCTION TIME (HR)					
	diameter	VD/v	temperature	SECTION NO.					
	m		K	1	2	3	4	5	6
1	0.0127	1700	338.15	0.75	0.75	0.75	0.75	0.75	0.75
2	0.0127	1700	348.15	0.75	0.75	0.75	0.75	0.75	0.75
3	0.0127	1700	358.15	0.75	0.75	0.75	0.75	0.75	0.75
4	0.0127	1300	338.15	0.75	0.75	0.75	0.75	0.75	0.75
5	0.0127	1300	358.15	0.75	0.75	0.75	0.75	0.75	0.75
6	0.0127	1300	348.15	0.75	0.75	0.75	0.75	0.75	0.75
7	0.0127	900	338.15	0.75	0.75	0.75	0.75	0.75	0.75
8	0.0127	900	348.15	0.75	0.75	0.75	0.75	0.75	0.75
9	0.0127	900	358.15	0.75	0.75	0.75	0.75	0.75	0.75
10	0.0095	1700	338.15	0.75	0.75	0.75	0.75	0.75	0.75
11	0.0095	1700	348.15	0.75	0.75	0.75	0.75	0.75	0.75
12	0.0095	1700	358.15	0.75	0.75	0.75	0.75	0.75	0.75
13	0.0095	1300	338.15	0.75	0.75	0.75	0.75	0.75	0.75
14	0.0095	1300	348.15	0.75	0.75	0.75	0.75	0.75	0.75
15	0.0095	1300	358.15	0.75	0.75	0.75	0.75	0.75	0.75
16	0.0095	900	338.15	0.75	0.75	0.75	0.75	0.75	0.75
17	0.0095	900	348.15	0.75	0.75	0.75	0.75	0.75	0.75
18	0.0095	900	358.15	0.75	0.75	0.75	0.75	0.75	0.75
19	0.0064	1700	338.15	0.75	0.75	0.75	0.75	0.75	0.75
20	0.0064	1700	348.15	0.75	0.75	0.75	0.75	0.75	0.75
21	0.0064	1700	358.15	0.75	1	1	0.75	1	1
22	0.0064	1300	338.15	0.75	0.75	0.75	0.75	0.75	0.75
23	0.0064	1300	348.15	0.75	0.75	0.75	0.75	0.75	0.75
24	0.0064	1300	358.15	0.75	1	1	1	1	0.75
25	0.0064	900	338.15	0.75	0.75	1	1	0.75	1
26	0.0064	900	348.15	0.75	1	0.75	0.75	0.75	0.75
27	0.0064	900	358.15	0.75	0.75	1	1	1	1

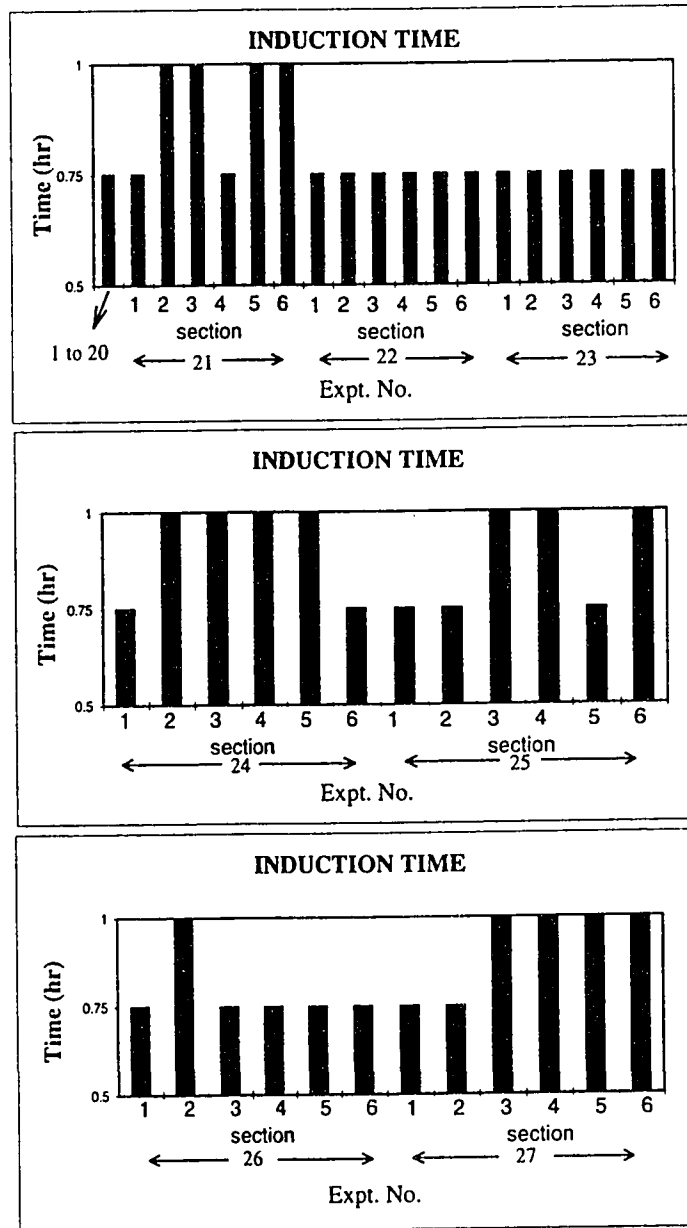


Figure 4.2: Induction time determined for the experimental study

diameters of 1/2 and 3/8 inch is 0.75 hour for all the six test sections irrespective of the values of other two parameters namely Reynolds number and tube surface temperature for the range studied in the experimental program. However, in 1/4 inch tube for few cases, the induction time noted was 1.0 hr but majority of the cases showed induction time of 0.75 hour. This difference of induction time was suspected to be due to the difference of surface roughness of 1/4 inch tube as compared to the other tubes. Surface roughness of the test sections was therefore measured using linear profiling system [73]. Two runs were made to determine the roughness and the results were averaged. The 1/2 and 3/8 inch test sections had a surface roughness of 100 microinch while the 1/4 inch diameter test section had a surface roughness of 60 microinch. The relatively smooth surface of the 1/4 inch test section delayed the initiation of scaling for a short period of time. This finding was inline with the observation made by Vatistas [2].

The above mentioned method of finding the induction time was compared with another approximate method of estimating the initiation time. In this method, it is assumed that the initial buildup of scale is linear with respect to time. A straight line joining first two data points, at two and four hours, is extended towards the x-axis and the x-intercept is determined. This intercept is infact the induction time of that particular test section. As an example, for the parameters of Experiment No. 16, if the line joining the first two data points in Fig. 4.1 is extended, it cuts the x-axis

at 1.2 hour. If this process is repeated for other test sections we obtain induction time for all the six test sections. The induction time, thus obtained, range between 0.9 to 1.25 hour for the six test sections as compared to 0.75 hour induction time calculated using the regression technique. Therefore the induction time calculated using this method can only be used as a first approximation of the actual induction time. Using this approximate technique, it was observed that the lines that were linearly extrapolated sometimes crossed each other and thus the induction time of the six test sections did not follow a particular trend with respect to the test section location. The results obtained are thus presented as a range of induction time as shown in Table 4.3.

In order to confirm the results obtained from the above regression technique, experiments were conducted to determine the onset time of scaling. Experiment was run for half hour and then the heat exchanger was dismantled to measure the mass gain in the test sections. No mass gain was observed. The test sections were then cleaned and the heat exchanger was assembled to start the experiment again. After one hour of running the experiment was stopped and mass gain in the test sections was noted to determine the fouling resistance in the test sections. Three such experiments were conducted for particular combinations of Re , D and T_s . It was observed that the results were within $\pm 6\%$ of that obtained through the regression procedure.

All the experiments discussed above were conducted for $CaCO_3$ solution con-

Table 4.3: Estimated range of induction time (obtained by linear extrapolation of first two data points)

EXPT NO.	Tube diameter	Re = VD/v	Tube surface temperature	Range of induction time for six test sections	
	m		K	from (hr)	to (hr)
1	0.0127	1700	338.15	0.75	1.1
2	0.0127	1700	348.15	0.75	1
3	0.0127	1700	358.15	0.7	1.25
4	0.0127	1300	338.15	0.75	1.05
5	0.0127	1300	358.15	1	1.2
6	0.0127	1300	348.15	0.9	1
7	0.0127	900	338.15	0.75	1.05
8	0.0127	900	348.15	0.9	1.05
9	0.0127	900	358.15	0.9	1.2
10	0.0095	1700	338.15	0.5	1.25
11	0.0095	1700	348.15	0.65	0.7
12	0.0095	1700	358.15	0.65	1.1
13	0.0095	1300	338.15	0.6	1.1
14	0.0095	1300	348.15	0.75	0.75
15	0.0095	1300	358.15	0.6	1.1
16	0.0095	900	338.15	0.9	1.25
17	0.0095	900	348.15	1.1	1.4
18	0.0095	900	358.15	0.8	1.2
19	0.0064	1700	338.15	1	1.4
20	0.0064	1700	348.15	0.6	0.75
21	0.0064	1700	358.15	0.9	1.1
22	0.0064	1300	338.15	0.95	1.2
23	0.0064	1300	348.15	0.8	1.1
24	0.0064	1300	358.15	1.05	1.25
25	0.0064	900	338.15	1.05	1.15
26	0.0064	900	348.15	0.75	1.15
27	0.0064	900	358.15	1.1	1.25

centration of 0.0006 moles/liter. In order to determine if the solution concentration plays any role in the induction time of the fouling, two experiments were conducted with different solution concentrations for a particular set of experimental parameters namely Re , T_s and D . The new concentration values for which the experiments were conducted were 0.0012 and 0.0003 moles/liter (experiment number 28 and 29 respectively). For the concentration of 0.0003 moles/liter, statistical results showed that the induction time of all the six test sections was determined to be 1.0 hour. The onset time for all six test sections was also calculated for the solution concentration of 0.0012 moles/liter and was found to be 0.25 hour. It was thus concluded that the solution concentration effects the onset time of the fouling. When the concentration increases initiation of fouling occurs rapidly as compared to lower solution concentration and the growth rate is expected to increase significantly with a higher concentration solution of $CaCO_3$. Chan et al. [30] based on their experimental study of silica fouling also concluded that the induction period is reduced with the increase in salt concentration in the solution.

4.2 Effect of thermal-hydraulic parameters on the growth rate of Fouling Resistance

The influence of Re , D and T_s on the growth rate of $CaCO_3$ scaling for some particular combinations of above mentioned parameters is discussed hereafter. As men-

tioned earlier the inner tube of the heat exchanger, subjected to fouling, was divided into six test sections which made it possible to study the variation of fouling resistance along the length of the heat exchanger. Two experiments were performed for new levels of $CaCO_3$ solution concentrations to study the effect of concentration on the growth rate of $CaCO_3$ scaling and is also mentioned hereunder.

4.2.1 Effect of Reynolds Number (Re)

Figure 4.3 illustrates the effect of Re on fouling resistance (R_f) versus time for test section number 5 of a 0.5 inch (0.0127 m) diameter tube maintained at a constant surface temperature of 338.15 K. It can be seen from the figure that the fouling resistance decreases with the increase of Re . This indicates that, perhaps due to increased shear stresses at increased fluid velocities, the rate of scale removal is higher than the rate of deposition. However, for the range of Re (900-1700), the effect on the scaling is not substantial. A similar observation was cited by Lee and Knudsen [33] based on their experimental study on asymptotic fouling resistance. They had observed that by varying the fluid velocities from 3 to 10 ft/sec (0.91 to 3.05 m/sec), there was no profound effect on the amount of $CaCO_3$ fouling resistance.

4.2.2 Effect of Tube Diameter (D)

The fouling resistance curves for three tube diameters are shown in Fig. 4.4. The curves shown are for test section number 6, $Re = 1700$ and the tube surface tem-

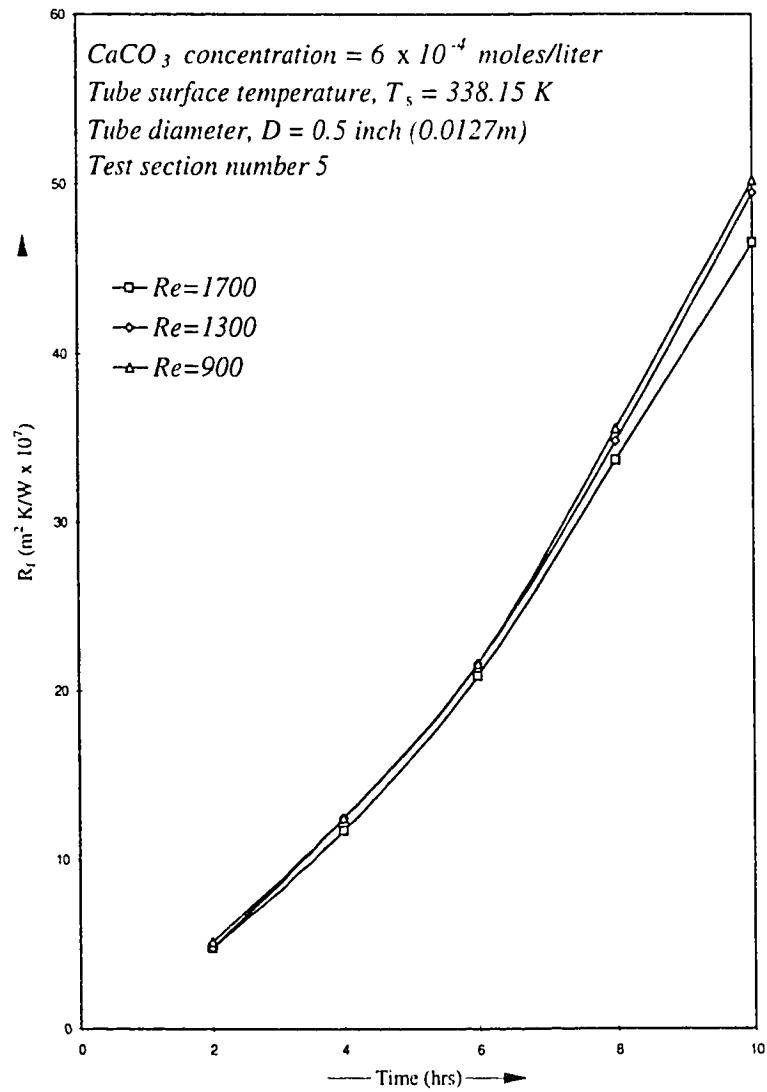


Figure 4.3: Effect of Reynolds No. on R_f

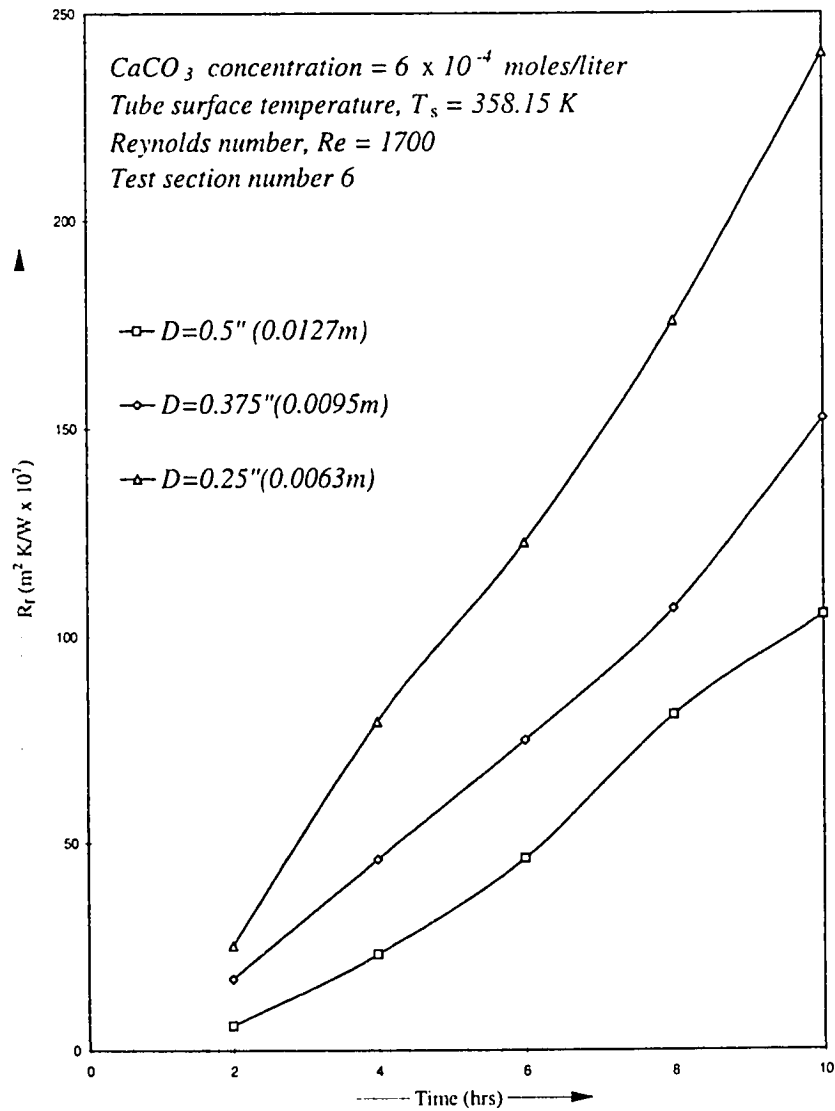


Figure 4.4: Effect of tube diameter on R_f

perature of 358.15 K. As is quite evident, from the figure, the tube diameter has a noticeable effect on the fouling resistance. Increase in diameter causes a decrease in the fouling resistance. This may be due to the reason that fouling is enhanced when a fluid with scaling characteristics is flowing in a tube of a relatively small diameter. The smaller cross sectional area is expected to provide more nucleation sites, as compared to a relatively flat surface, and results in an increase in the rate of fouling growth. It is worth mentioning that although Re is the same for all the three test section diameters, velocity of the fluid flowing in the smallest test section (0.25 inch) is the largest. Thus apparently this test section is thought to have the least fouling resistance. However it was observed that the 0.25 inch test section had more fouling resistance than the other test sections. This is due to the fact that the tube diameter effect is much more profound as compared to the effect of velocity on R_f . Thus the diameter effect dominates over the velocity effect and due to this reason the test section of 0.25 inch diameter has the maximum fouling resistance.

After two hours of running, tube diameter of 0.25 inch (0.00635 m) exhibits about 3 times more fouling resistance than that of the 0.5 inch (0.0127 m) tube. Similarly, after 10 hours, fouling resistance in the 0.25 inch (0.00635 m) tube is more than twice that of the 0.5 inch (0.0127 m) tube. Watkinson and Martinez [35] have observed similar trends for $CaCO_3$ asymptotic fouling resistance using copper tubes with various diameters ranging from 0.0053 to 0.02 m.

4.2.3 Effect of Tube Outer Surface Temperature (T_s)

Experiments were also conducted for three tube surface temperatures and the sample results are shown in Fig. 4.5 which demonstrates the effect of surface temperature on R_f . The curves shown are of section number 6 of the 0.5 inch (0.0127 m) diameter for $Re = 1700$. As explained earlier, $CaCO_3$ salts have inverse solubility characteristics i.e., the fouling resistance increases with an increase in temperature. The figure shows that as time passes the effect of temperature becomes more pronounced. However, at two hours, the effect of temperature variation is less significant. After 10 hours of running, R_f of tube at 358.15 K is more than twice that of the same tube maintained at 338.15 K. Similar results are obtained by Watkinson and Martinez [34] for the asymptotic fouling resistance in the same temperature range as considered in our study (i.e., 338.15 to 358.15 K). Also data obtained from experiments conducted by Parry et al. [74] show similar trends of increasing fouling resistance with temperature.

4.2.4 Effect of Tube Length

It was observed that the fouling resistance increased along the test sections of the heat exchanger. Since the fluid was being heated as it passed through the heat exchanger thus the increase in deposits was expected. Although the deposits increased along the length, for different experiments the increase in growth of these deposits

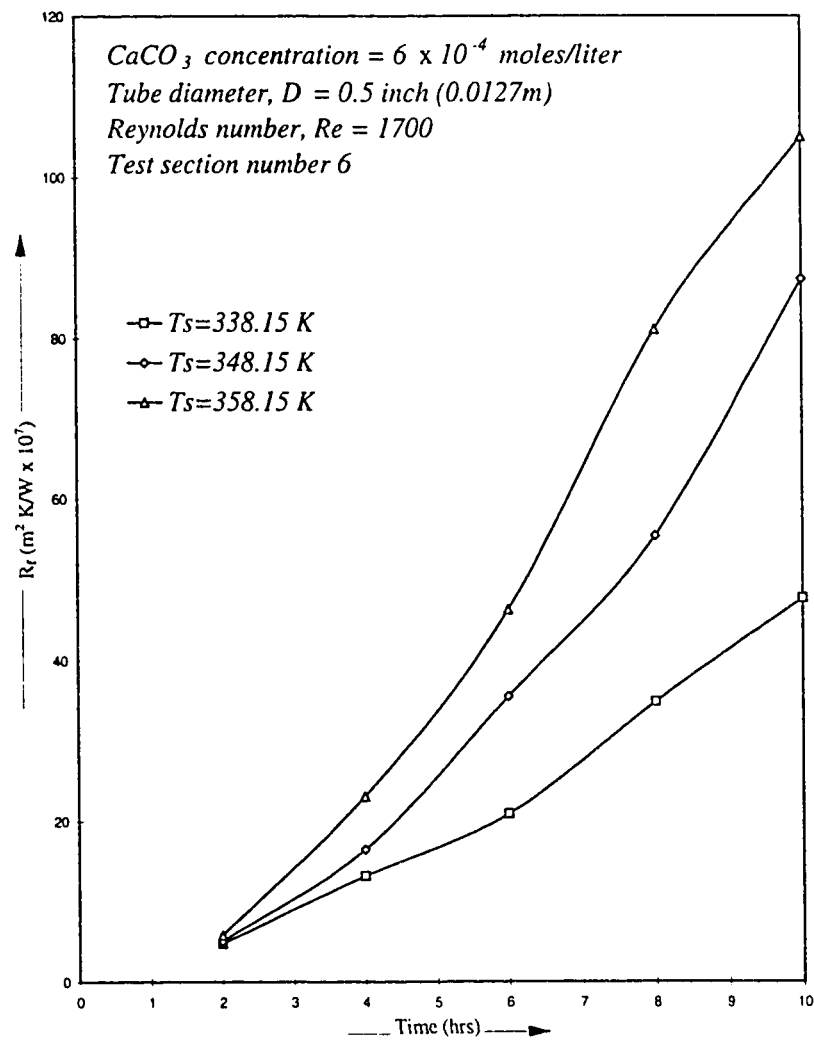


Figure 4.5: Effect of tube surface temperature on R_f

was somewhat random and did not follow a particular trend. A typical variation of the fouling resistance along the six test sections is shown in Fig. 4.6. The resistance shown is for tube diameter of 0.0127 m at surface temperature of 338.15 K for Reynolds number of 1300 after 10 hours of running. Experiments conducted by Manzoor [36] showed that the fouling resistance decreases with the length of the heat exchanger. This might be due to the fact that the fluid was being cooled as it passed through the heat exchanger. Similarly Chan et al. [30] also concluded that when the brine solution was being cooled in a double pipe heat exchanger, fouling resistance decreased along the length of the heat exchanger. In the present study, since the salt solution was being heated as it passed through the inner tube of the heat exchanger therefore increase in fouling resistance along the length was expected.

4.2.5 Effect of $CaCO_3$ concentration

Two experiments were conducted with new $CaCO_3$ solution concentrations for keeping Re , T_s and D fixed. The fouling resistance was found to be increasing with increase in the concentration. The effect of $CaCO_3$ concentration for section number 6 of the 0.0127m diameter tube is shown in Fig. 4.7. The tube diameter was 0.5 inch (0.0127m) at surface temperature of 348.15 K and the Reynolds number was fixed at 900. It can be observed that the fouling resistance doubles with doubling the concentration. The fouling resistance after two hours of running with concentration

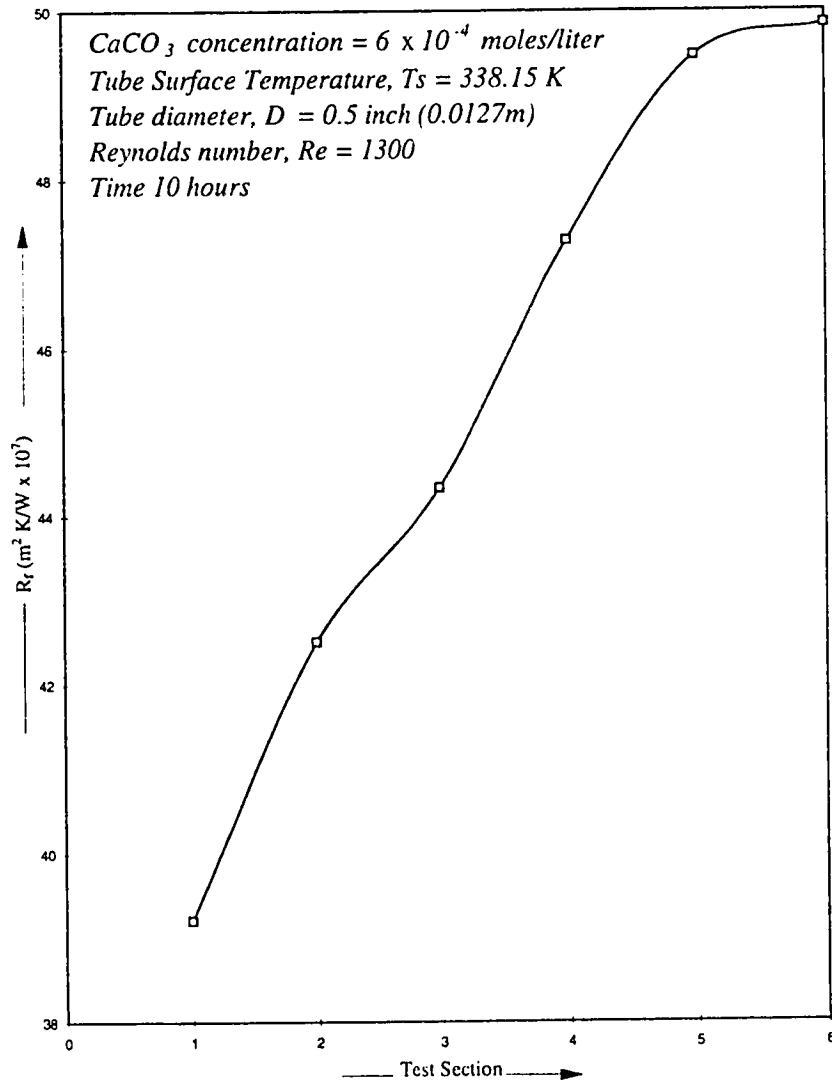


Figure 4.6: Variation of R_f along the test sections

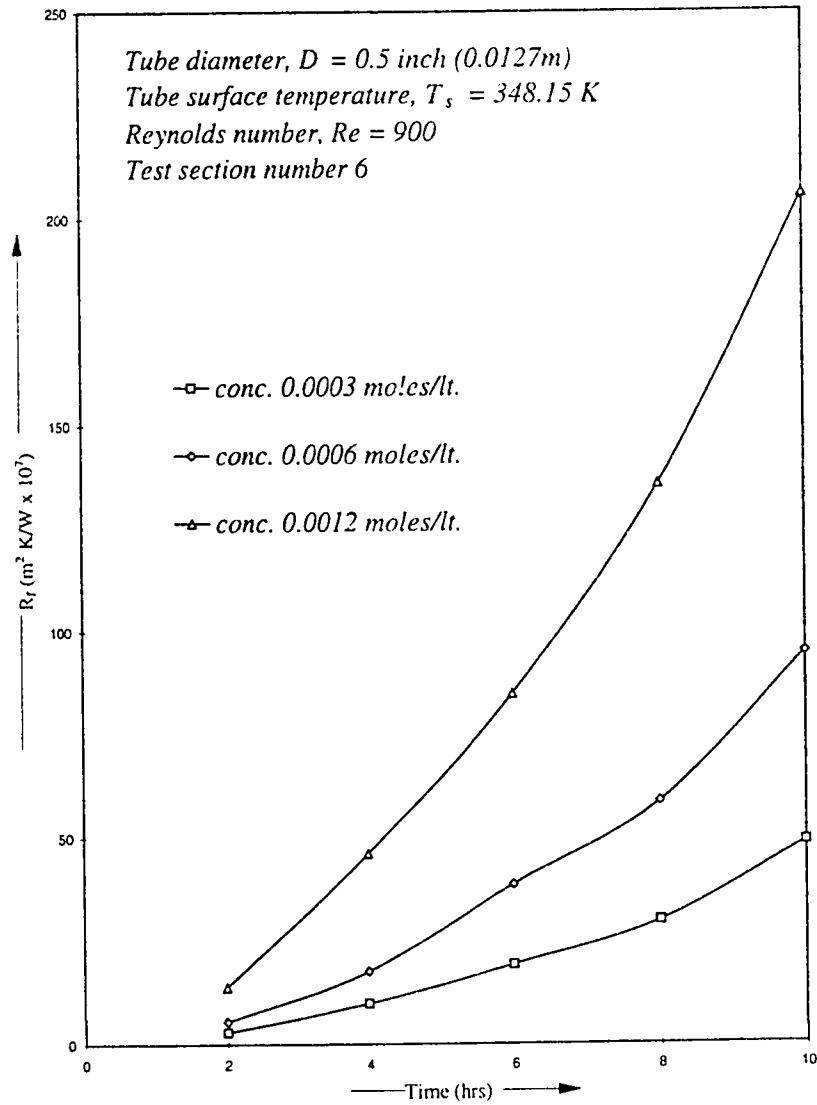


Figure 4.7: Effect of $CaCO_3$ concentration on R_f

of 0.0012 moles/liter is almost four times that of the solution with concentration of 0.0003 moles/liter. This trend follows throughout the experiment for all the five test runs. Coates and Knudsen [34] also observed that the calcium content has a significant effect on the scaling characteristics and reported that an increase in the content increased the fouling resistance quite profoundly.

4.3 Fouling Resistance Models

Dimensionless fouling resistance models for six test sections for R_f as a function of time, Reynolds number, tube diameter and tube surface temperature have been developed based on the data collected from experiments. “Microsoft Excel” was used for the development of regression models. The form of models for all the test sections are the same and is presented hereunder:

$$R_f^* = A [t^*]^B, \quad (4.1)$$

where

$$\begin{aligned} A = & a_0 + a_1(Re^*) + a_2(D^*) + a_3(T^*) + a_4(Re^*T^*) \\ & + a_5(D^*T^*) + a_6(D^{*2}) + a_7(T^{*2}) + a_8(T^*Re^{*2}) \end{aligned} \quad (4.2)$$

and

$$B = b_0 + b_1(Re^*) + b_2(D^*) + b_3(T^*) + b_4(Re^*D^*) + b_5(Re^*T^*) + b_6(D^*T^*)$$

$$+b_7(D^{*2}) + b_8(T^{*2}) + b_9(D^{*2}R\epsilon^*) + b_{10}(D^{*2}T^*) + b_{11}(T^{*2}D^*). \quad (4.3)$$

The coefficients of the parameters in the equations of A and B for the models developed for the six test sections are shown in Table 4.4.

Test	Coefficients								
Sect.	a ₀	a ₁	a ₂	a ₃	a ₄	a ₅	a ₆	a ₇	a ₈
1	-12.90	-0.018	11.811	15.097	-0.144	-14.83	-1.494	2.754	0.043
2	-9.556	0.203	-0.386	11.752	-0.371	-2.344	-7.298	-6.276	0.024
3	-10.21	-0.542	2.138	12.515	0.306	-5.173	5.975	-4.759	0.087
4	-13.024	-1.417	11.282	15.529	1.109	-14.87	-0.200	1.809	0.176
5	-9.793	-1.265	1.705	12.173	0.988	-4.949	5.793	-4.391	0.153
6	-8.535	-1.041	-1.134	10.889	0.817	-2.084	6.873	-5.455	0.107

Test	Coefficients											
Sect.	b ₀	b ₁	b ₂	b ₃	b ₄	b ₅	b ₆	b ₇	b ₈	b ₉	b ₁₀	b ₁₁
1	984.360	1.140	-1204	-2049	-1.407	0.395	2579.5	-80.98	1064.9	1.509	80.702	-1357.8
2	331.869	-2.580	-223.2	-703.6	-0.131	2.330	560.59	-77.04	373.52	-0.277	77.867	-337.63
3	564.722	-4.528	-674.5	-1188	-2.167	7.003	1500.0	-84.92	623.39	2.597	85.948	-828.11
4	645.693	-5.092	-803.6	-1362	-1.419	6.749	1782.9	-92.90	717.23	1.670	94.655	-982.334
5	602.829	-2.600	-772.0	-1270	-1.531	4.348	1701.4	-83.17	668.33	1.717	84.979	-932.478
6	464.531	-1.269	-628.7	-983.4	-0.810	2.183	1402.4	-82.13	520.65	0.918	84.745	-777.443

Table 4.4: Coefficients of A and B of the R_f models

It was observed from the data, for the range of parameters studied, values of A vary between 0.14 and 1.04, while B varies between 1.27 and 1.99. As the tube surface temperature increased it resulted in an increase in the value of A. But value of A was reduced when Reynolds number and tube diameter were increased. Similarly variation in B was found to be inversely proportional to the Reynolds number and tube diameter. The effect of tube surface temperature on B was found to be somewhat random. Notice that the parameters in the above model have been non-dimensionalized using the maximum parametric values, mentioned in the nomenclature, for which the experiments have been performed. This has resulted in models of quite high coefficients of determination (R^2) ranging from 0.983 to 0.996. For general representation of fouling resistance in the inner tube of the heat exchanger average values of the six test sections were calculated and based on these data a dimensionless regression model was developed for the fouling resistance. The model was same as mentioned in equation 4.1 with values of A and B as follows

$$A = -10.908 - 0.733(Re^*) + 4.503(D^*) + 13.207(T^*) + 0.505(Re^*T^*) - 7.712(D^*T^*) + 3.993(D^{*2}) - 2.639(T^*D^{*2}) + 0.098(T^*Re^{*2}) \quad (4.4)$$

and

$$B = 669.920 - 2.164(Re^*) - 843.840(D^*) - 1405.180(T^*) - 5.553(Re^*D^*) + 4.044(Re^*T^*) + 1854.330(D^*T^*) - 84.440(D^{*2}) + 736.390(T^{*2})$$

$$+3.880(D^{*2}Re^*) + 83.720(D^{*2}T^*) - 1008.990(T^{*2}D^*). \quad (4.5)$$

4.3.1 Model Adequacy

It should be mentioned that evaluating model adequacy is an important part of any model building problem. Montgomery and Peck [75] have discussed several applicable methods. Residual analysis was adopted for this study. The model is used to predict the fouling resistance and then residuals are calculated (i.e., the difference between observed and predicted values of R_f). Figures 4.8 to 4.14 show the observed versus the predicted values of the fouling resistance whereas normal probability plots of the residuals are shown in Figs. 4.15 to 4.21. Small departures from the normality (i.e., straight line) are statistically acceptable. No obvious model inadequacies are observed from these plots. It is also important to examine plots of residuals versus the predicted values of fouling resistance [75], to detect common patterns such as horizontal bands, double bows and curved bands.

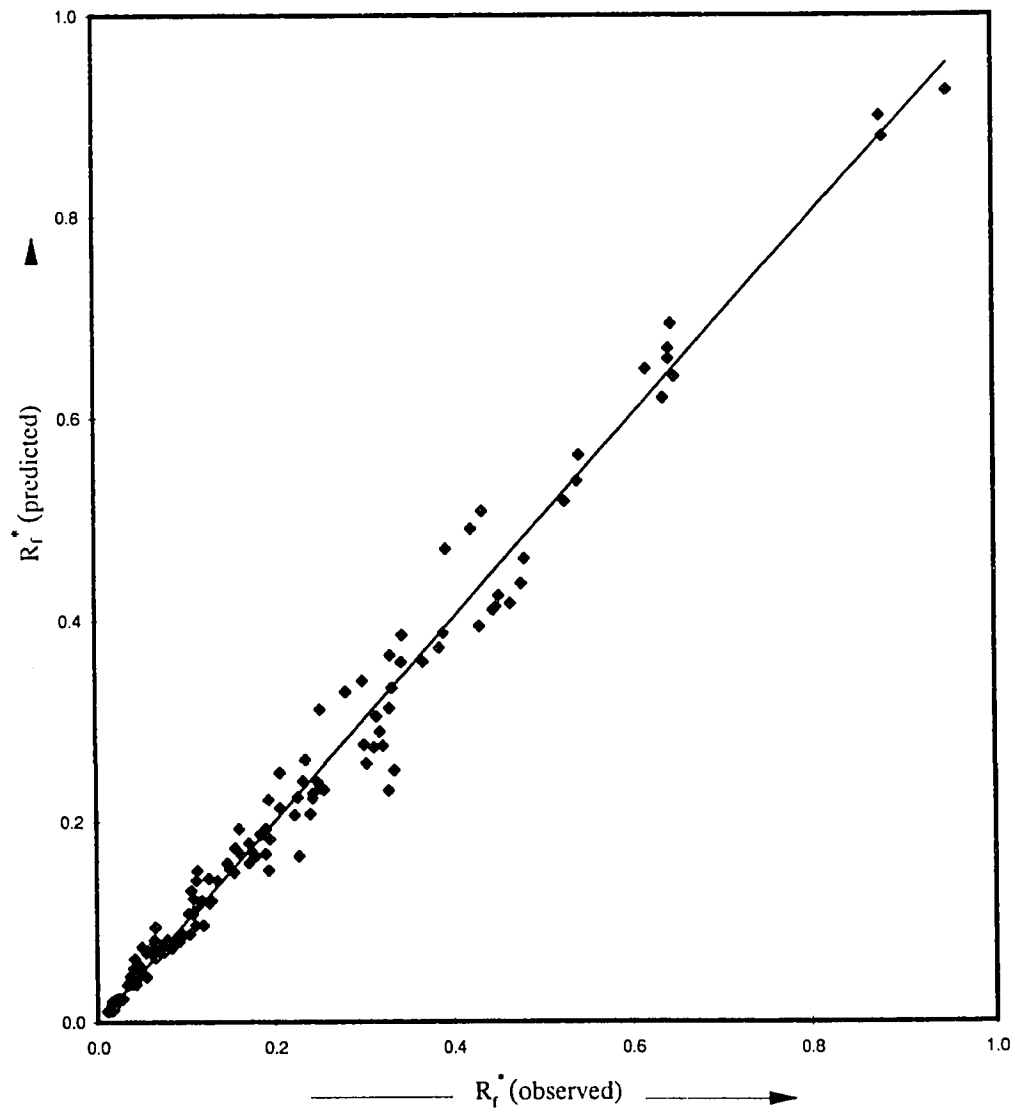


Figure 4.8: Observed R_f versus predicted R_f for model of test section 1

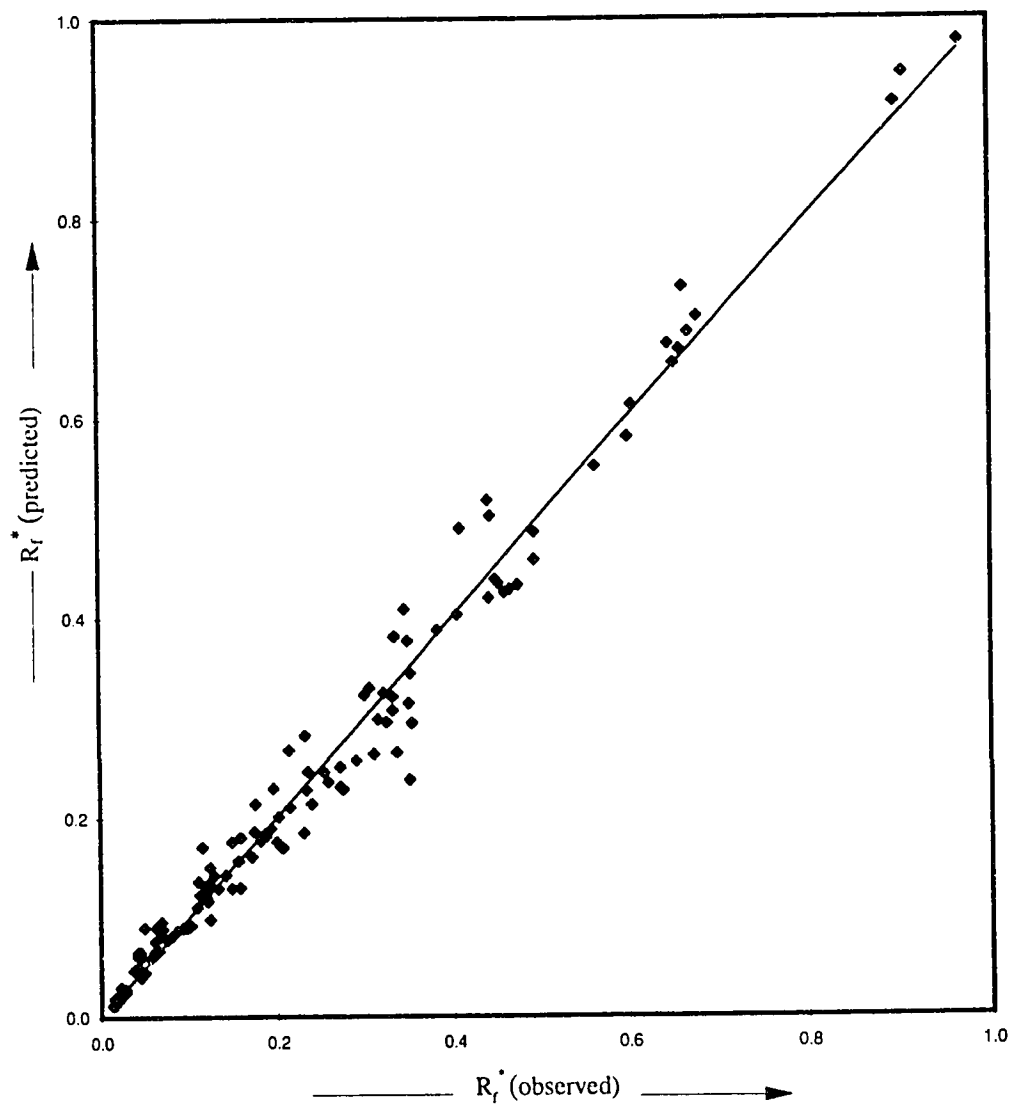


Figure 4.9: Observed R_f versus predicted R_f for model of test section 2

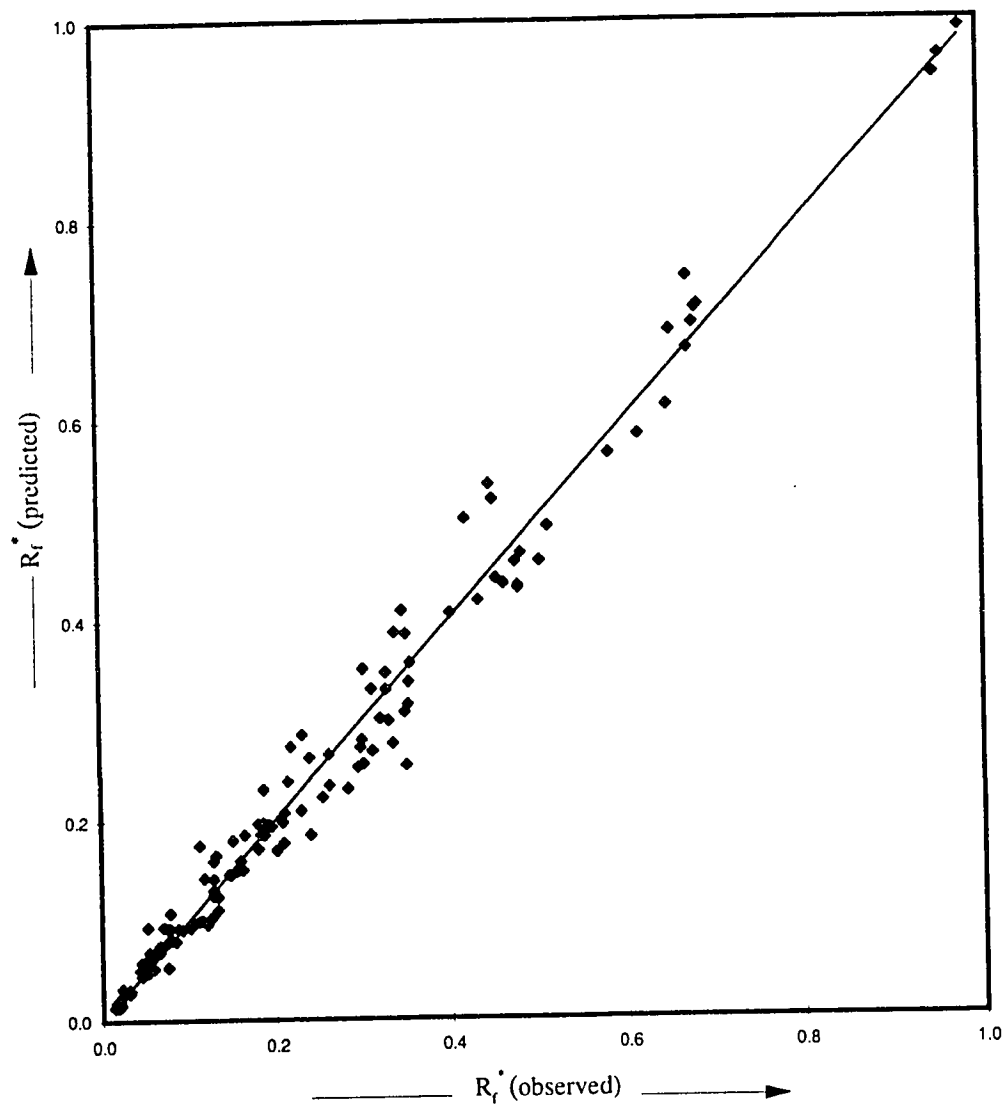


Figure 4.10: Observed R_f versus predicted R_f for model of test section 3

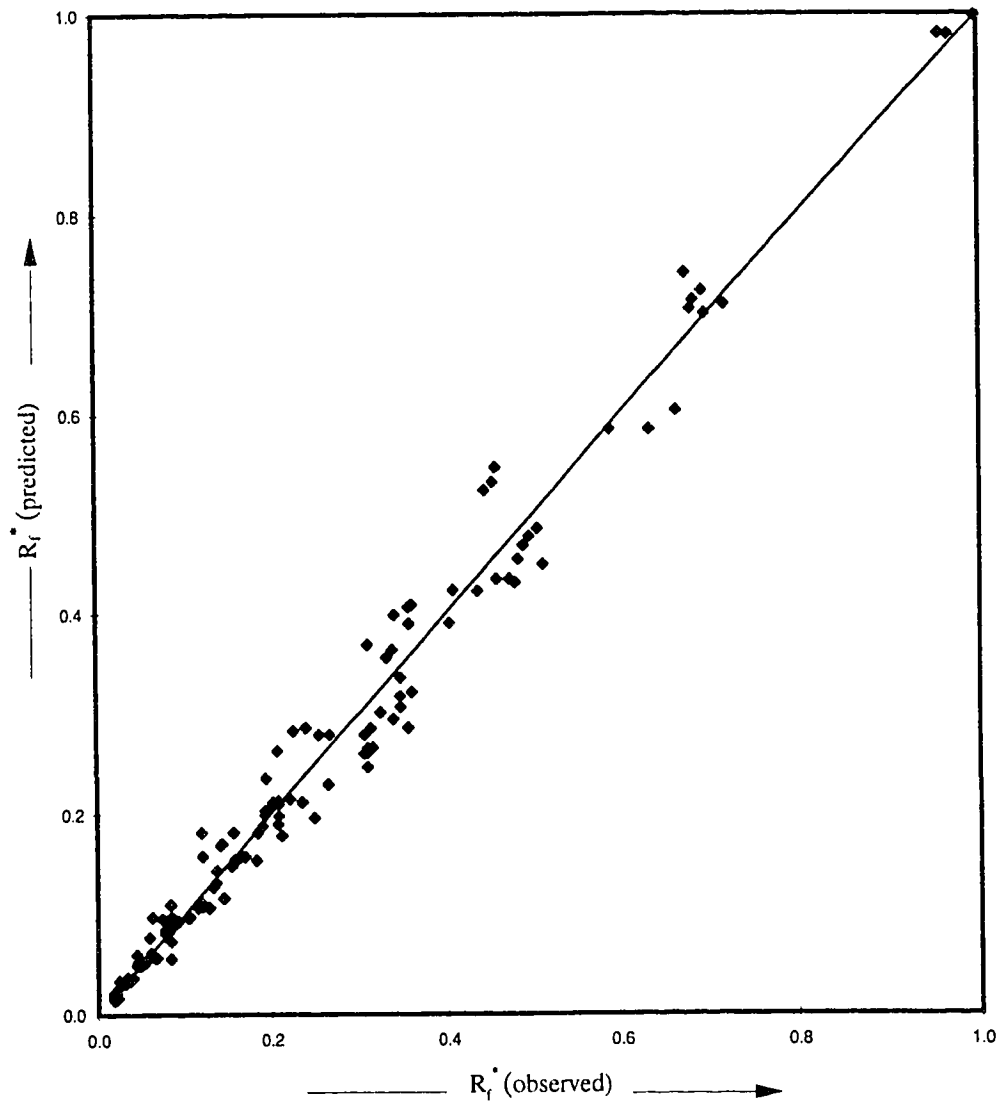


Figure 4.11: Observed R_f versus predicted R_f for model of test section 4

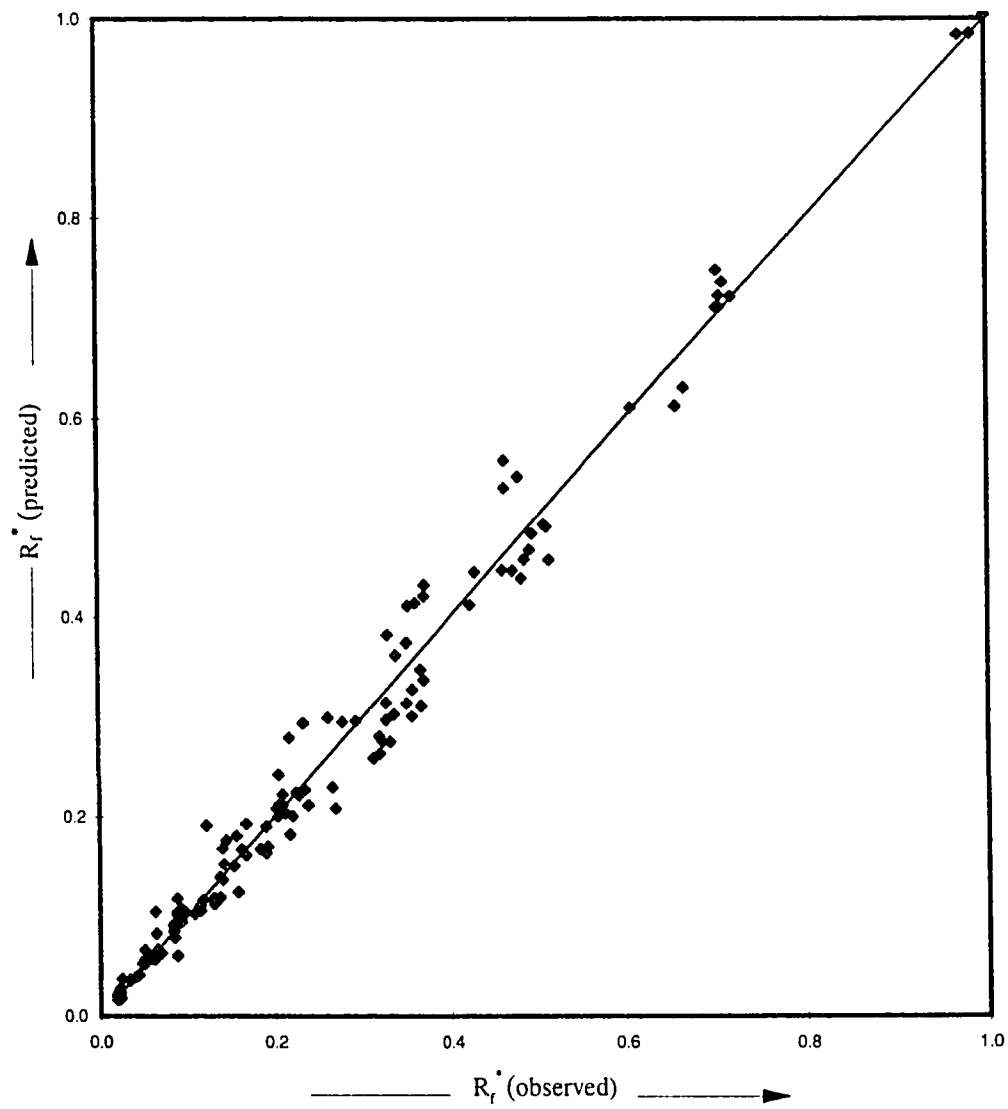


Figure 4.12: Observed R_f versus predicted R_f for model of test section 5

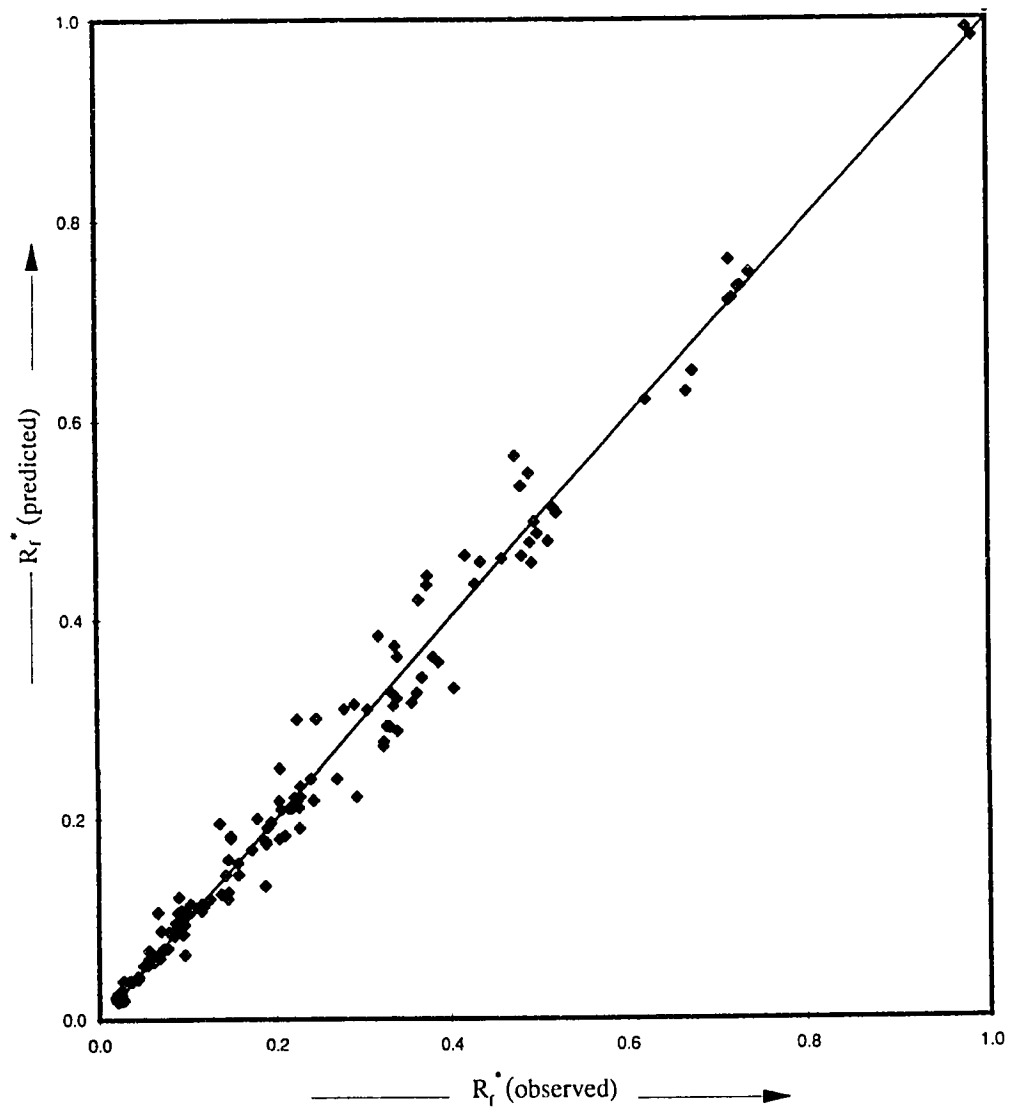


Figure 4.13: Observed R_f versus predicted R_f for model of test section 6

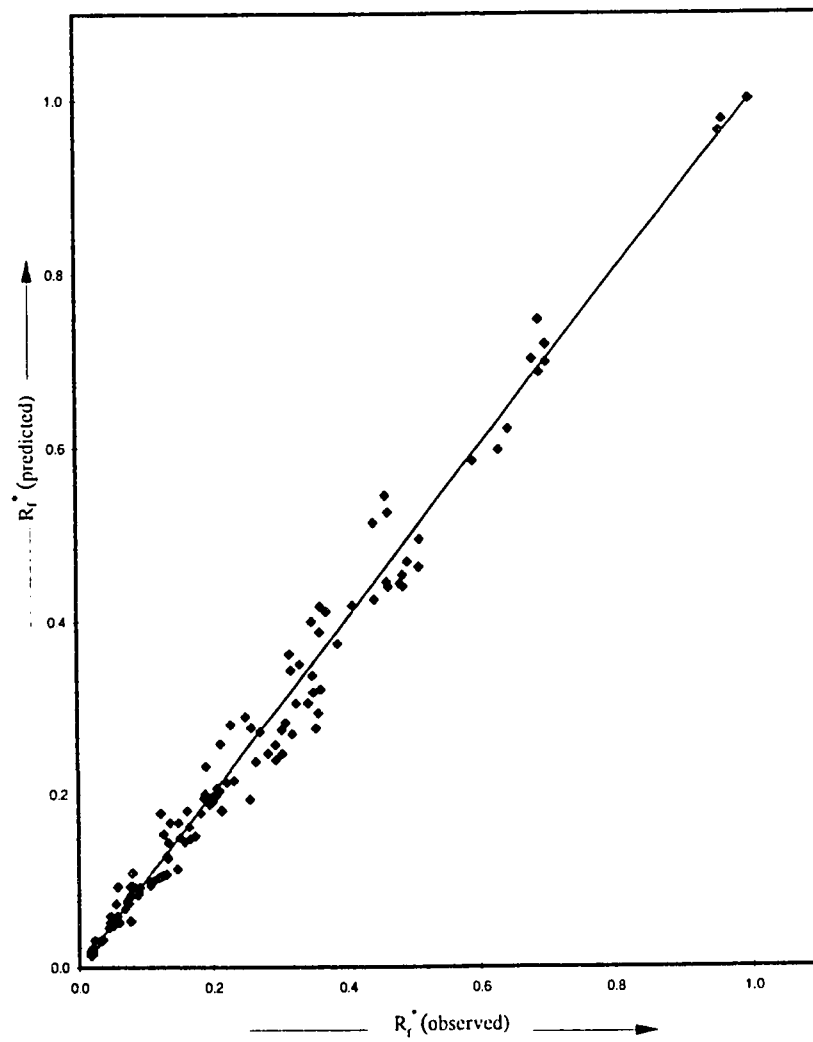


Figure 4.14: Observed R_f versus predicted R_f for average R_f model

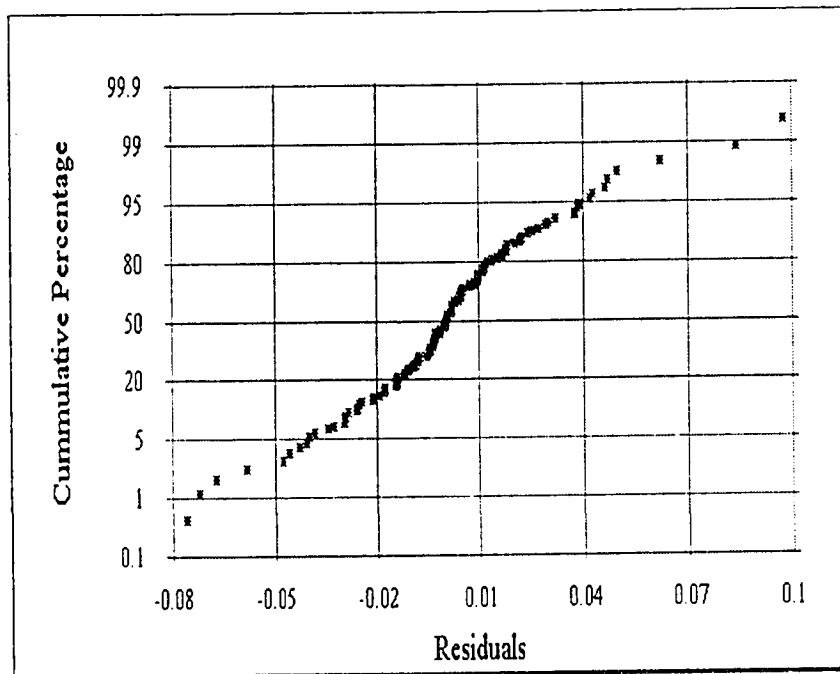


Figure 4.15: Normal probability plot for model of test section 1

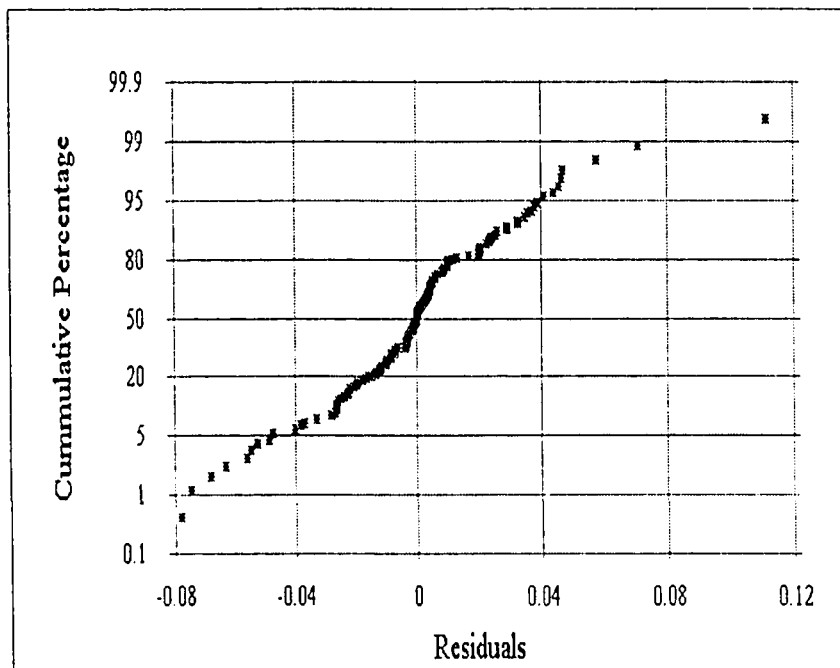


Figure 4.16: Normal probability plot for model of test section 2

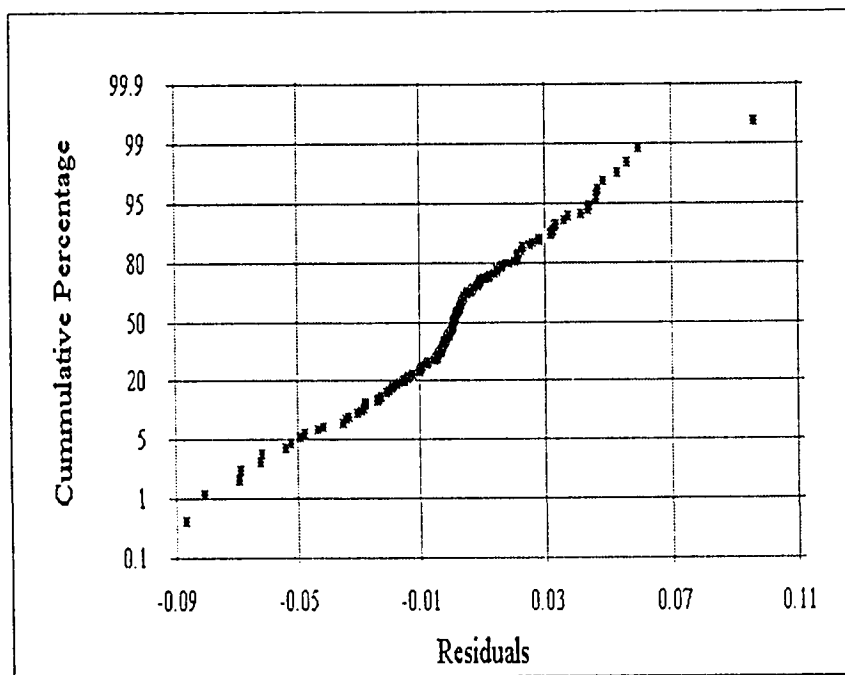


Figure 4.17: Normal probability plot for model of test section 3

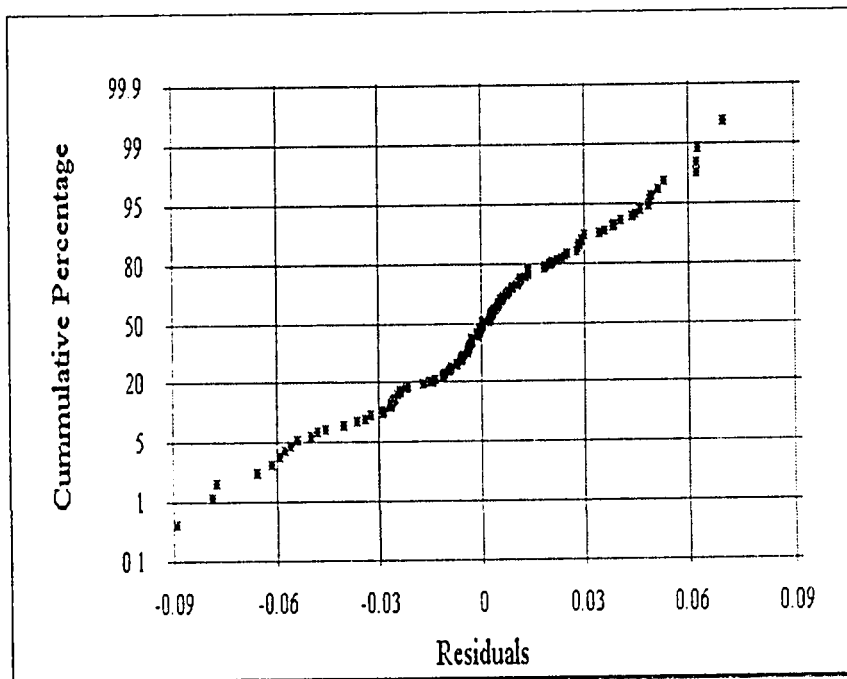


Figure 4.18: Normal probability plot for model of test section 4

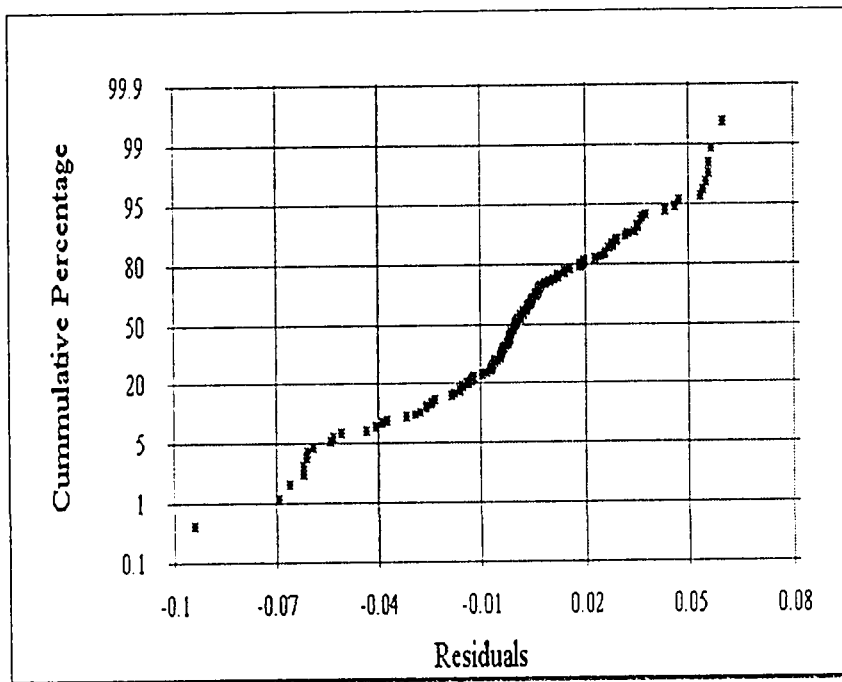


Figure 4.19: Normal probability plot for model of test section 5

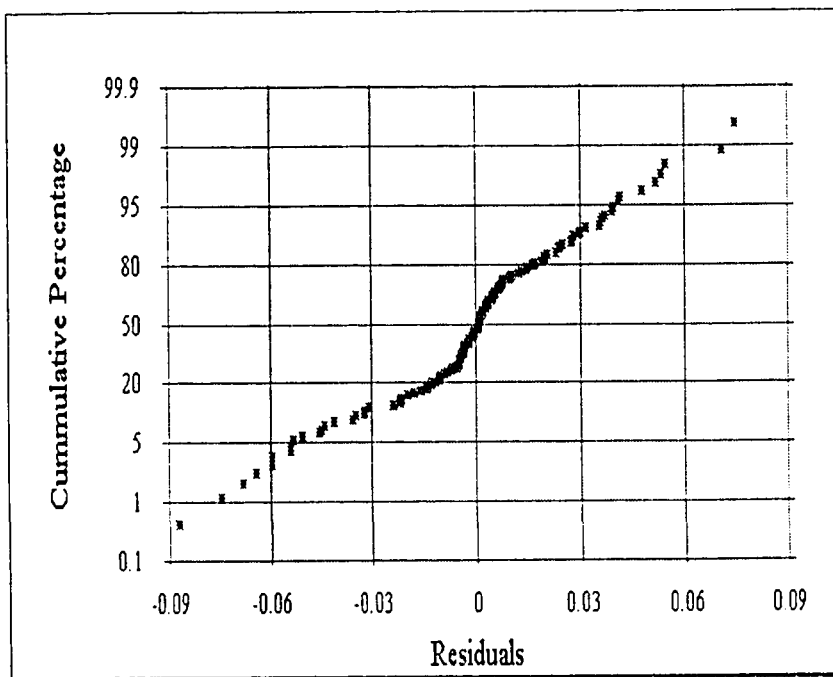


Figure 4.20: Normal probability plot for model of test section Q

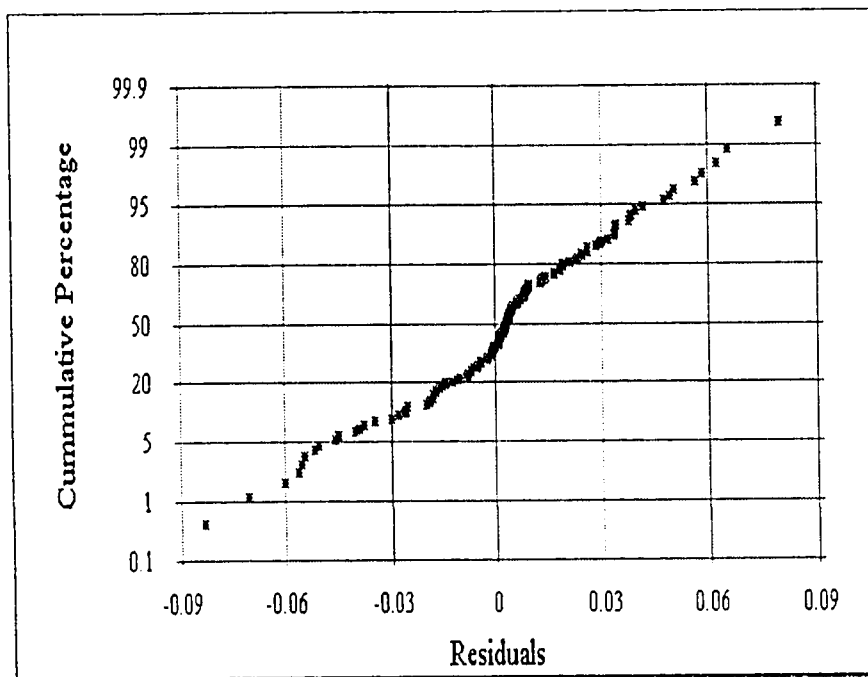


Figure 4.21: Normal probability plot for model of average R_f

Figures 4.22 to 4.28 show plots between the predicted values of R_f and residuals which indicate no apparent defects in the developed model. The fouling resistance models thus developed are quite suitable to predict R_f , within the range of experimental parameters shown in Table 3.1, for the six test sections and for calculating average fouling resistance.

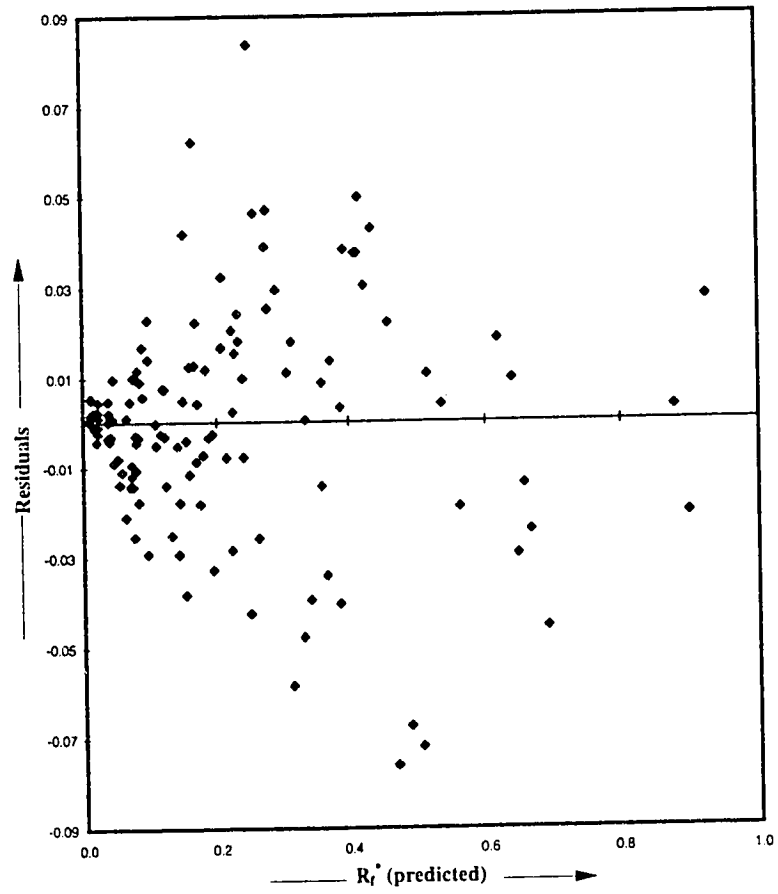


Figure 4.22: Predicted fouling resistance versus residuals for model of section 1

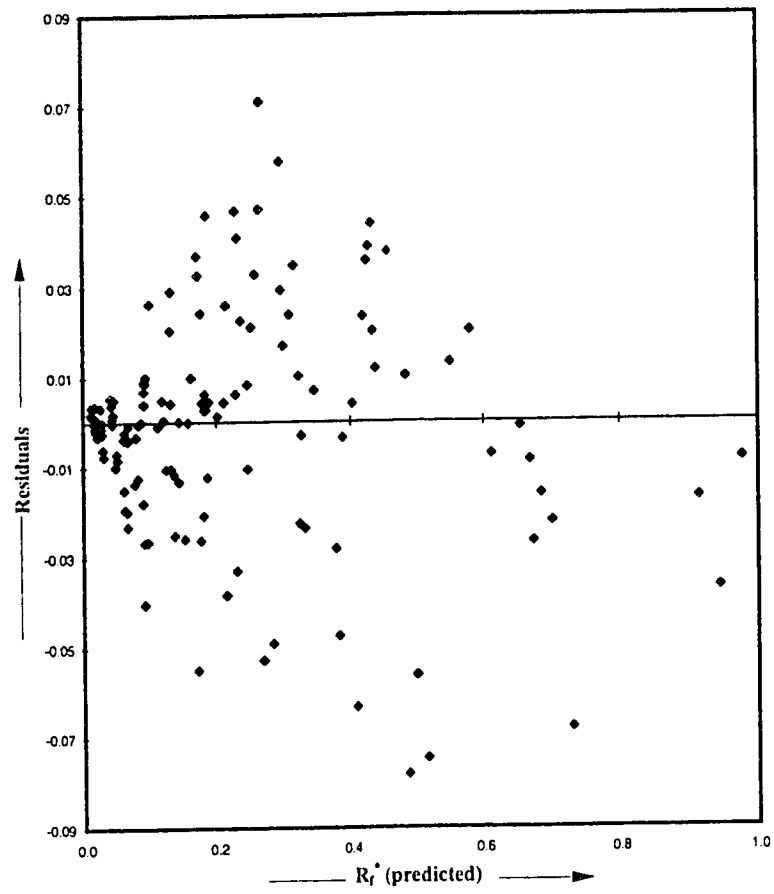


Figure 4.23: Predicted fouling resistance versus residuals for model of section 2

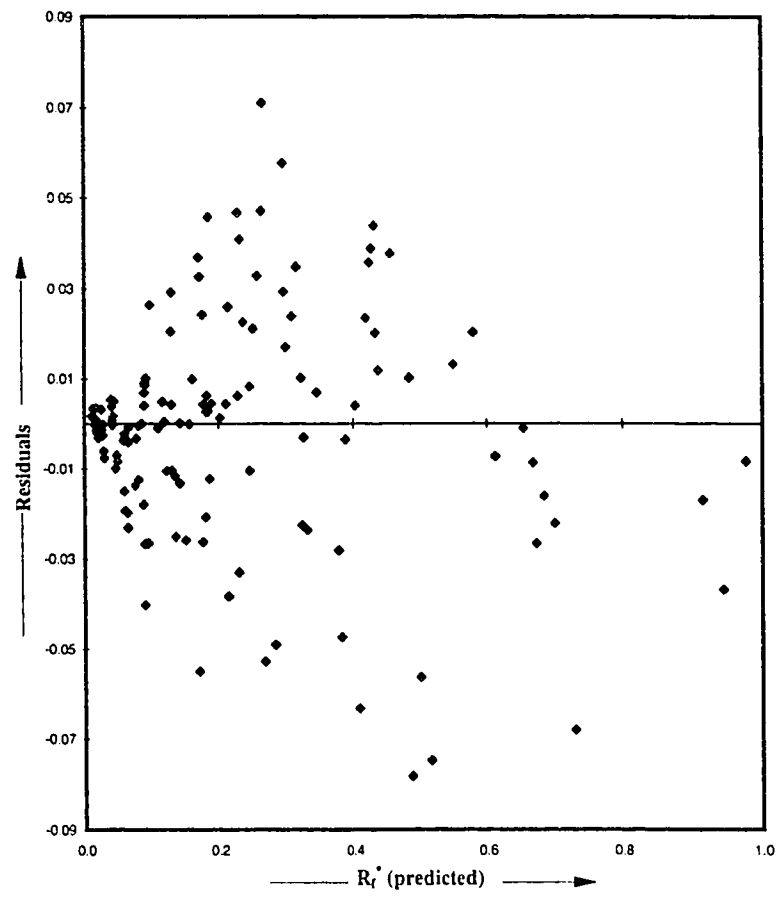


Figure 4.24: Predicted fouling resistance versus residuals for model of section 3

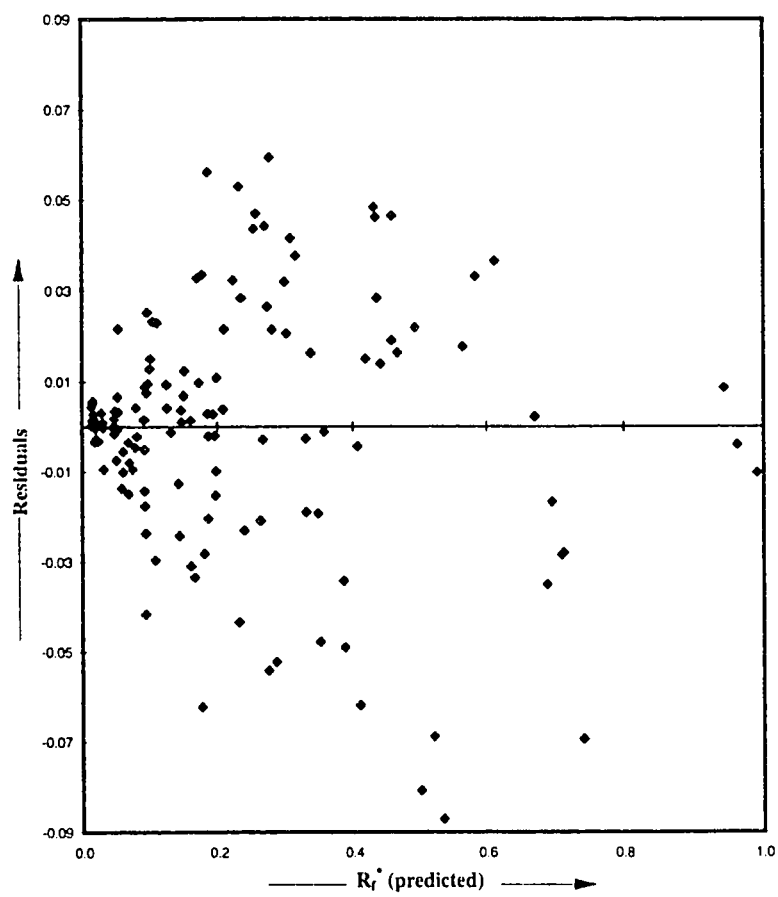


Figure 4.25: Predicted fouling resistance versus residuals for model of section 4

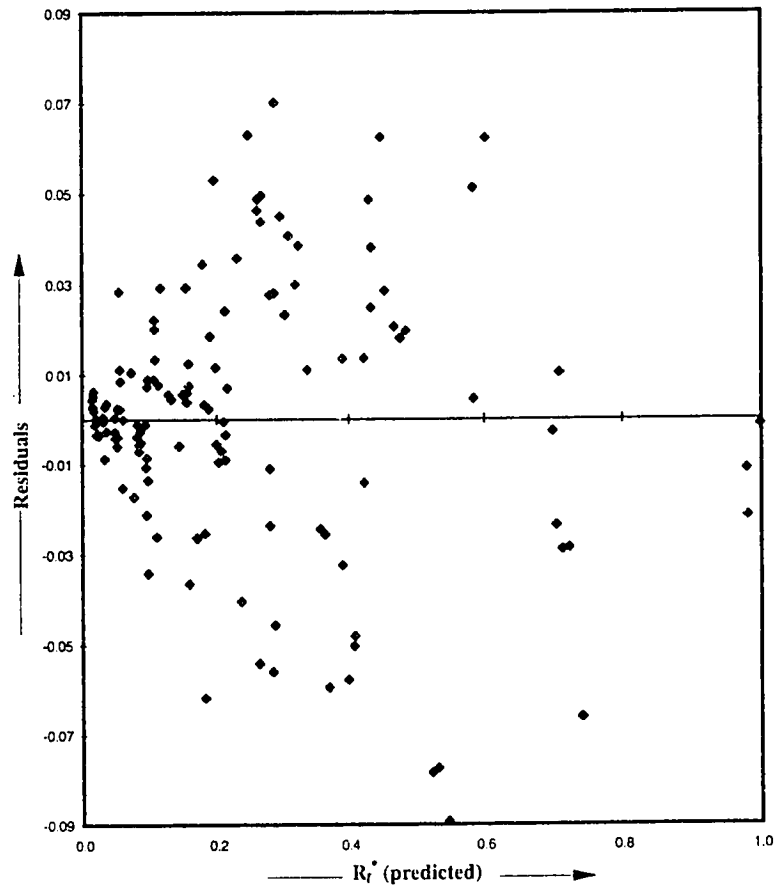


Figure 4.26: Predicted fouling resistance versus residuals for model of section 5

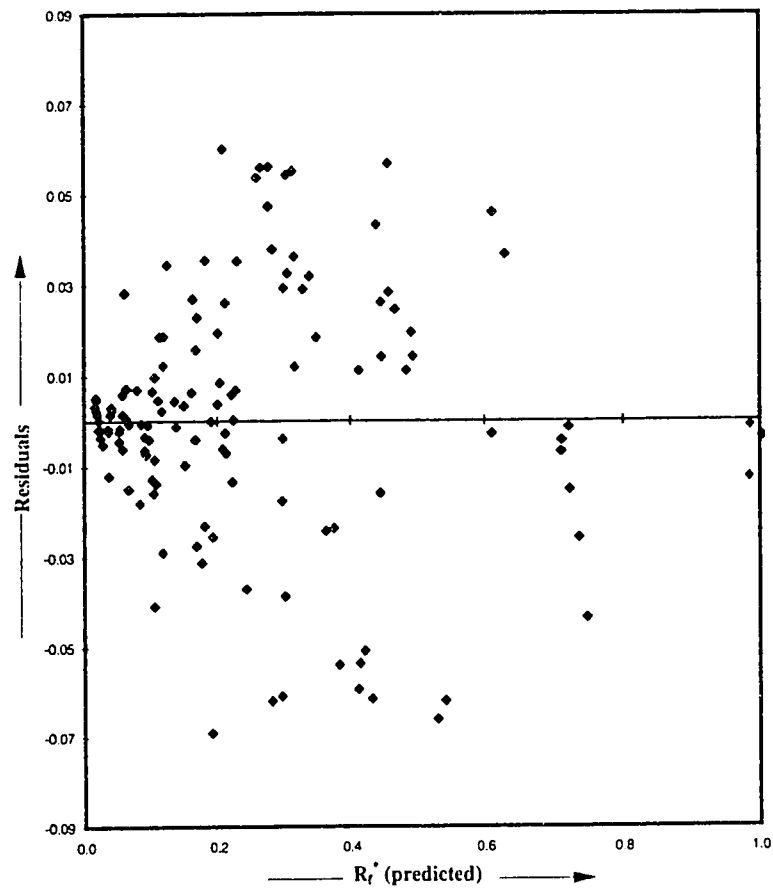


Figure 4.27: Predicted fouling resistance versus residuals for model of section 6

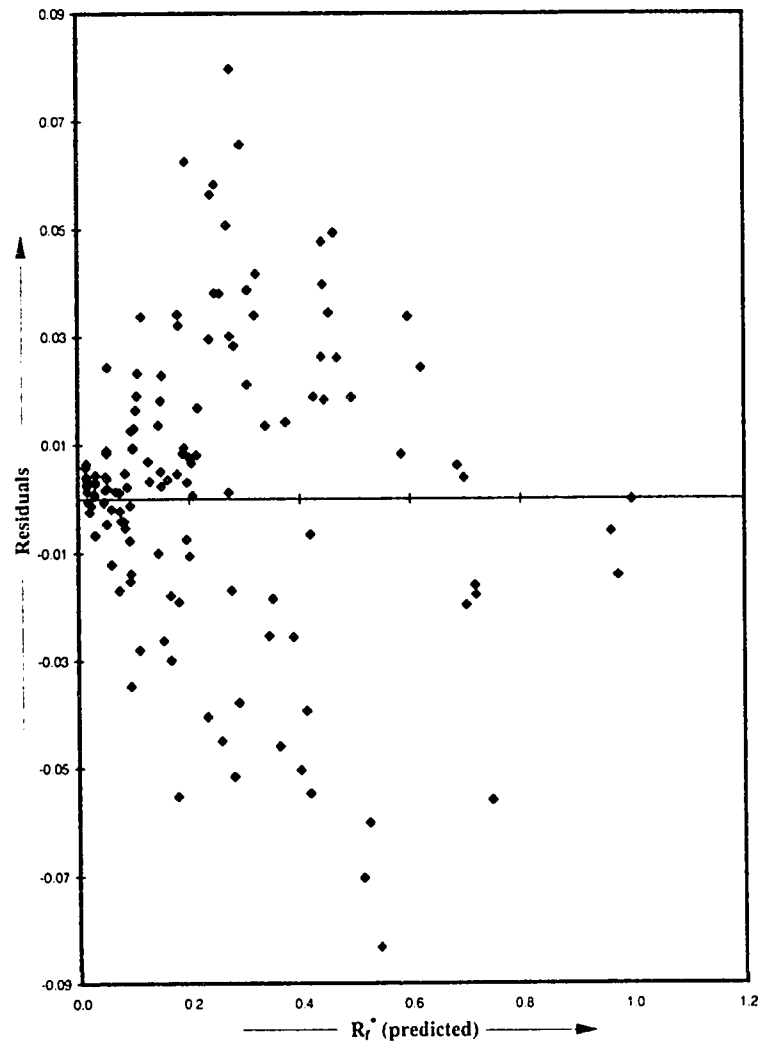


Figure 4.28: Predicted fouling resistance versus residuals for model of average R_f

4.4 Application

The research carried out can be useful for the design and operation stages of the heat exchangers. The experimental study and data analysis resulted in determining the influence of Reynolds number, tube diameter, tube surface temperature, scaling salt concentration and heat exchanger length on the fouling resistance. The effect of tube diameter on the fouling resistance will be helpful during the design stage of the heat exchangers. Depending upon the application, if the design has a provision to use two different tube diameters then in order to reduce the growth rate of fouling, using larger diameter seems appropriate. During the operation of the heat exchanger the results of Reynolds number effect and tube surface temperature effect on the fouling resistance can be utilized. The effect of tube length on the fouling resistance can be applied for analysis purpose to study the variation of R_f along the length of the heat exchanger.

The heat exchanger has to be cleaned when the fouling resistance reaches a critical value beyond which the efficiency of the heat exchanger drops below the required value. Using the fouling resistance models, the time taken to reach the critical value of fouling resistance can be determined and cleaning schedules of the heat exchangers can be developed. Such fouling resistance models can be used to predict fouling resistance in the tube for some specified values of parameters within

the range of investigated parameters.

Chapter 5

Concluding Remarks

An experimental investigation was carried out aimed at evaluating the effects of Reynolds number, tube diameter, tube outer surface temperature and solution concentration on the $CaCO_3$ scaling in a double-pipe heat exchangers. The objective of the study was to determine the influence of above mentioned thermal-hydraulic parameters on the onset time and growth rate of $CaCO_3$ scaling. Furthermore, dimensionless models have been developed to estimate fouling resistance in the heat exchangers after a given period of operation for some specified values of Re, D and T_s . The conclusions are enumerated hereunder.

- (1) It was observed that Reynolds number, tube diameter and tube outer surface temperature have no effect on the onset time of deposition. However, these parameters play a vital role in the later growth of the scaling. The data were statistically analysed and induction time was calculated by a simple regres-

sion technique. The results were then confirmed by actual experimentation. Experiments were then conducted to determine the effect of $CaCO_3$ concentration on the onset time of scaling. It was observed that the induction time was reduced when the concentration was increased.

- (2) The fouling resistance data of $CaCO_3$ scaling was presented to study the influence of tube surface temperature, Reynolds number and tube diameter. It was observed that the influence of Reynolds number in the range investigated ($Re = 900-1700$) is almost negligible. However, the influence of tube outer surface temperature and tube diameter on the fouling growth is found to be appreciable for the range investigated. The reason for the variation of fouling resistance as a function of surface temperature and tube diameter is explained by considering the inverse solubility characteristics of $CaCO_3$ and tube surface effects. In addition to the above mentioned parameters, effect of $CaCO_3$ concentration in the solution on the growth rate of scaling has also been studied. It was concluded that when the solution concentration is doubled we get twice the fouling resistance. The variance of fouling resistance with the length of the heat exchanger was also studied and compared with the results of previous investigators.
- (3) The data obtained from experiments are presented in the form of six dimensionless fouling resistance models each representing a test section of the inner

tube of the heat exchanger for estimation and prediction purpose. A model to predict the average fouling resistance has also been presented. In this regard, all the variables in the model are non-dimensionalized with respect to the respective maximum values considered in this study. The models thus developed have been investigated in somewhat more detail by observing the normal probability plot of residuals. In addition, several other statistical checks are also made to assess the suitability of the models. No apparent model defects are noticed. It is thus concluded that the fouling resistance models may be considered as reliable models within the range of experimental parameters investigated in the present study.

5.1 Recommendations for Future Research

Fouling related research has vast prospects and this area needs a lot of attention considering the impact of fouling. Effects of surface characteristics and salt concentration on the fouling resistance of some combination of inverse solubility characteristics salts can be studied. The heat exchanger should be tested in the turbulent regime to gather experimental data for asymptotic fouling resistance. The study can be carried out for a shell and tube heat exchanger in which sophisticated fouling measuring devices should be used so that online data acquisition system can be employed instead of using mass gain technique to measure the fouling resistance.

Bibliography

- [1] T. R. Bott, editor. *Fouling of Heat Exchangers*. Elsevier, Netherlands, 1995.
- [2] E. F. Melo, T. R. Bott, and C. A. Bernardo. *Fouling Science and Technology - NATO ASI Series*. Kluwer Academic Publishers, Washington D.C., 1987.
- [3] E.F.C. Somerscales. Fouling of heat transfer surfaces: An historical review. *Heat Transfer Engineering*, 11(1):19-36, 1990.
- [4] Gilmour C.H. No fooling-no fouling. *Chemical Engineering Progress*, 61(7):1 - 12, 1965.
- [5] J. Taborek, T. Aoki, R.B. Ritter, J.W. Palen, and J.G. Knudsen. Fouling: The major unresolved problem in heat transfer. *Chemical Engineering Progress*, 68(2):59-67, 1972.
- [6] V. Ganapathy. Fouling-the silent heat transfer thief. *Hydrocarbon processing*, pages 49-52, 1992.

- [7] B. A. Garrett-Price, S. A. Smith, R. L. Watts, J. G. Knudsen, W. J. Marner, and J. W. Suitor, editors. *Fouling of Heat Exchangers*. Noyes, New Jersey, 1985.
- [8] J. G. Knudsen. Conquer cooling water fouling. *Chemical Engineering Progress*, pages 42–48, 1991.
- [9] T. R. Bott, editor. *Heat Exchanger Fouling, The challenge*. Elsevier, Netherlands, 1992.
- [10] A. M. Pritchard. *Fouling of Heat Transfer Equipment*, pages 2–4. Hemisphere Publishing Corporation, Washington D.C., 1979.
- [11] P. A. Thackery. The cost of fouling in heat exchanger plant. In A. M. Pritchard, editor, *Fouling-Science or Art*, Guildford, U.K, March 27-28 1979.
- [12] W. L. Van Nostrand, S. H. Leach, and J. L. Haluska. *Fouling of Heat Transfer Equipment*, pages 619–643. Hemisphere Publishing Corporation, Washington D.C., 1979.
- [13] R. Steinhagen, H. M. Steinhagen, and K. Maani. Problems and costs due to heat exchanger fouling in New Zealand industries. *Heat Transfer Engineering*, 14(1):19–30, 1993.

- [14] P. L. Curlett and A. M. Impagliazzo. The impact of condenser tube fouling on powerplant design and economics. In *20th National Heat Transfer Conference*. Milwaukee, August 1981.
- [15] S. S. Penner, S. B. Alpert, J. M. Beer, I. Bozzuto, C. R. Glassman, R. B. Knust, Markert Jr., A. K. Oppenheim, L. D. Smoot, R. E. Sommerland, C. L. Wagoner, I. Wender, W. Wolowowdiuk, and K. E Yeager. Developing coal-combustion technologies. *Prog. Energy Combust. Sci.*, 10(1):87–144, 1984.
- [16] H. A. Schlesinger. Economics of alternatives for OTEC biofouling protection. In *OTEC Biofouling and Corrosion Symposium*, Seattle, October 1977.
- [17] J. L. Kasper, W. Chow, J. Graham, and Y. G. Musalli. Use and cost of chlorination systems. *Power Engineering*, pages 54–57, October 1983.
- [18] W. A. Hendrix and G. H. Hoyos. Coserving boiler energy. *Chemical Engineering*, 86(28):77–78, 1979.
- [19] Betz Ltd. Water treatment for boilers. *Processing*, July/August 1980.
- [20] R. J. Terrell. The economics of cooling - from birth onwards. In *Fouling and Cleaning of Heat Exchangers*, Liverpool, March 1986.
- [21] P. Hinckley. How to avoid problems of waste heat boilers. *Chemical Engineering*, 82(18):94–98, 1975.

- [22] J. G. Collier. Reliability problems of heat transfer equipment. *Heat Transfer Engineering*, 4(34):51-62, 1983.
- [23] *Tubular Exchange Manufacturers Association 5th edition*. New York, 1968.
- [24] J. Taborek and G. Aurioles. Effect of 1988 TEMA standards on mechanical and thermo-hydraulic design of shell and tube heat-exchangers. *AIChE Symposium Series*, 85(269):79-83, 1989.
- [25] J. M. Chenoweth. Final report of the HTRI/TEMA committee to review the fouling section of the TEMA standards. *Heat Transfer Engineering*, 11(1):73-107, 1990.
- [26] E. F. C. Somerscales. *Fouling of Heat Transfer Equipment*. Hemisphere Publishing Corporation, Washington D.C., 1979.
- [27] P. A. Pilavachi and J. D. Isdale. European community research and development strategy in the field of heat exchanger fouling projects. *Heat Recovery Systems and CHP*, 13(2):133-138, 1993.
- [28] S. Kakac and A. E. Bergles, editors. *Heat Exchangers*. Hemisphere Publishing Corporation, Washington D.C., 1981.
- [29] P. J. Fryer. Modelling the behaviour of heat exchangers undergoing scaling. *Geothermics*, 18:89-96, 1989.

- [30] S. H. Chan, H. Rau. C. DeBellis, and Neusen K. F. Silica fouling of heat transfer equipment-experiments and model. *Journal of Heat Transfer*, 110:841–849, 1988.
- [31] R. W. Morse and J. G. Knudsen. Effect of alkalinity on the scaling of simulated cooling tower water. *The Canadian Journal of Chemical Engineering*, 55:272–278, 1977.
- [32] M. Story and J. G. Knudsen. The effect of heat transfer surface temperature on the scaling behaviour of simulated cooling tower water. *AIChE Symposium Series*, 74(124):25–30, 1978.
- [33] S. H. Lee and J. G. Knudsen. Scaling characteristics of cooling tower water. *ASHRAE Transactions*, 85(1):281–302, 1979.
- [34] K. E. Coates and J. G. Knudsen. Calcium carbonate scaling characteristics of cooling tower water. *ASHRAE Transactions*, 86(2):68–91, 1980.
- [35] A.P. Watkinson and O. Martinez. Scaling of heat exchanger tubes by calcium carbonate. *Journal Of Heat Transfer*, 97:504–508, 1975.
- [36] Manzoor ul Haq. Reliability-based maintenance strategies for heat-exchangers subject to fouling. Master's thesis, KFUPM KSA., 1995.
- [37] A. M. Konings. Guide values for the fouling resistances of cooling water with different types of treatment for design of shell-and-tube heat exchangers. *Heat Transfer Engineering*, 10(4):54–61, 1989.

- [38] A.K. Meitz S.I. Haider, R.L. Webb. An experimental study of tube-side fouling resistance in water-chiller-flooded evaporators. *ASHRAE Transactions*, 98(2):86–103, 1992.
- [39] J. G. Knudsen. Coping with cooling water fouling in tubular heat exchangers. *AIChE Symposium Series*, 85(269):1–12, 1989.
- [40] S.H. Chan, Z.J. Chen, and P. He. Effect of sodium and potassium chlorides on silica fouling. *AIChE Symposium series*, 89:86–103, 1993.
- [41] E.M.H. Khater B.D. Crittenden. Fouling from vaporizing kerosine. *Journal of Heat Transfer*, 109:583–589, 1987.
- [42] S.T. Kolaczowski B.D. Crittenden and T.Takemoto. Use of in-tube inserts to reduce fouling from crude oils. *AIChE Symposium series*, 89(295):300–307, 1993.
- [43] A. P. Watkinson. Fouling of augmented heat transfer tubes. *Heat Transfer Engineering*, 11(3):57–65, 1990.
- [44] N.H. Kim and R.L. Webb. Experimental study of particulate fouling in enhanced water chilled condensor tubes. *Ashrae transactions*, 98(2):507–515, 1989.
- [45] S.A. Crittenden, B.D.and Hout and N.J. Alderman. Model experimnets of chemical reaction fouling. *Chem Engr Res Des*, 65:165–169, 1987.

- [46] B.D. Crittenden, S.T. Kolaczowski, and I.L. Cowney. Fouling of crude oil preheat heat-exchangers. *Transactions of IChemE*, 70(1):547–557, 1992.
- [47] B.D. Crittenden, S.T. Kolaczowski, T. Takenoto, and M.J. Gough. Use of matrix inserts to control hydrocarbon fouling. *IChemE Proc 10th Int Heat Transfer Conference*, pages 213–218. 1994.
- [48] S. R. Yang, J. M. Wang, G. D. Zai, and R. H. Kim. Investigation of heat transfer augments as a fouling cleaner and its optimum geometry in the tube side of a condenser. *Experimental Thermal and Fluid Science*, 5:795–802, 1992.
- [49] S. Manohar. Field testing of a probe to measure fouling in an industrial flue gas stream. *Heat Transfer Engineering*, 14:51–61, 1993.
- [50] W.L. Owens. A simple device for measuring fouling in heat exchanger tubes. *Journal Of Solar Energy Engineering*, 108:135–139, 1986.
- [51] G. Dickakian. *Heat Transfer Equipment Fundamentals, Design, Applications and Operating Problems - HTD V108*, pages 331–336. ASME, United Engineering Center, New York, 1990.
- [52] D. C. Thompson and Bridgewater. Plant demonstration of a technique to measure the local fouling resistance. *ICHEME Symposium Series No. 129*, pages 979–985, 1992.

- [53] E. F. C. Somerscales. *Fouling of Heat Transfer Equipment*. Hemisphere Publishing Corporation, Washington D.C., 1979.
- [54] G. Zhang, T.R. Bott, and C.R. Benrose. Reduced partical deposition in air cooled heat exchangers. *Heat Transfer Engineeirng*, 13(2):81-87, 1992.
- [55] C. B. Panchal and D. S. Saccar. *Fouling and Enhancement Interactions - HTD V164*, pages 9-15. ASME, United Engineering Center, New York, 1991.
- [56] D. Hasson. *Fouling of Heat Tranfer Equipment*, pages 527-568. Hemisphere Publishing Corporation, Washington D.C., 1979.
- [57] C. A. Branch and H. M. M. Steinhagen. Influence of scaling on the performance of shell-and-tube heat exchangers. *Heat Transfer Enginecring*, 12(2):37-45, 1991.
- [58] J. E. Hesselgreaves. The effect of system parameters on the fouling performance of heat exchangers. *ICHEME Symposium Series No. 129*, pages 995-1006, 1992.
- [59] S.G. Yiantsios and A.J. Karabelas. Fouling of tube surfaces; modeling of removal kinetics. *AIChE Journal*, 40(11):1804-1813. November 1994.
- [60] S. Brown. Coping with fouling in heat exchangers. *Process Engineering*, pages 37-38, 1991.
- [61] R. H. Kim. *Fouling and Enhancement Interactions - HTD V164*, pages 39-45. ASME, United Engineering Center, New York, 1991.

- [62] J.L. Hughes. *Containment heat exchangers tube side cleaning program - HTD V14*, pages 9–13. ASME, United Engineering Center, New York, 1991.
- [63] A. Bejan and J.V. Vargas. When to defrost a refrigerator, and when to remove the scale from the heat exchanger of a power plant. *Int. J. Heat and Mass Transfer*, 37(3):523–532, 1994.
- [64] O. V. Tretyakov, V. G. Kristskiy, and P. S. Styazhkin. Improved prediction of the formation of calcium carbonate scale in heat exchangers of secondary loops of conventional thermal and nuclear power plants. *Heat Transfer - Soviet Research*, 23(4):532–538, 1991.
- [65] S. Duffuaa and M.O. Budair. Scale removal from heat exchangers: Using energy utilization techniques as a schedule criterion. *Applied Energy*, 47:77–85, 1994.
- [66] C. B. Panchal and A. P. Watkinson. Chemical reaction fouling model for single-phase heat transfer. *AIChE Symposium Series*, 89(289):323–334, 1993.
- [67] L. Oufer and J. G. Knudsen. Modelling chemical reaction fouling under sub-cooled boiling conditions. *AIChE Symposium Series*, 89(289):308–313, 1993.
- [68] C.B. Panchal and A.P. Watkinson. Chemical reaction fouling model for single-phase heat transfer. *AIChE Symposium series*, 89(295):86–103, 1993.
- [69] K. F. Neusen, S. H. Chian, and D. Z. Zhou. *Heat Transfer in Geophysical and Geothermal Systems*, volume 76, pages 45–50. ASME HTD, New York, 1987.

- [70] J. G. Knudsen. *Fouling in Heat Exchange Equipment - HTD V17*. ASME, United Engineering Center, New York, 1981.
- [71] Betz Laboratories Inc. *Handbook Of Industrial Water Conditioning 7th edition*. USA, 1976.
- [72] W. L. Masterten and C. N. Hurley. *Chemistry, Principles and Reactions*. Saunders Publishers, Philadelphia, 1989.
- [73] Kalpakjian. Serope. *Manufacturing Processes for Engineering Materials*. Addison Wesley Publishing Company, Massachusetts, 1985.
- [74] D. J. Pary and D. Hawthorn. Fouling of powerstation condensers within the Marylands Region of the C.E.G.B. In J.G. Somerscales, E.F.C.and Knudsen, editor, *Fouling of Heat Transfer Equipment*, pages 569–586. Hemisphere, 1979.
- [75] D. C. Montgomery and E. A. Peck. *Introduction to Linear Regression Analysis*. Wiley, New York, 1985.

Appendices

Appendix-A includes all heat exchanger drawings. Uncertainty analysis of the experimental study is described in Appendix-B. Results of chemical solution analysis are shown in Appendix C. Data collected from the experimental study are presented in tabular and graphical forms in Appendices D and E respectively. A sample calculation of the fouling resistance has been discussed in the Appendix-F. All steps required to calculate R_f from the measured mass gain due to fouling are mentioned. Results of test section surface analysis are presented in Appendix-G. Sensitivity analysis was carried out to determine the change in R_f^* that resulted by varying the parameters slightly from their base value ($Re^*=0.76$, $D^*=0.75$ and $T_s^*=0.97$). As an example percentage change in R_f^* was determined resulting due to a change of 10% in the values of the parameters. The results are shown in Appendix-H. Scale was removed from the test sections and was analyzed under SEM (Scanning Electron Microscope) and EDX (Energy Dispersive X-rays) to identify the nature of the scale. The scale removed was crystalline and soft. It did not strongly adhere to the surface of the test section. The results of SEM and EDX are shown in Appendix-I.

Appendix A

Heat Exchanger Drawings

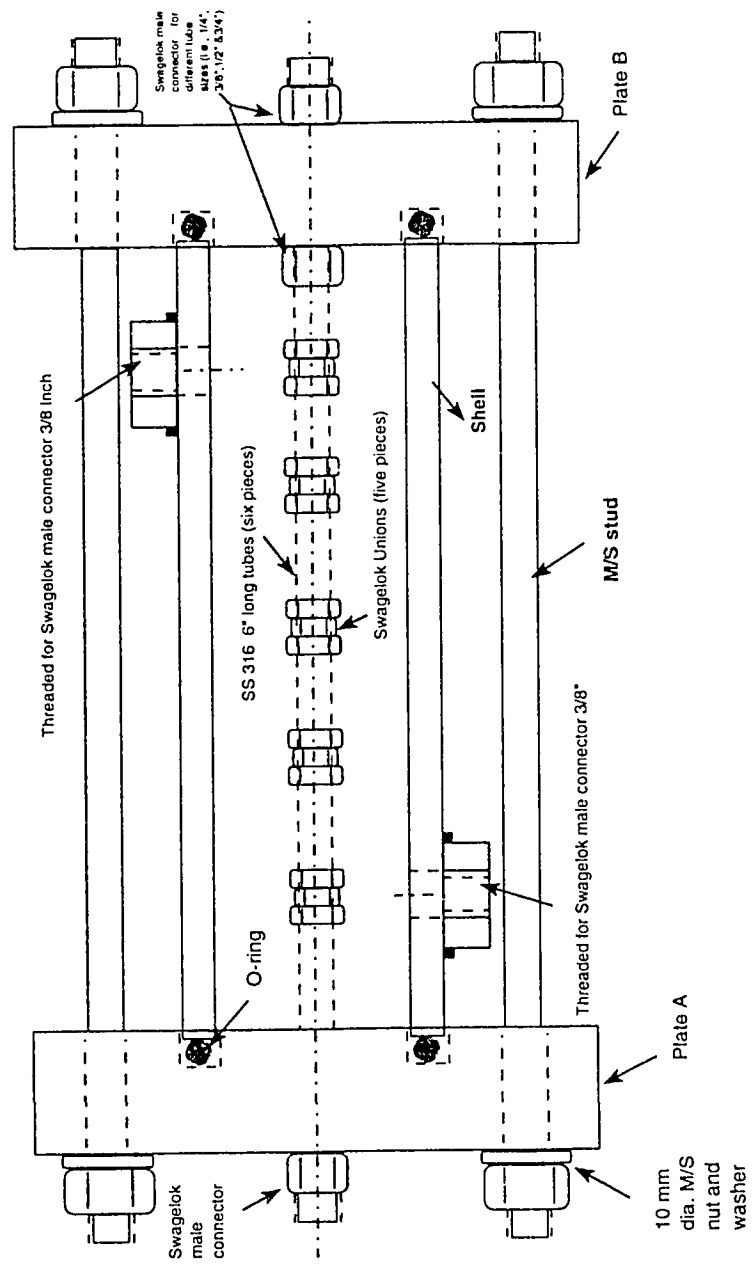


Figure A.1: Assembly drawing of the heat exchanger

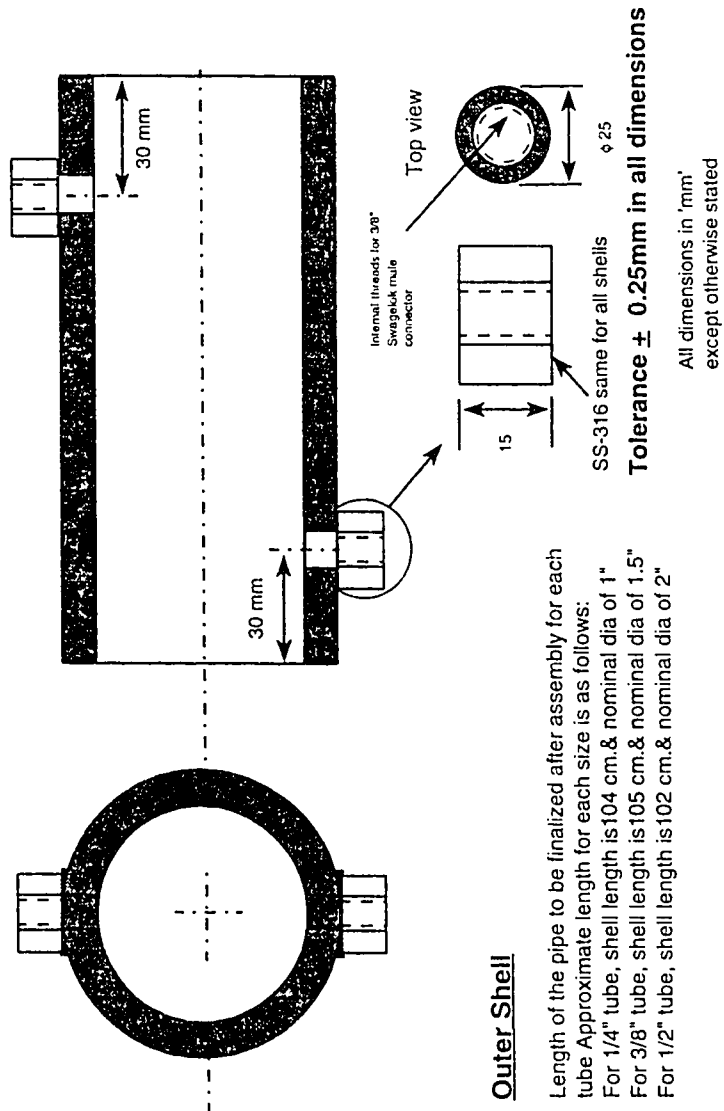
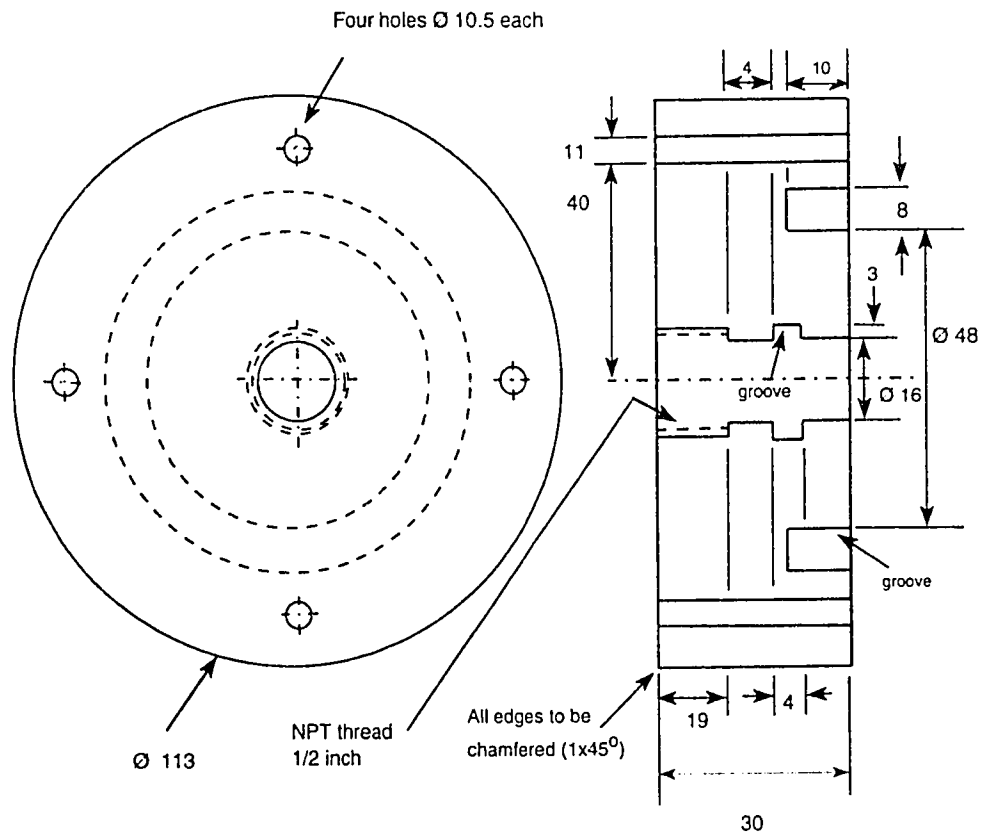


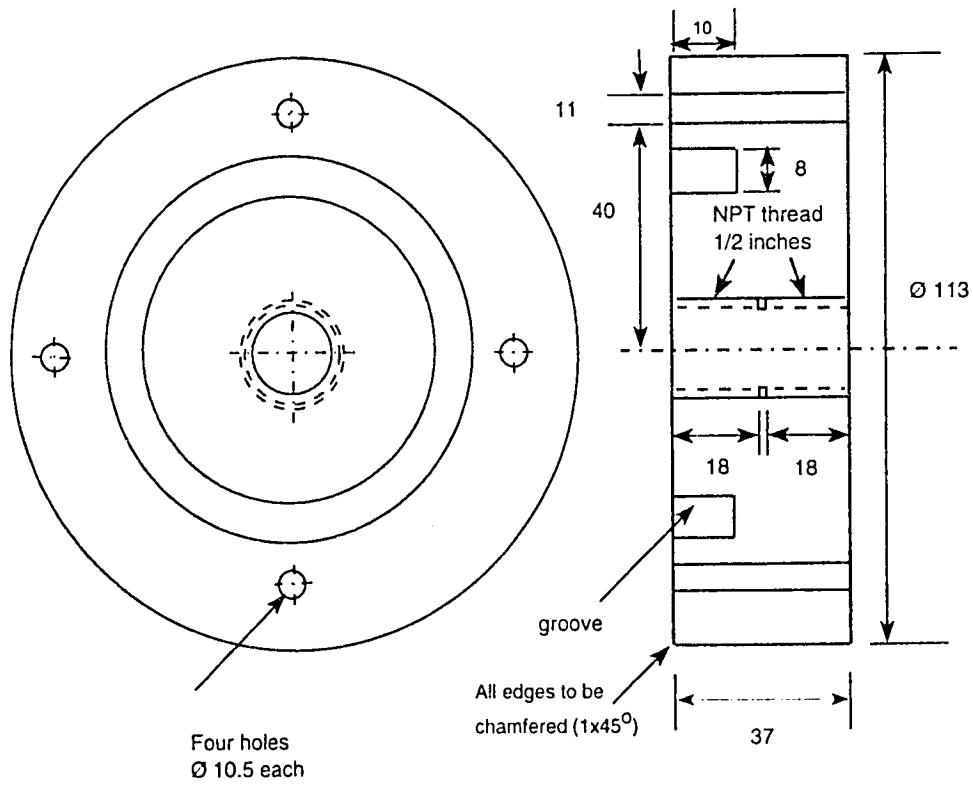
Figure A.2: Schematic of the heat exchanger shell



All dimensions in 'mm'
except otherwise stated

**Tolerance ± 0.25 mm
in all dimensions**

Figure A.3: Drawing of plate A of 1/2 inch tube heat exchanger



**Tolerance ± 0.25 mm
in all dimensions**

All dimensions in 'mm'
except otherwise stated

Figure A.4: Drawing of plate B of 1/2 inch tube heat exchanger

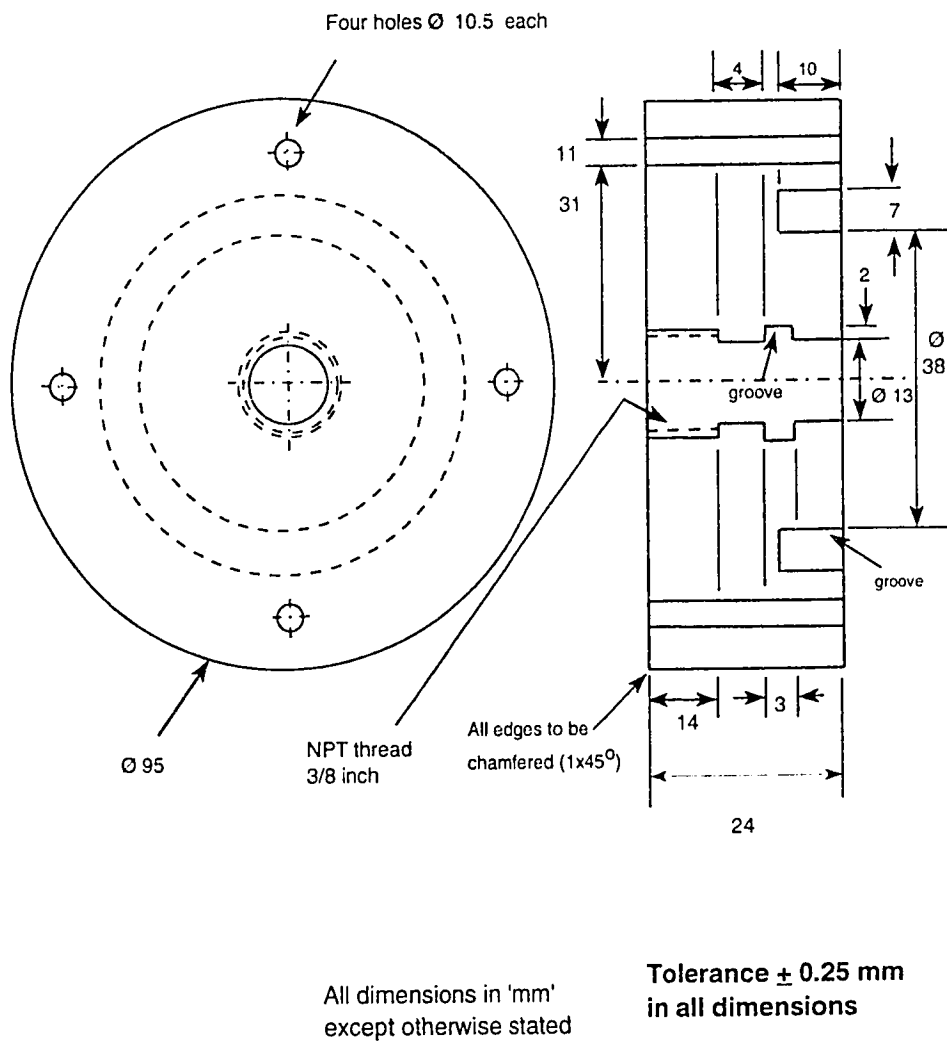
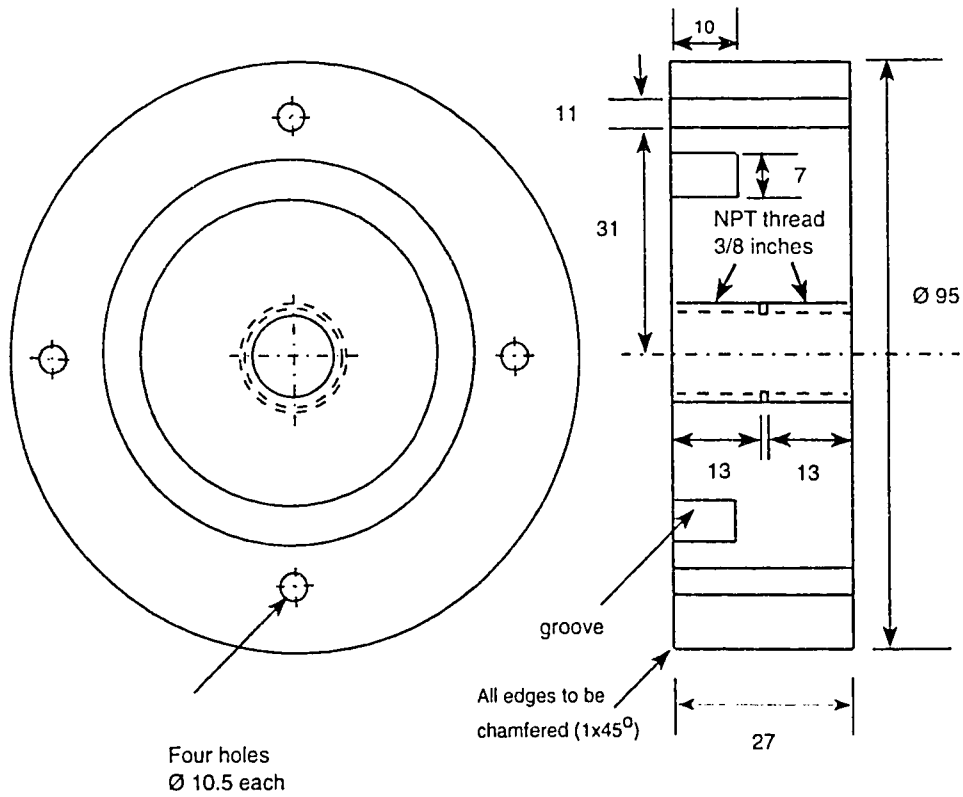


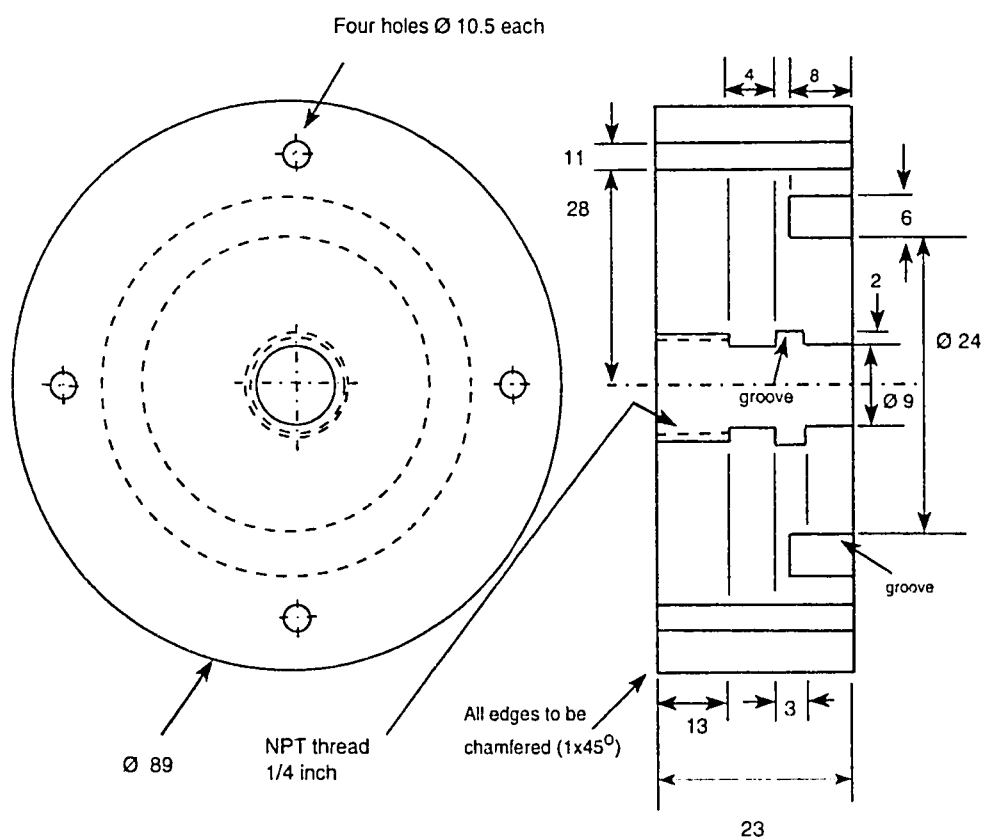
Figure A.5: Drawing of plate A of 3/8 inch tube heat exchanger



**Tolerance ± 0.25 mm
in all dimensions**

All dimensions in 'mm'
except otherwise stated

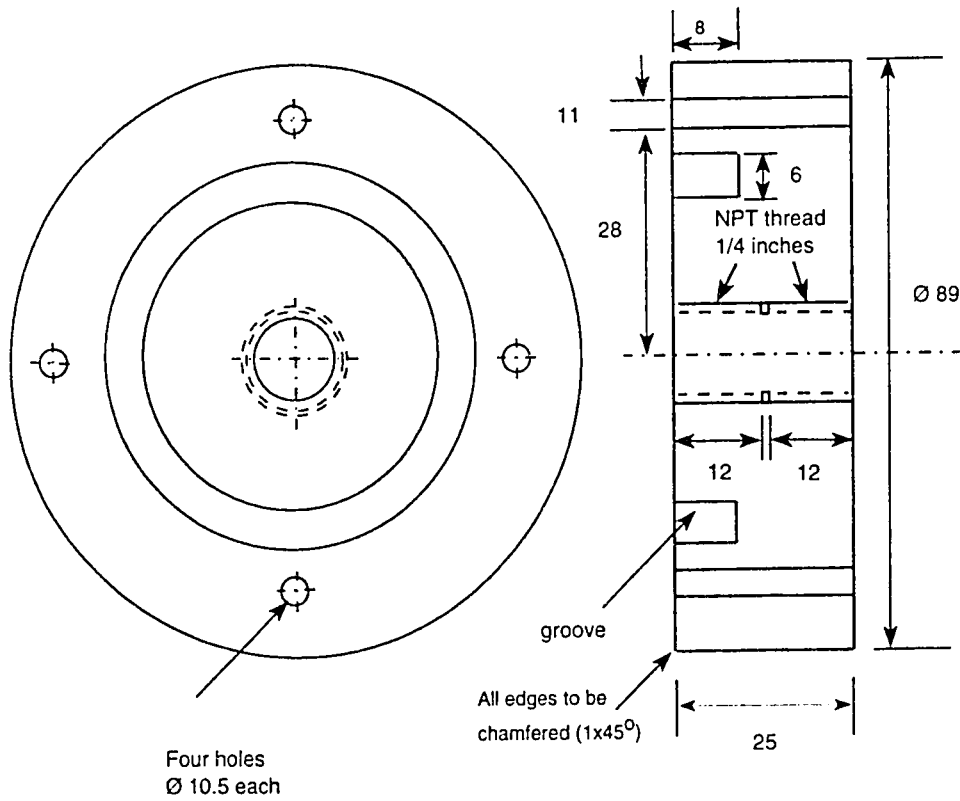
Figure A.6: Drawing of plate B of 3/8 inch tube heat exchanger



All dimensions in 'mm'
except otherwise stated

**Tolerance ± 0.25 mm
in all dimensions**

Figure A.7: Drawing of plate A of 1/4 inch tube heat exchanger



**Tolerance ± 0.25 mm
in all dimensions**

All dimensions in 'mm'
except otherwise stated

Figure A.8: Drawing of plate B of 1/4 inch tube heat exchanger

Appendix B

Uncertainty analysis

Mass gain technique was used to determine the fouling resistance. The accuracy of the weighing scale used was ± 0.1 mg. It was calculated that an error of ± 0.1 mg resulted in $\pm 0.3\%$ difference in the measurement of R_f .

In calculating the Reynolds number time taken to fill 500 ml beaker was noted. From the fouling resistance model it was determined that an error of ± 1 sec, in the measurement of time, produced $\pm 0.13\%$ difference in the R_f .

Temperature was measured with an accuracy of $\pm 1^\circ\text{F}$. This accuracy could result in a $\pm 1.878\%$ difference in the fouling resistance calculation.

Appendix C

Results of Chemical Solution

Analysis

Table C.1: Results of chemical solution analysis

All units mg/l except for conductivity in microsiemens
and density in grams/ml.

Parameters	Distilled water	Condition at inlet of HE	Condition at exit of HE
Barium	< 0.05	< 0.05	< 0.05
Calcium	< 0.02	22	12
Magnesium	< 0.05	< 0.05	< 0.05
Potassium	< 0.2	< 0.2	< 0.2
Sodium	< 0.2	28.5	29
Strontium	< 0.05	< 0.05	< 0.05
Chloride	0.37	41.35	42.83
Sulphate	< 0.2	< 0.2	< 0.2
Carbonate	ND	26.97	10.71
TDS	2.19	116	103
Conductivity	4.42	233	207
Ph	6.39	9.73	9.34
Density	0.9993	0.9996	0.9997

Appendix D

Data Obtained from the Experiments

Table D.1: Data of Experiments 1, 2 and 3

EXPT. # 1

Fouling Resistance ($\text{m}^2 \text{K/W} \times 10^7$)						
time (hr)	Sect 1	Sect 2	Sect 3	Sect 4	Sect 5	Sect 6
2	3.661	3.661	4.393	4.393	4.759	4.759
4	8.787	9.153	10.984	11.350	11.716	13.181
6	14.647	16.844	19.409	20.142	20.874	20.874
8	25.272	29.303	32.603	33.336	33.702	34.802
10	37.736	41.770	44.337	45.071	46.538	47.639

EXPT. # 2

Fouling Resistance ($\text{m}^2 \text{K/W} \times 10^7$)						
time (hr)	Sect 1	Sect 2	Sect 3	Sect 4	Sect 5	Sect 6
2	4.027	4.393	4.393	4.759	4.759	5.125
4	10.252	10.984	11.350	12.083	15.379	16.478
6	25.638	26.738	28.204	29.303	33.702	35.536
8	47.272	50.574	49.473	50.941	53.877	55.345
10	80.316	85.461	85.829	86.931	86.931	87.299

EXPT. # 3

Fouling Resistance ($\text{m}^2 \text{K/W} \times 10^7$)						
time (hr)	Sect 1	Sect 2	Sect 3	Sect 4	Sect 5	Sect 6
2	4.393	4.759	4.759	5.125	5.491	5.857
4	11.350	10.984	12.449	20.508	20.874	23.073
6	28.937	29.303	31.503	44.704	46.538	46.208
8	54.611	58.648	62.319	74.805	78.846	81.088
10	80.684	85.461	86.564	98.697	103.478	104.987

Table D.2: Data of experiments 4, 5 and 6

EXPT. # 4

Fouling Resistance ($\text{m}^2 \text{K/W} \times 10^7$)						
time (hr)	Sect 1	Sect 2	Sect 3	Sect 4	Sect 5	Sect 6
2	4.027	4.027	3.661	4.393	4.759	4.759
4	9.153	10.252	10.618	11.350	12.449	13.548
6	15.745	17.211	18.310	20.508	21.607	21.607
8	26.738	30.036	31.503	33.702	34.802	35.536
10	39.203	42.503	44.337	47.272	49.473	49.840

EXPT. # 5

Fouling Resistance ($\text{m}^2 \text{K/W} \times 10^7$)						
time (hr)	Sect 1	Sect 2	Sect 3	Sect 4	Sect 5	Sect 6
2	4.393	4.393	5.125	5.125	5.491	5.857
4	13.548	14.280	18.310	20.508	21.607	23.439
6	29.303	29.670	32.603	35.536	38.836	45.805
8	55.712	56.446	59.015	60.851	65.623	71.499
10	81.786	82.153	82.153	82.888	89.504	99.064

EXPT. # 6

Fouling Resistance ($\text{m}^2 \text{K/W} \times 10^7$)						
time (hr)	Sect 1	Sect 2	Sect 3	Sect 4	Sect 5	Sect 6
2	4.027	4.027	4.759	4.759	5.491	5.491
4	10.252	10.252	13.181	14.647	15.745	16.844
6	26.005	27.104	28.937	29.670	34.436	36.269
8	47.272	48.006	52.776	50.941	53.143	54.978
10	81.419	85.829	86.931	87.299	88.034	91.710

Table D.3: Data of experiments 7, 8 and 9

EXPT. # 7

Fouling Resistance ($\text{m}^2 \text{K/W} \times 10^7$)						
time (hr)	Sect 1	Sect 2	Sect 3	Sect 4	Sect 5	Sect 6
2	4.027	4.027	4.393	4.393	5.125	5.125
4	9.885	10.252	10.984	10.984	12.449	13.548
6	16.112	16.844	19.043	20.508	21.607	21.974
8	27.471	30.403	32.236	34.802	35.536	36.269
10	39.203	42.870	45.805	47.639	50.207	50.207

EXPT. # 8

Fouling Resistance ($\text{m}^2 \text{K/W} \times 10^7$)						
time (hr)	Sect 1	Sect 2	Sect 3	Sect 4	Sect 5	Sect 6
2	4.027	4.759	4.759	4.759	5.125	5.491
4	10.618	10.252	13.548	15.013	16.112	17.577
6	26.371	27.471	31.503	32.603	34.436	38.469
8	47.639	49.473	51.675	54.244	57.180	58.648
10	78.846	86.196	85.461	88.034	90.240	94.652

EXPT. # 9

Fouling Resistance ($\text{m}^2 \text{K/W} \times 10^7$)						
time (hr)	Sect 1	Sect 2	Sect 3	Sect 4	Sect 5	Sect 6
2	5.491	5.125	5.125	5.491	5.491	5.857
4	13.548	15.013	18.310	19.409	21.241	23.439
6	30.770	31.503	31.503	35.169	38.469	46.538
8	56.813	57.547	59.015	62.319	67.827	71.132
10	83.991	85.094	85.829	88.034	90.607	102.375

Table D.4: Data of experiments 10, 11 and 12

EXPT. # 10

Fouling Resistance ($\text{m}^2 \text{K/W} \times 10^7$)						
time (hr)	Sect 1	Sect 2	Sect 3	Sect 4	Sect 5	Sect 6
2	2.764	3.870	4.976	5.529	5.529	4.976
4	9.954	10.507	11.613	11.060	12.167	12.167
6	19.361	21.022	22.683	22.683	22.683	23.237
8	33.207	34.870	36.532	37.641	37.641	38.195
10	50.396	52.615	56.500	57.610	58.165	59.275

EXPT. # 11

Fouling Resistance ($\text{m}^2 \text{K/W} \times 10^7$)						
time (hr)	Sect 1	Sect 2	Sect 3	Sect 4	Sect 5	Sect 6
2	4.976	5.529	5.529	6.082	6.082	6.635
4	12.167	12.167	12.720	15.487	15.487	16.040
6	27.667	28.221	27.667	29.329	29.883	33.207
8	50.396	52.615	53.725	55.390	57.055	60.386
10	80.944	81.500	82.612	83.168	85.949	89.287

EXPT. # 12

Fouling Resistance ($\text{m}^2 \text{K/W} \times 10^7$)						
time (hr)	Sect 1	Sect 2	Sect 3	Sect 4	Sect 5	Sect 6
2	8.294	10.507	12.720	14.380	15.487	17.147
4	27.667	32.653	35.978	38.749	39.858	45.958
6	55.390	62.051	64.273	65.384	71.494	74.829
8	89.843	93.739	98.192	99.862	104.875	106.546
10	128.847	137.778	142.245	143.921	148.391	152.303

Table D.5: Data of experiments 13, 14 and 15

EXPT. # 13

Fouling Resistance ($\text{m}^2 \text{K/W} \times 10^7$)						
time (hr)	Sect 1	Sect 2	Sect 3	Sect 4	Sect 5	Sect 6
2	2.764	3.317	3.870	4.423	5.529	6.635
4	9.401	11.060	12.167	12.167	12.720	14.933
6	23.237	24.898	26.005	26.005	26.559	28.221
8	36.532	38.195	39.304	40.413	40.967	42.076
10	61.496	63.162	64.273	64.828	64.828	65.939

EXPT. # 14

Fouling Resistance ($\text{m}^2 \text{K/W} \times 10^7$)						
time (hr)	Sect 1	Sect 2	Sect 3	Sect 4	Sect 5	Sect 6
2	5.529	5.529	7.741	7.741	8.294	8.847
4	16.594	15.487	17.147	18.254	21.576	22.683
6	35.978	36.532	37.087	38.195	40.967	43.739
8	57.610	57.055	57.055	58.720	63.717	68.161
10	84.281	84.281	84.837	87.062	90.400	91.513

EXPT. # 15

Fouling Resistance ($\text{m}^2 \text{K/W} \times 10^7$)						
time (hr)	Sect 1	Sect 2	Sect 3	Sect 4	Sect 5	Sect 6
2	10.507	11.060	13.827	16.594	17.147	18.254
4	30.991	36.532	38.195	39.304	44.849	49.841
6	62.607	66.494	73.162	74.829	79.832	82.056
8	94.295	99.306	105.989	106.546	115.462	118.249
10	132.195	146.714	150.626	155.098	160.689	163.486

Table D.6: Data of experiments 16, 17 and 18

EXPT. # 16

Fouling Resistance ($\text{m}^2 \text{K/W} \times 10^7$)						
time (hr)	Sect 1	Sect 2	Sect 3	Sect 4	Sect 5	Sect 6
2	3.317	3.317	3.317	4.423	4.976	5.529
4	11.060	12.167	12.720	13.273	14.380	16.040
6	27.113	30.437	30.991	31.545	32.099	35.424
8	46.512	49.841	51.505	52.060	53.170	55.390
10	74.273	75.940	76.496	77.052	78.164	79.276

EXPT. # 17

Fouling Resistance ($\text{m}^2 \text{K/W} \times 10^7$)						
time (hr)	Sect 1	Sect 2	Sect 3	Sect 4	Sect 5	Sect 6
2	6.082	6.082	7.188	7.741	8.294	8.294
4	22.683	24.344	24.898	25.452	28.221	28.775
6	43.739	45.958	45.958	46.512	49.841	50.396
8	73.717	77.052	78.720	79.276	79.832	81.500
10	109.331	109.889	111.003	112.118	112.675	112.675

EXPT. # 18

Fouling Resistance ($\text{m}^2 \text{K/W} \times 10^7$)						
time (hr)	Sect 1	Sect 2	Sect 3	Sect 4	Sect 5	Sect 6
2	9.401	11.060	14.380	16.040	17.147	18.808
4	31.545	38.749	39.858	41.521	47.067	51.505
6	60.941	70.939	73.717	76.496	82.056	83.168
8	95.409	108.217	113.232	115.462	118.807	120.480
10	132.754	147.832	158.452	162.367	162.927	165.164

Table D.7: Data of experiments 19, 20 and 21

EXPT. # 19

Fouling Resistance ($\text{m}^2 \text{ K/W} \times 10^7$)						
time (hr)	Sect 1	Sect 2	Sect 3	Sect 4	Sect 5	Sect 6
2	4.566	6.850	7.612	9.896	9.896	10.658
4	20.565	24.378	25.141	28.193	28.193	28.193
6	41.937	44.993	44.993	51.110	51.875	53.404
8	76.380	79.447	80.981	84.817	85.585	88.655
10	114.020	116.329	117.099	117.099	117.869	120.949

EXPT. # 20

Fouling Resistance ($\text{m}^2 \text{ K/W} \times 10^7$)						
time (hr)	Sect 1	Sect 2	Sect 3	Sect 4	Sect 5	Sect 6
2	15.991	15.991	15.991	19.040	20.565	20.565
4	38.117	38.881	40.409	48.816	51.110	52.640
6	61.823	73.313	76.380	80.981	82.515	83.283
8	96.334	100.176	102.482	108.634	113.251	117.869
10	151.031	157.986	159.532	166.493	172.685	175.008

EXPT. # 21

Fouling Resistance ($\text{m}^2 \text{ K/W} \times 10^7$)						
time (hr)	Sect 1	Sect 2	Sect 3	Sect 4	Sect 5	Sect 6
2	18.278	19.803	20.565	20.565	22.853	25.141
4	58.761	66.417	69.482	75.613	76.380	79.447
6	105.558	112.481	117.099	117.869	120.179	122.490
8	155.667	159.532	164.173	170.363	171.911	175.782
10	215.358	219.247	232.480	234.037	237.154	240.272

Table D.8: Data of experiments 22, 23 and 24

EXPT. # 22

Fouling Resistance ($\text{m}^2 \text{K/W} \times 10^7$)						
time (hr)	Sect 1	Sect 2	Sect 3	Sect 4	Sect 5	Sect 6
2	6.089	6.089	7.612	8.373	10.658	10.658
4	22.090	23.615	27.430	29.719	28.956	30.482
6	42.701	45.758	47.287	47.287	50.345	54.169
8	77.913	80.981	86.352	84.817	87.120	90.190
10	117.099	120.949	123.260	124.801	125.571	125.571

EXPT. # 23

Fouling Resistance ($\text{m}^2 \text{K/W} \times 10^7$)						
time (hr)	Sect 1	Sect 2	Sect 3	Sect 4	Sect 5	Sect 6
2	15.229	14.467	15.991	19.040	20.565	19.040
4	44.993	44.229	45.758	51.110	55.700	54.935
6	68.715	78.680	80.214	82.515	85.585	82.515
8	103.251	108.634	110.173	110.942	117.099	120.179
10	157.213	165.720	166.493	167.267	175.782	178.106

EXPT. # 24

Fouling Resistance ($\text{m}^2 \text{K/W} \times 10^7$)						
time (hr)	Sect 1	Sect 2	Sect 3	Sect 4	Sect 5	Sect 6
2	18.278	18.278	21.328	21.328	23.615	25.904
4	59.526	67.183	72.547	75.613	80.981	83.283
6	110.173	114.020	116.329	119.409	120.949	121.719
8	158.759	161.079	165.720	175.782	172.685	177.331
10	214.581	221.581	234.037	236.375	240.272	238.713

Table D.9: Data of experiments 25, 26 and 27

EXPT. # 25

Fouling Resistance ($\text{m}^2 \text{K/W} \times 10^7$)						
time (hr)	Sect 1	Sect 2	Sect 3	Sect 4	Sect 5	Sect 6
2	6.850	6.850	7.612	9.135	10.658	10.658
4	22.853	22.853	29.719	31.245	32.009	33.535
6	41.937	47.287	51.110	51.110	51.110	55.700
8	77.146	80.981	80.214	84.817	89.422	93.262
10	117.869	120.949	125.571	123.260	124.801	127.112

EXPT. # 26

Fouling Resistance ($\text{m}^2 \text{K/W} \times 10^7$)						
time (hr)	Sect 1	Sect 2	Sect 3	Sect 4	Sect 5	Sect 6
2	14.467	13.705	15.229	19.803	20.565	20.565
4	46.522	48.816	48.051	49.580	54.935	55.700
6	73.313	74.846	74.080	75.613	80.214	77.913
8	106.327	107.865	109.403	111.712	113.251	116.329
10	157.986	161.852	164.173	164.946	171.911	175.008

EXPT. # 27

Fouling Resistance ($\text{m}^2 \text{K/W} \times 10^7$)						
time (hr)	Sect 1	Sect 2	Sect 3	Sect 4	Sect 5	Sect 6
2	18.278	15.229	19.040	20.565	22.853	25.141
4	59.526	57.230	74.080	75.613	77.913	80.214
6	110.942	110.942	117.869	120.949	124.030	127.883
8	157.213	163.399	167.267	169.589	173.459	180.430
10	232.480	236.375	239.492	243.390	244.170	244.170

Table D.10: Data of experiments 28 and 29

EXPT. # 28

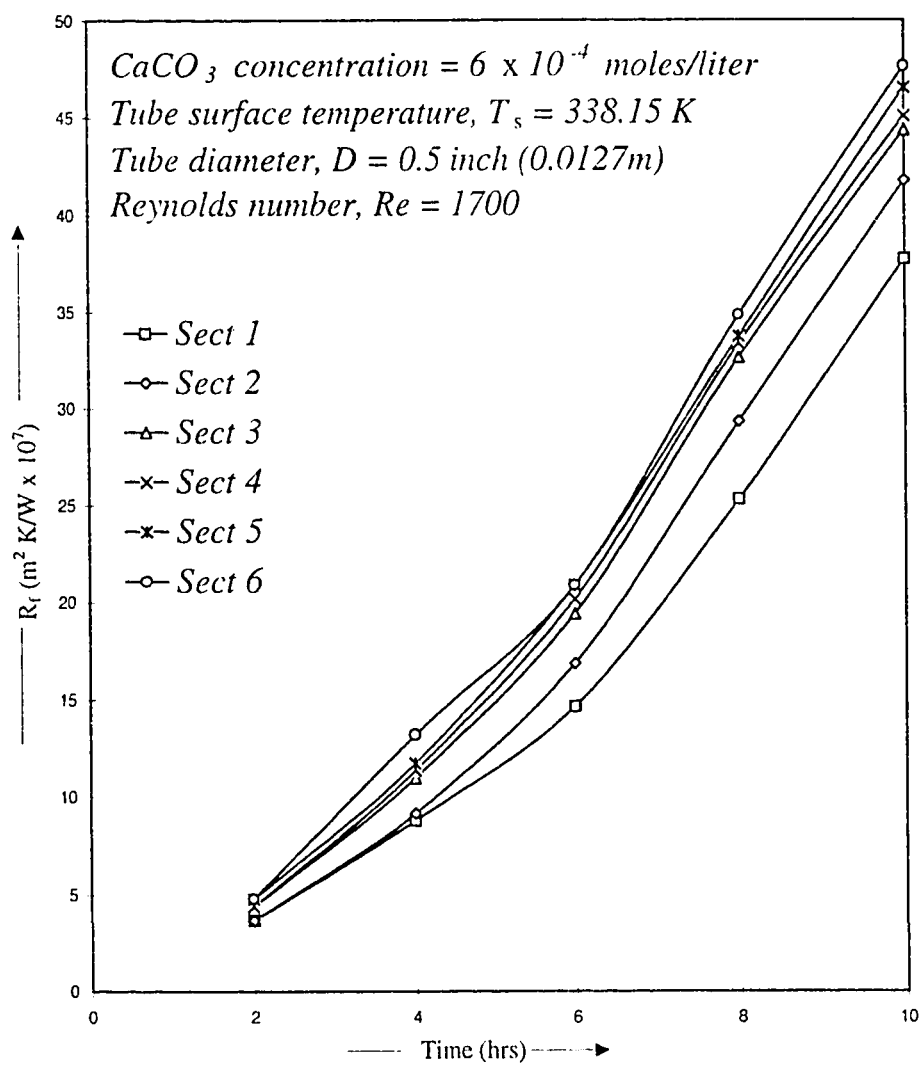
Fouling Resistance ($\text{m}^2 \text{K/W} \times 10^7$)						
time (hr)	Sect 1	Sect 2	Sect 3	Sect 4	Sect 5	Sect 6
2	11.533	10.911	11.863	12.193	13.877	13.767
4	30.953	40.413	43.200	44.044	45.108	46.098
6	54.794	58.648	69.810	72.858	76.275	84.726
8	106.973	110.837	115.768	122.505	128.139	135.507
10	168.876	186.412	187.668	194.428	199.712	205.626

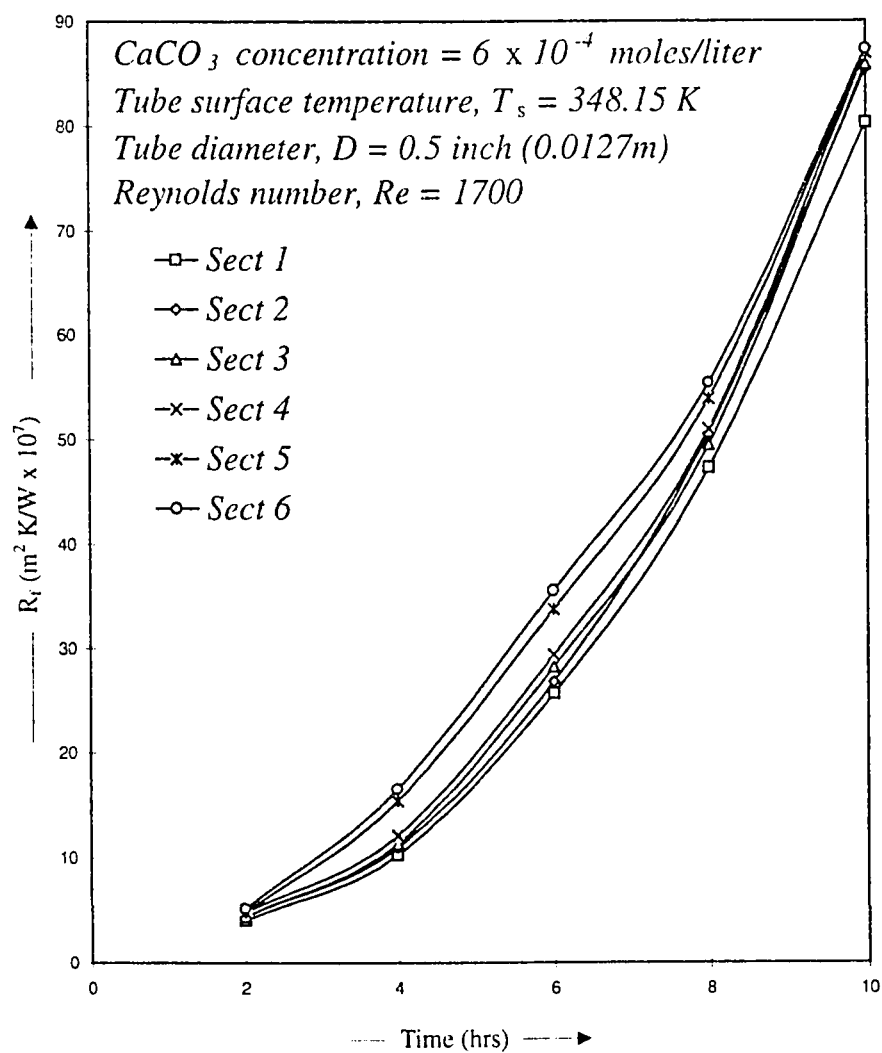
EXPT. # 29

Fouling Resistance ($\text{m}^2 \text{K/W} \times 10^7$)						
time (hr)	Sect 1	Sect 2	Sect 3	Sect 4	Sect 5	Sect 6
2	1.830	2.233	2.745	2.562	2.928	2.928
4	5.491	5.564	6.040	8.054	9.519	9.885
6	13.914	14.354	14.830	16.478	17.211	19.043
8	22.707	25.675	27.287	28.570	28.937	29.670
10	36.636	41.806	44.521	45.071	48.006	48.740

Appendix E

Data in Graphical Form

Figure E.1: R_f vs time of experiment No.1

Figure E.2: R_f vs time of experiment No.2

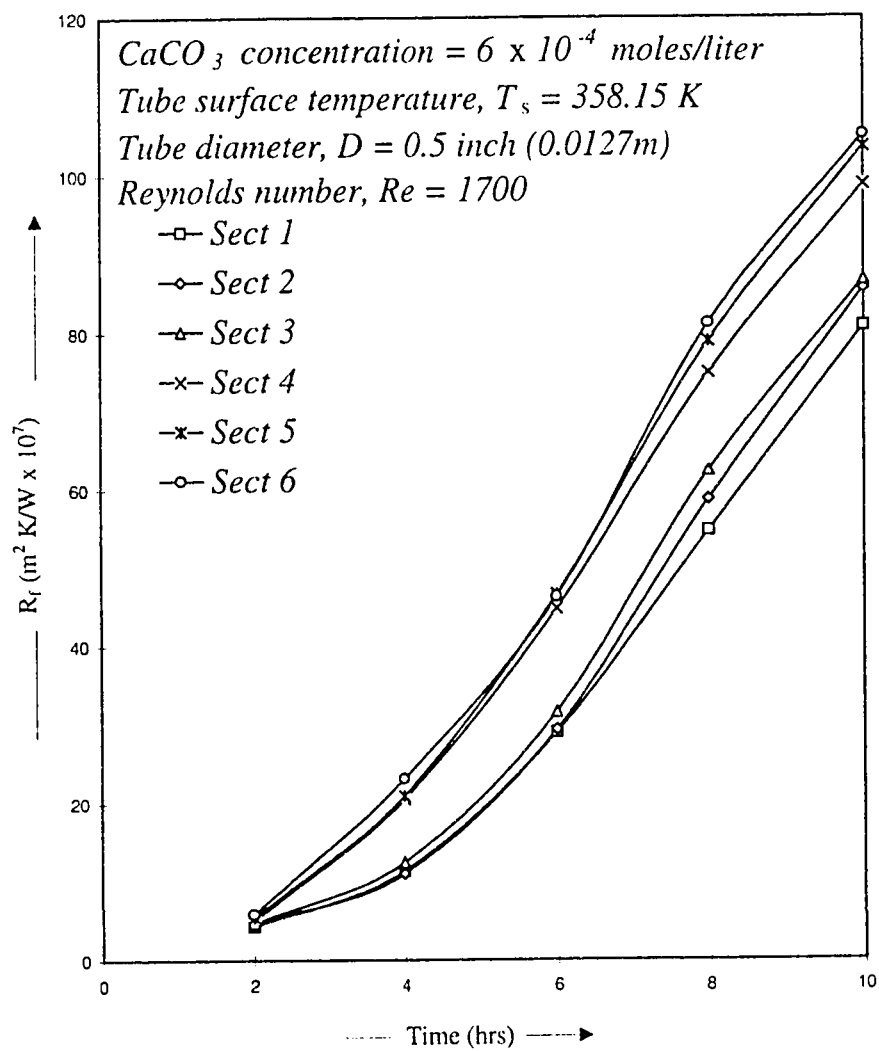
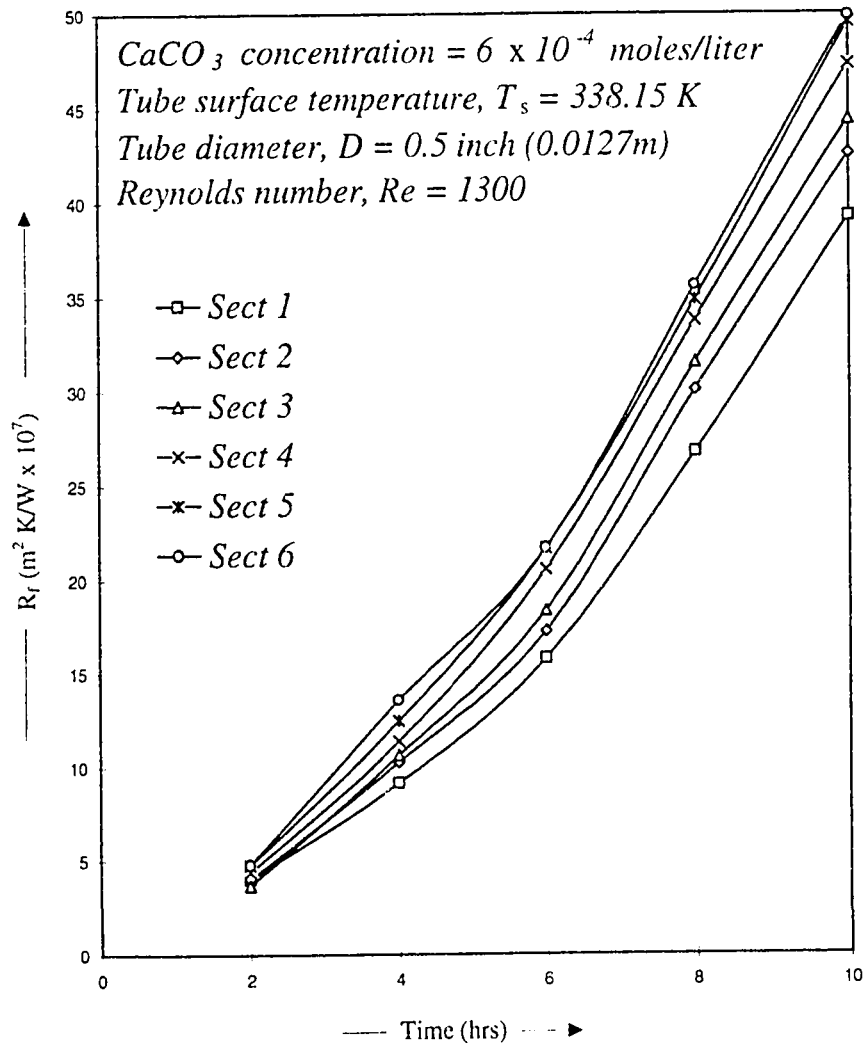


Figure E.3: R_f vs time of experiment No.3

Figure E.4: R_f vs time of experiment No.4

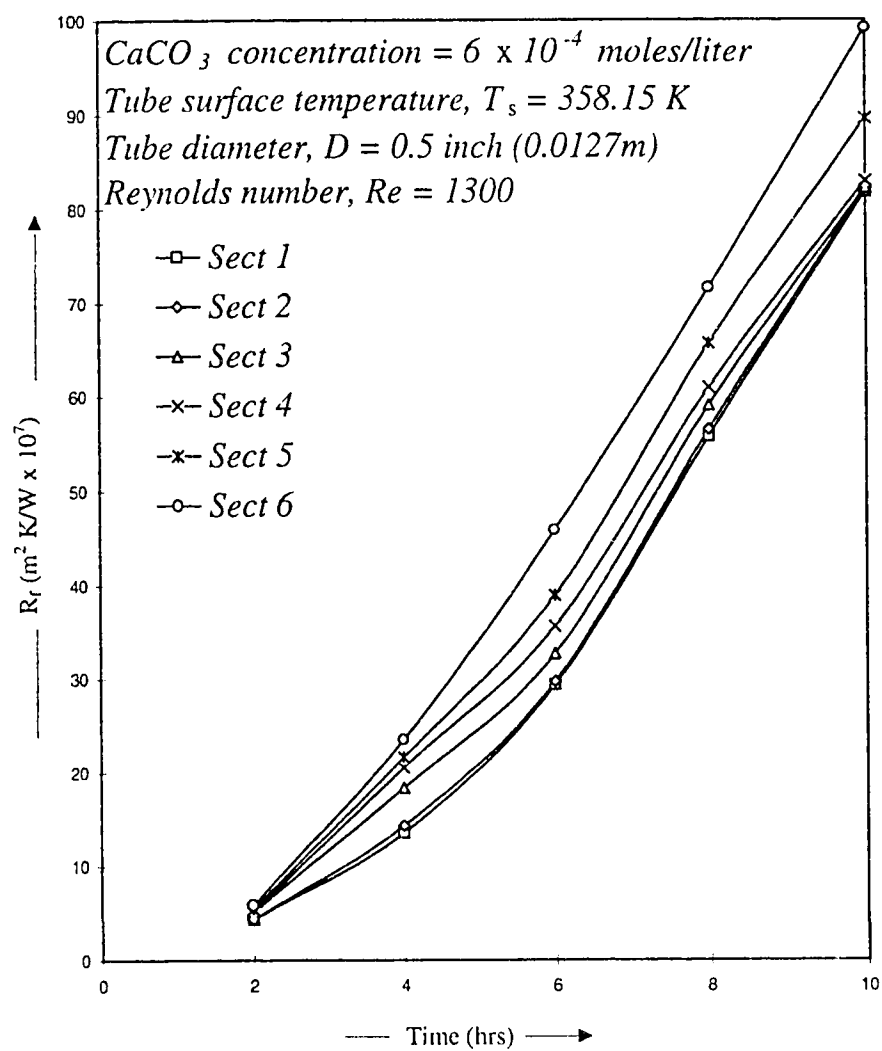


Figure E.5: R_f vs time of experiment No.5

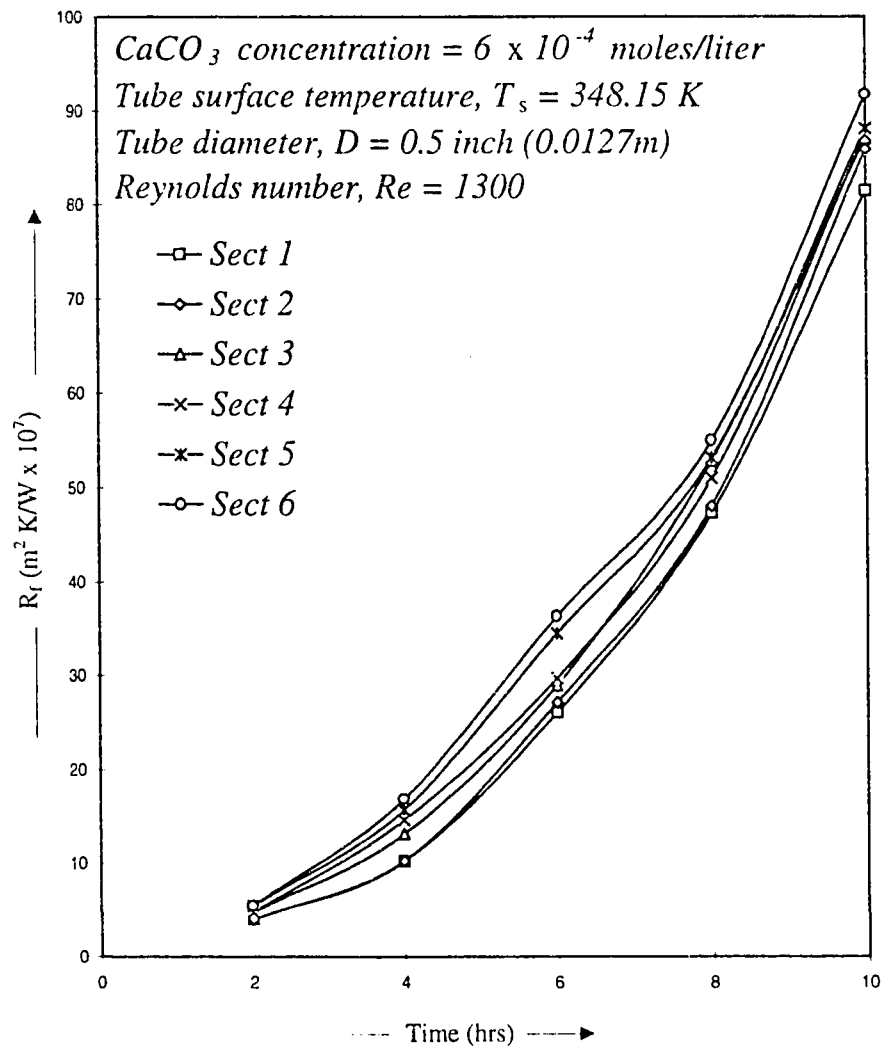


Figure E.6: R_f vs time of experiment No.6

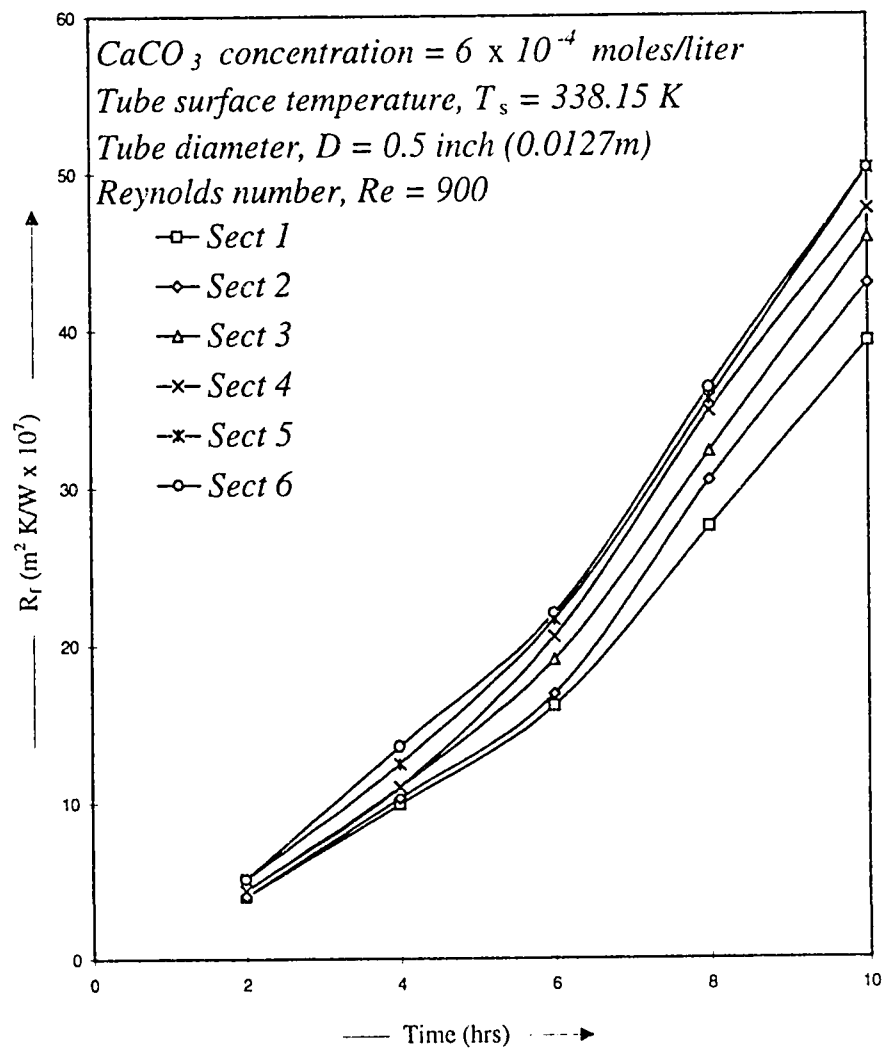
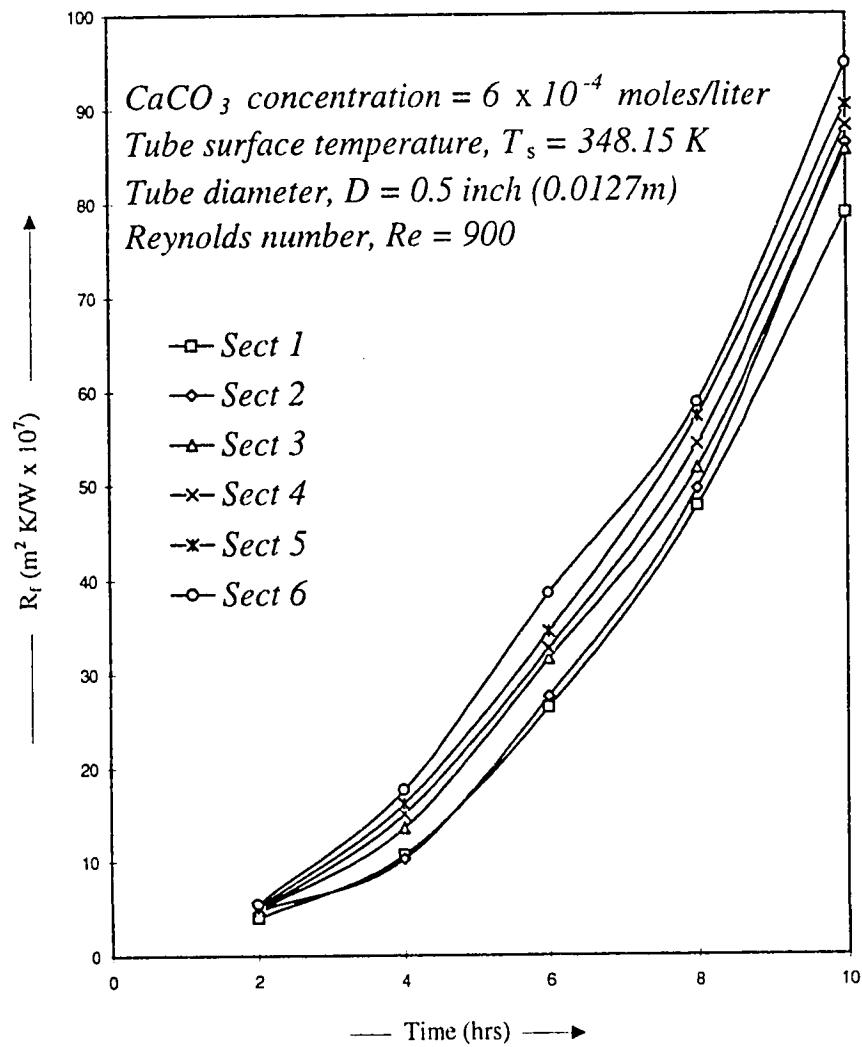
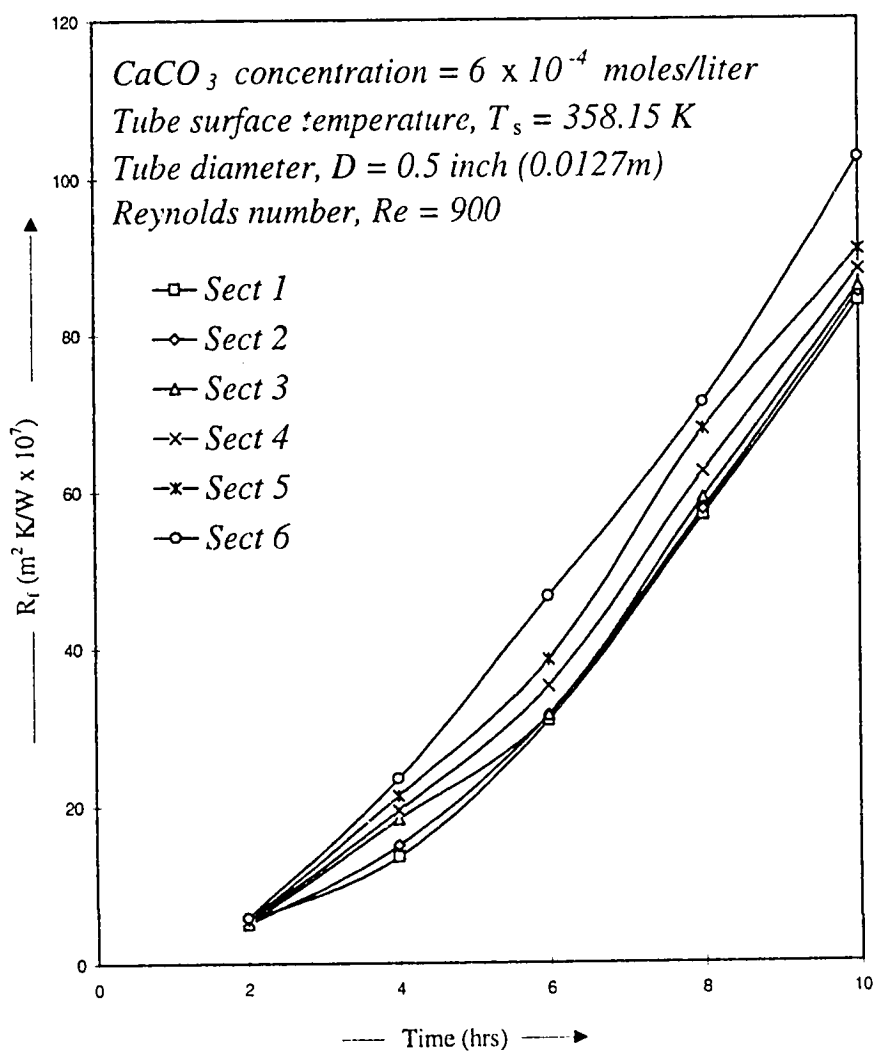


Figure E.7: R_f vs time of experiment No.7

Figure E.8: R_f vs time of experiment No.8

Figure E.9: R_f vs time of experiment No.9

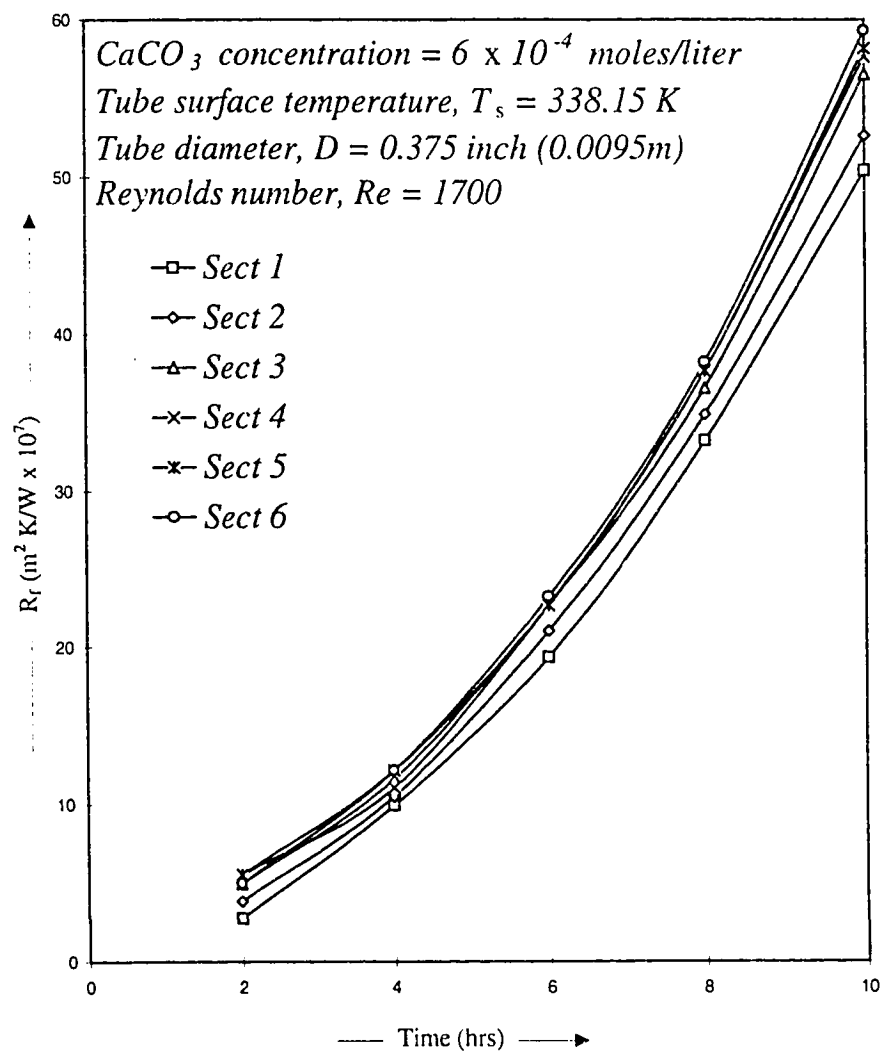
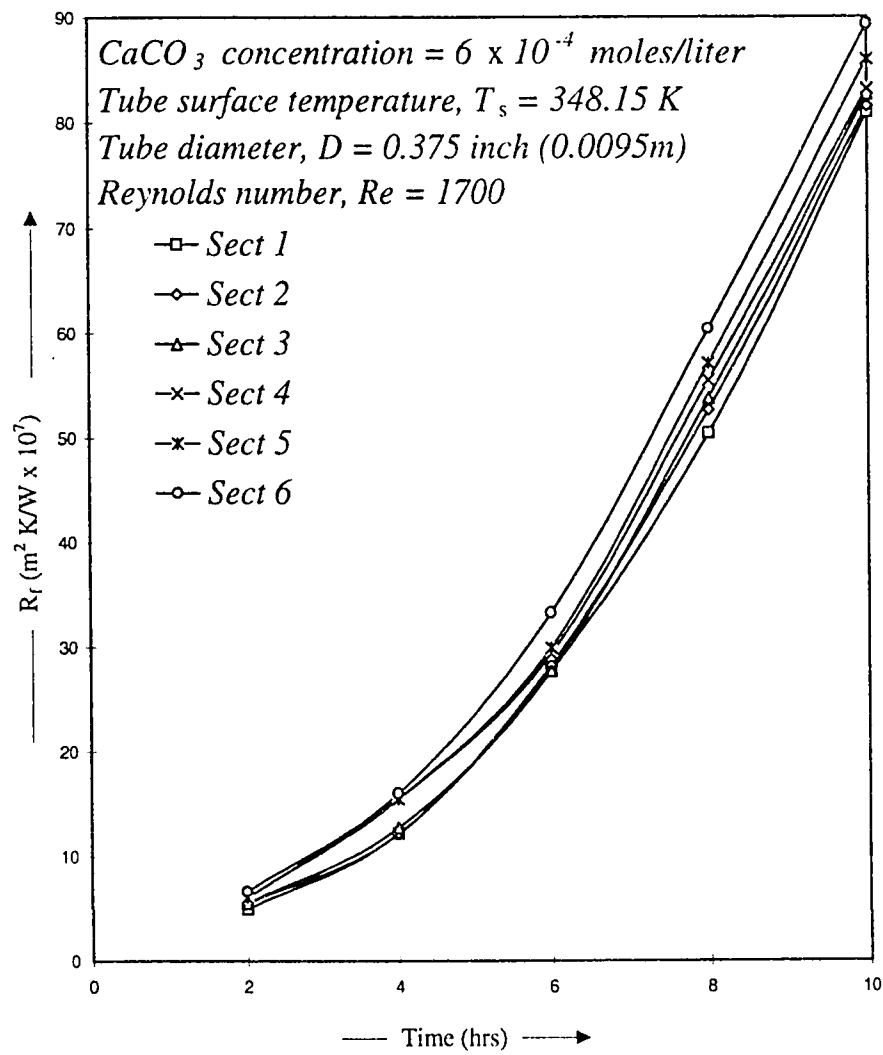


Figure E.10: R_f vs time of experiment No.10

Figure E.11: R_f vs time of experiment No.11

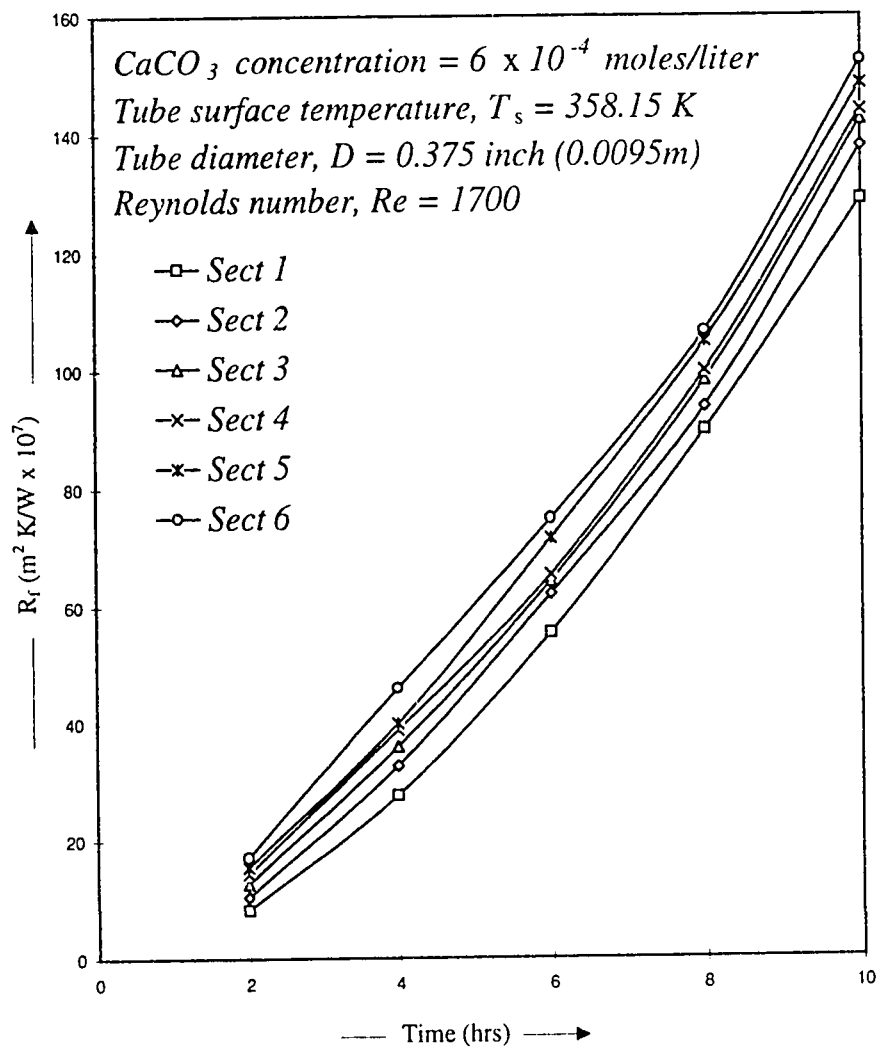


Figure E.12: R_f vs time of experiment No.12

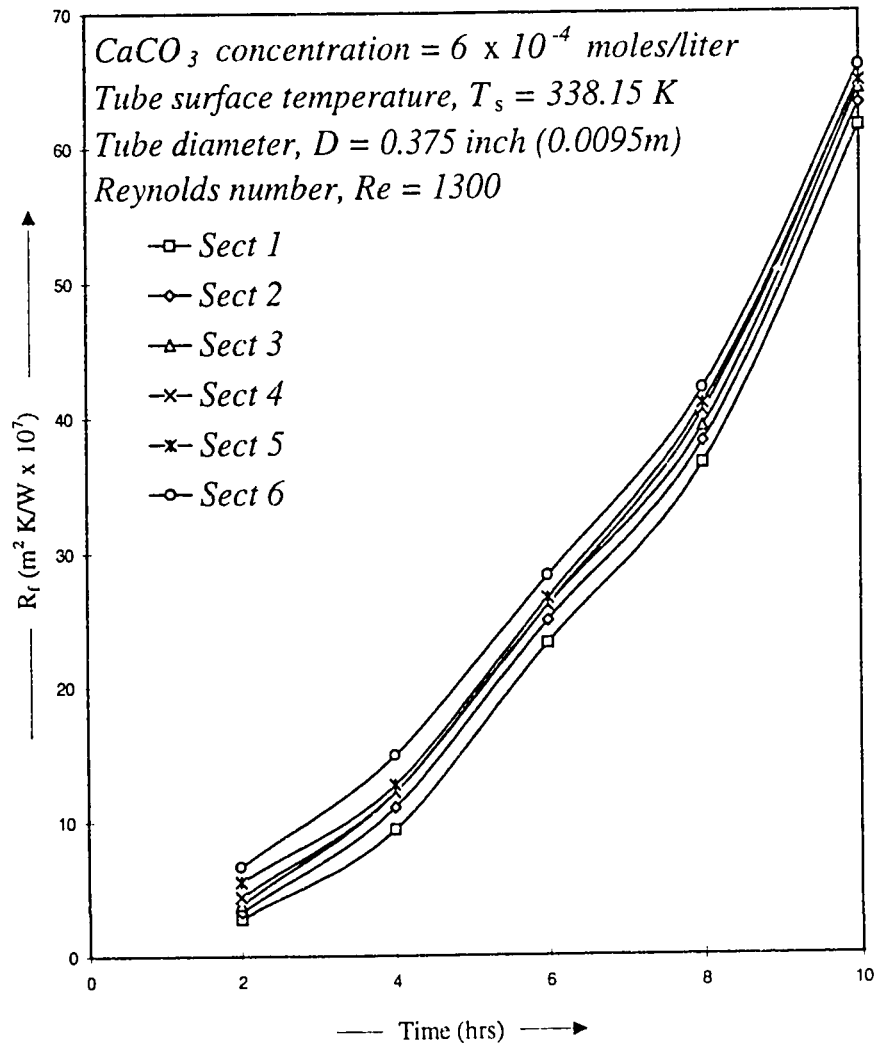


Figure E.13: R_f vs time of experiment No.13

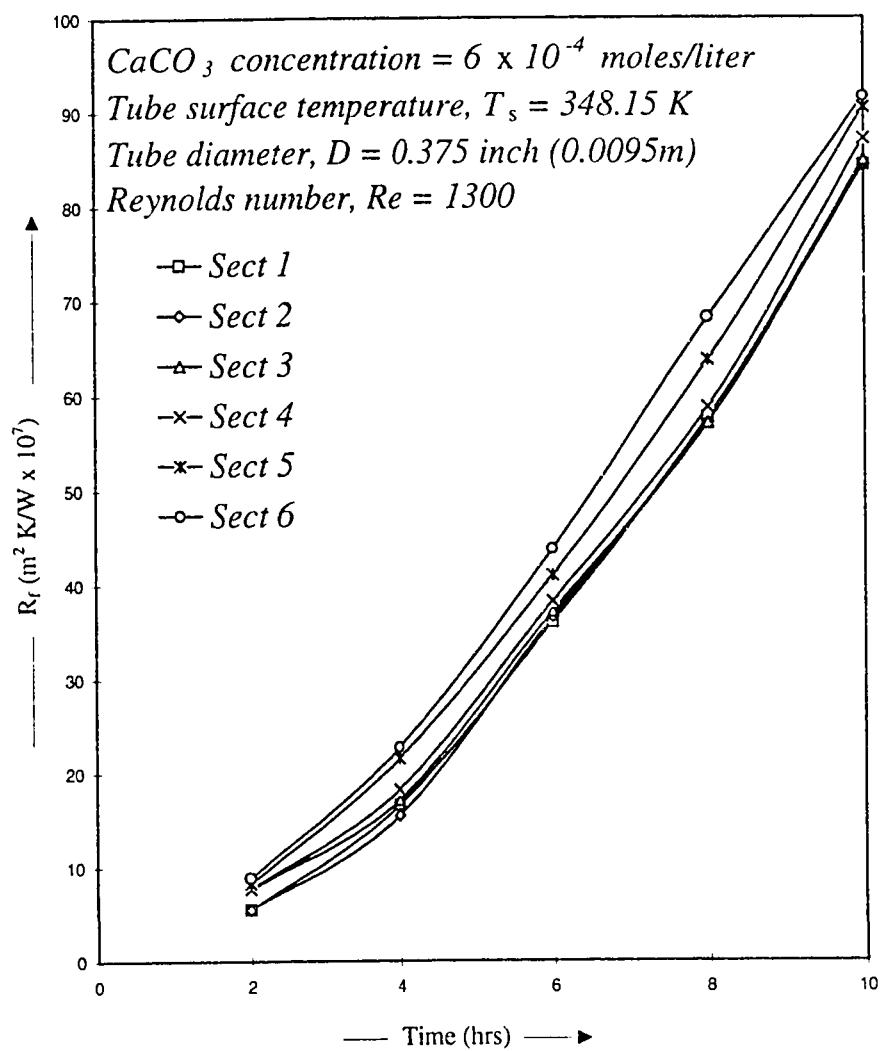


Figure E.14: R_f vs time of experiment No.14

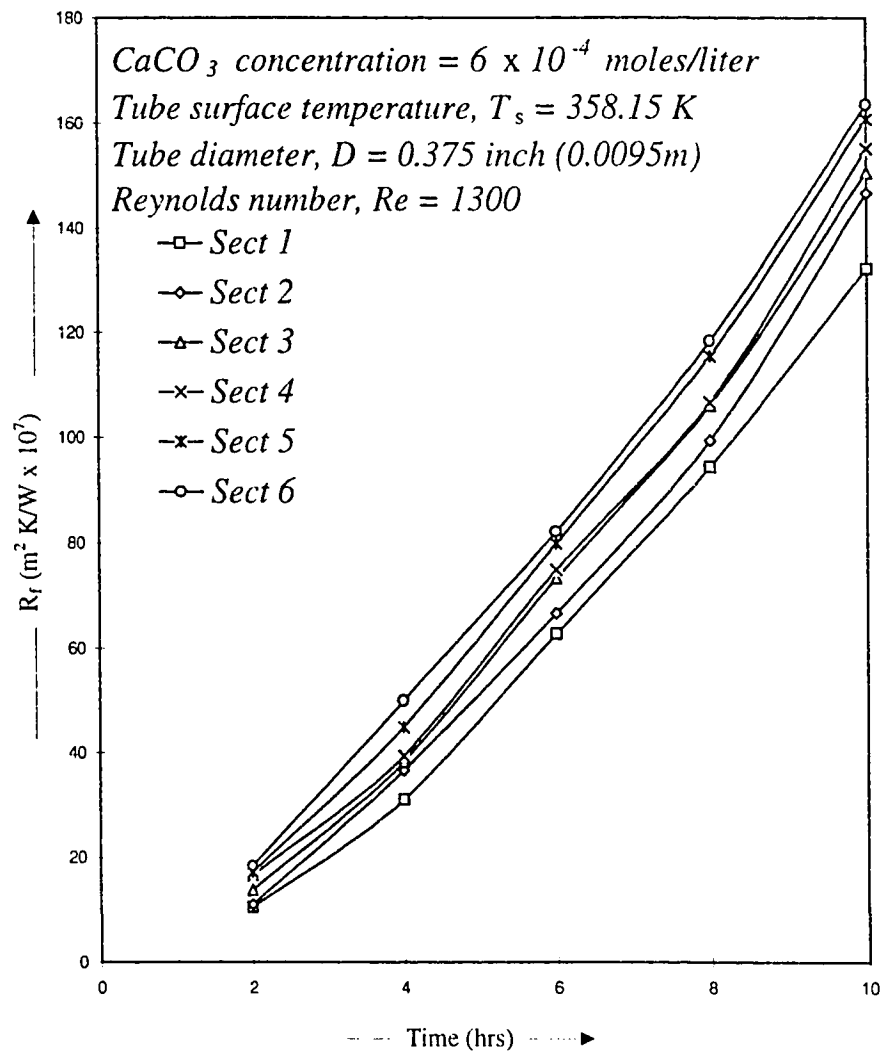
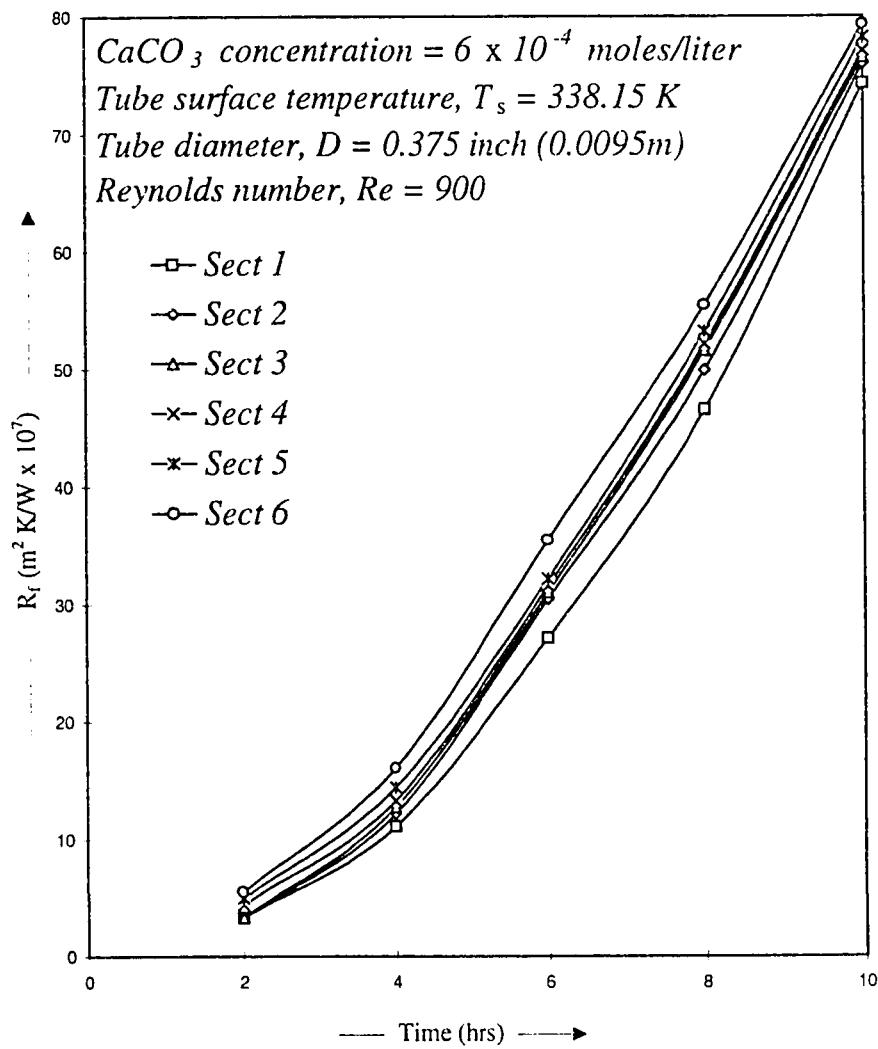


Figure E.15: R_f vs time of experiment No.15

Figure E.16: R_f vs time of experiment No.16

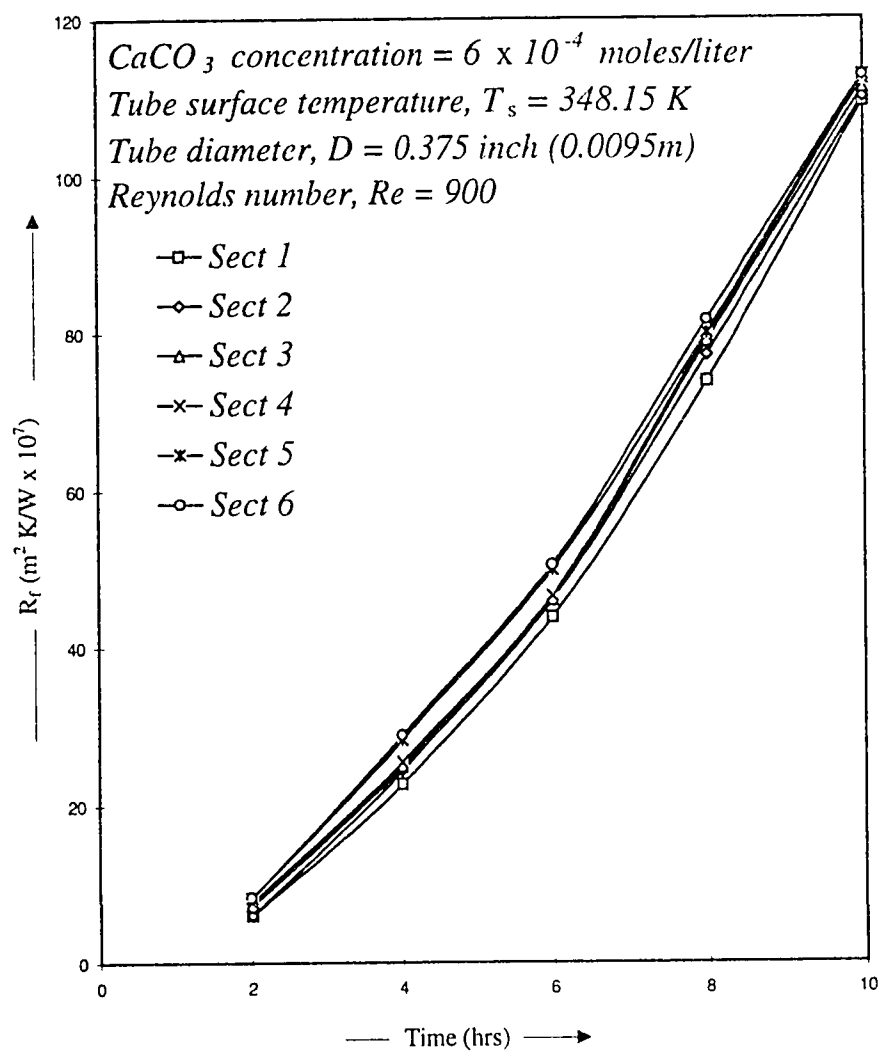
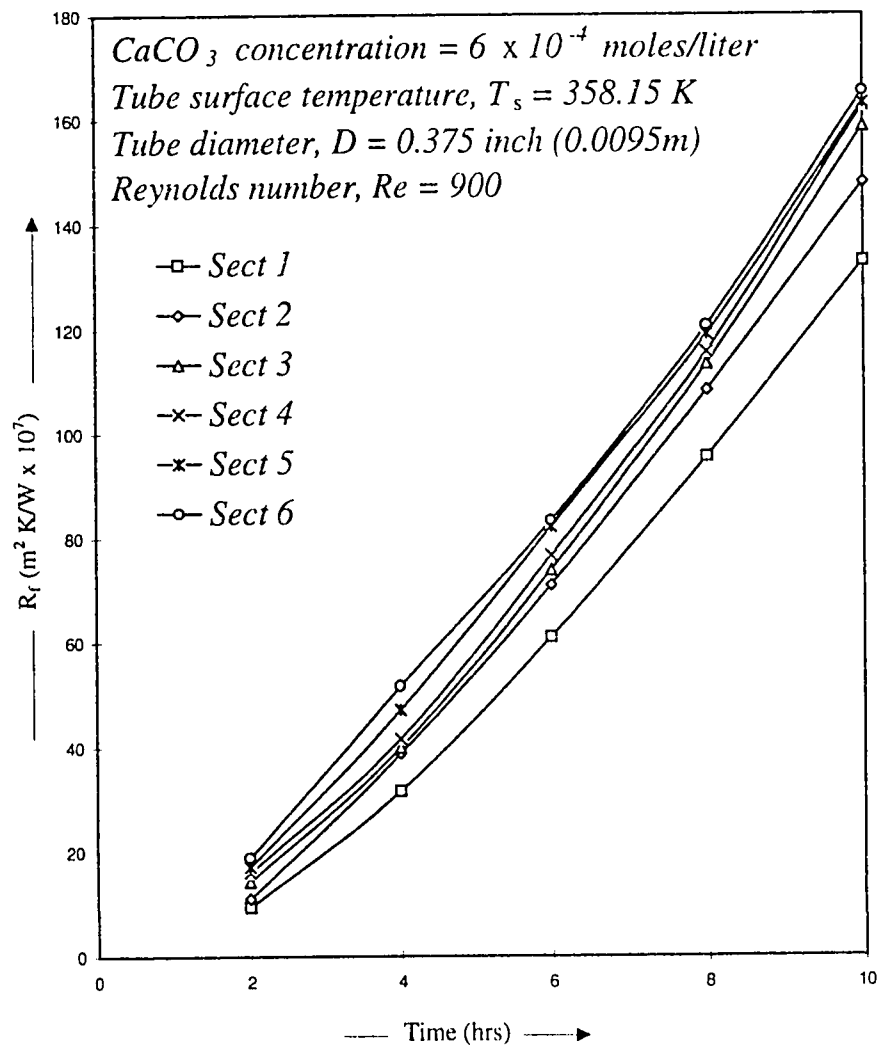
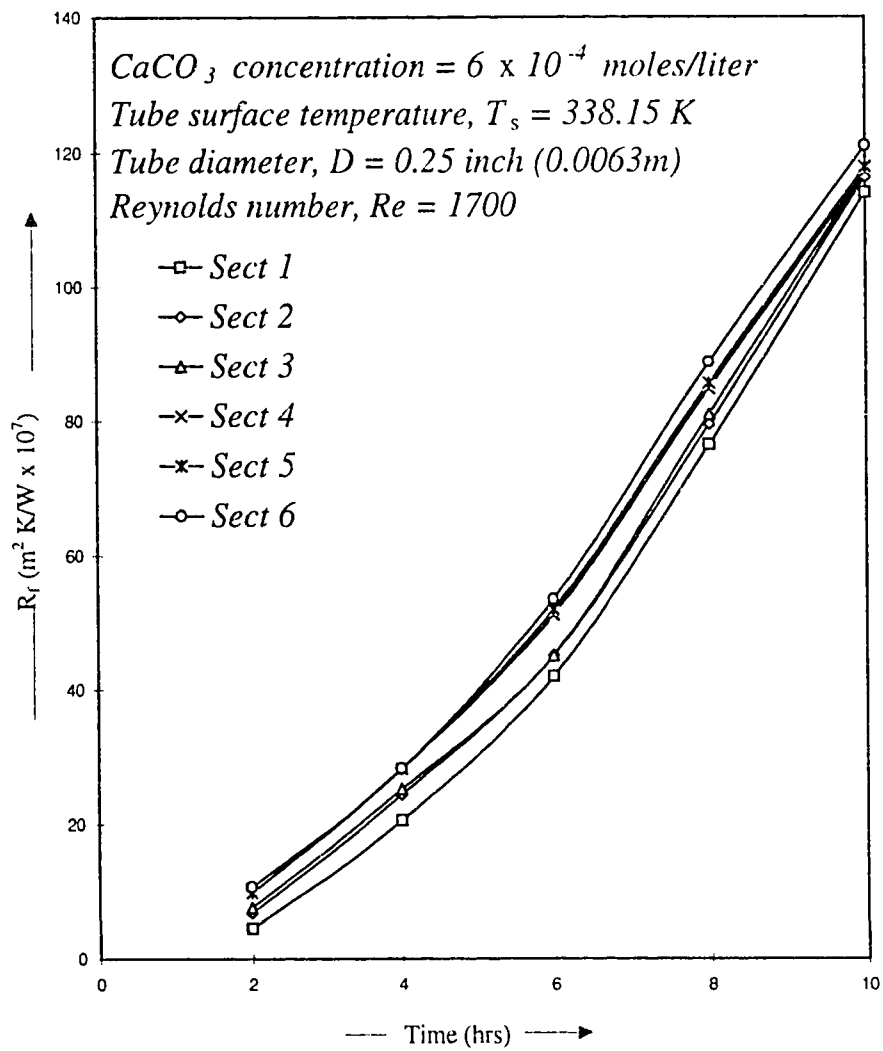
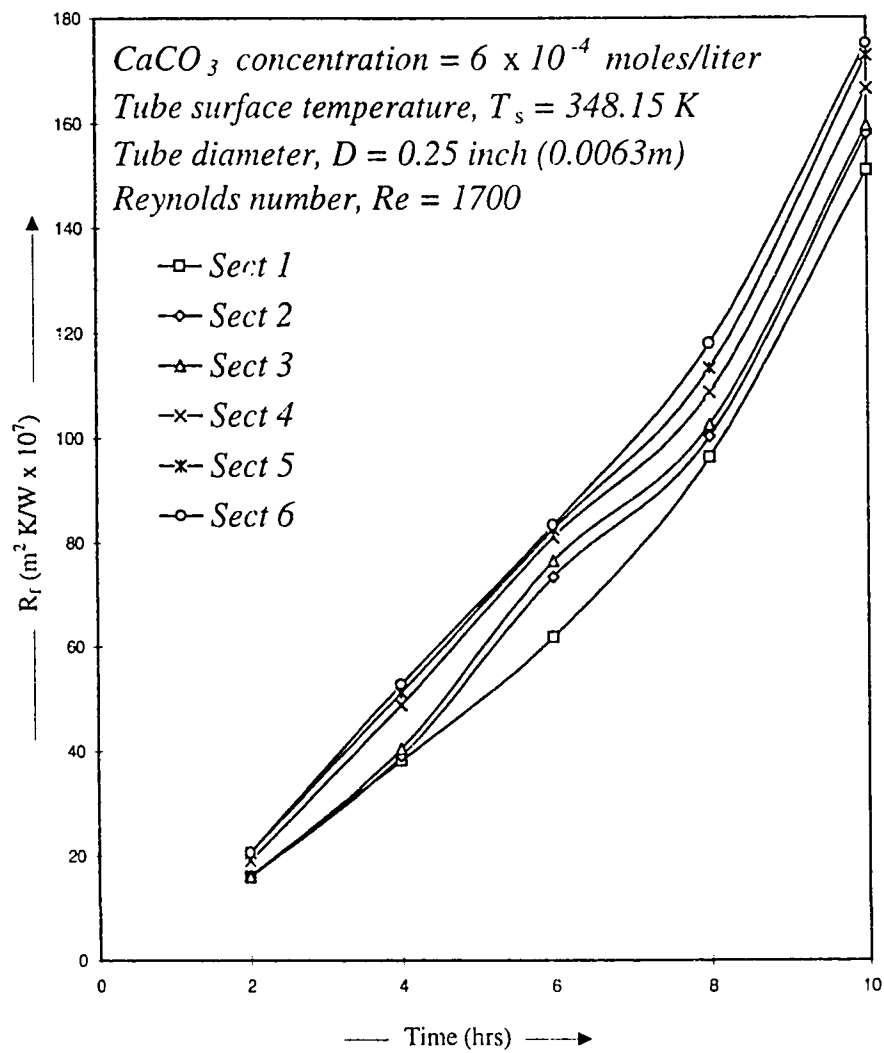
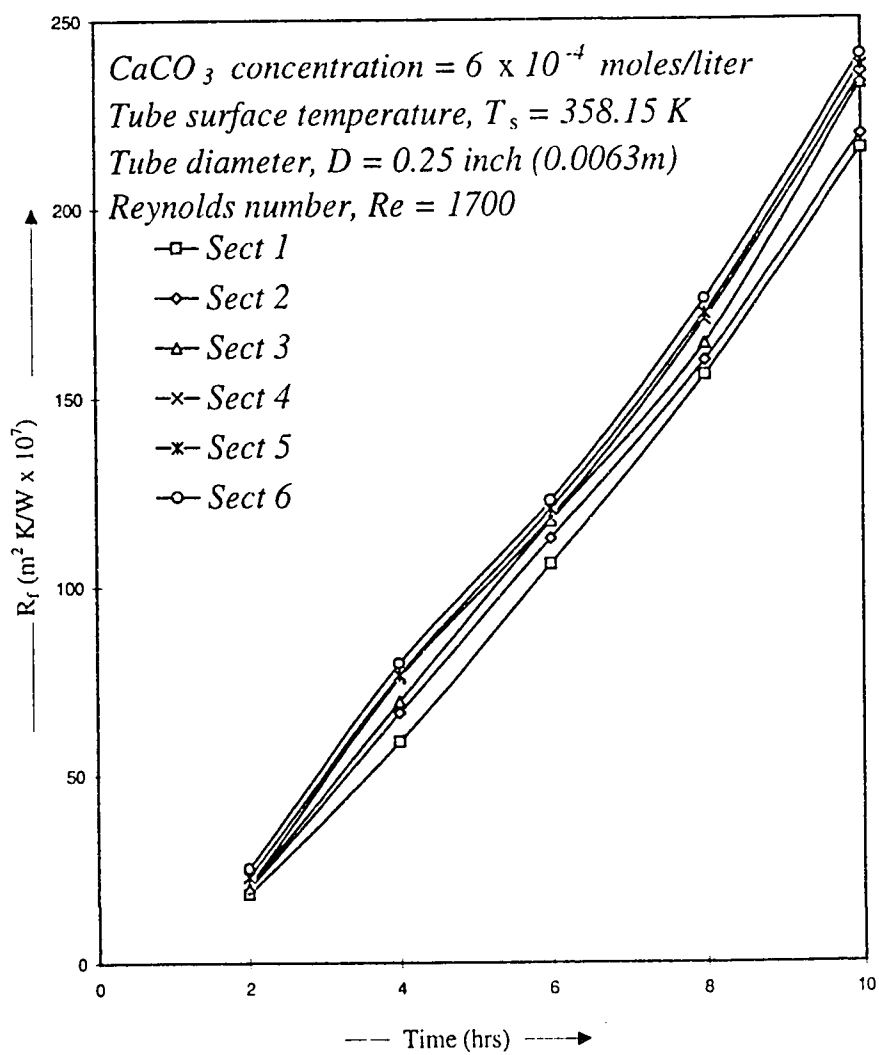


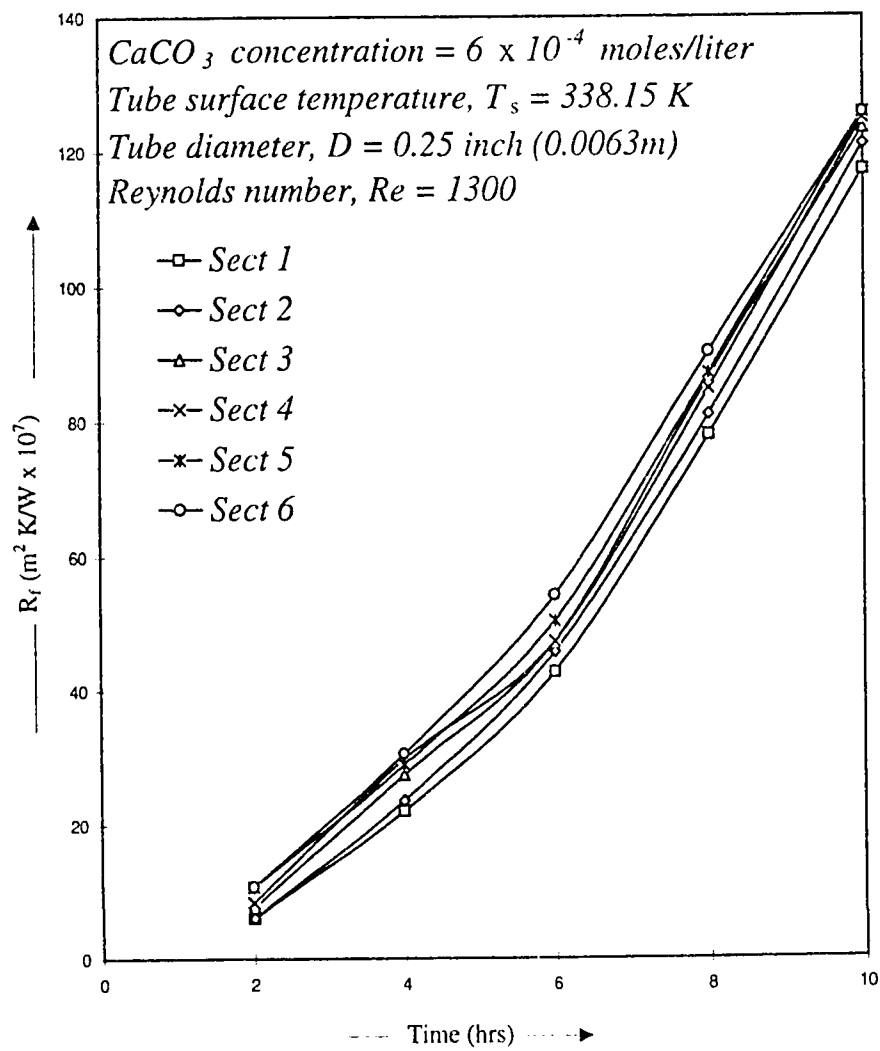
Figure E.17: R_f vs time of experiment No.17

Figure E.18: R_f vs time of experiment No.18

Figure E.19: R_f vs time of experiment No.19

Figure E.20: R_f vs time of experiment No.20

Figure E.21: R_f vs time of experiment No.21

Figure E.22: R_f vs time of experiment No.22

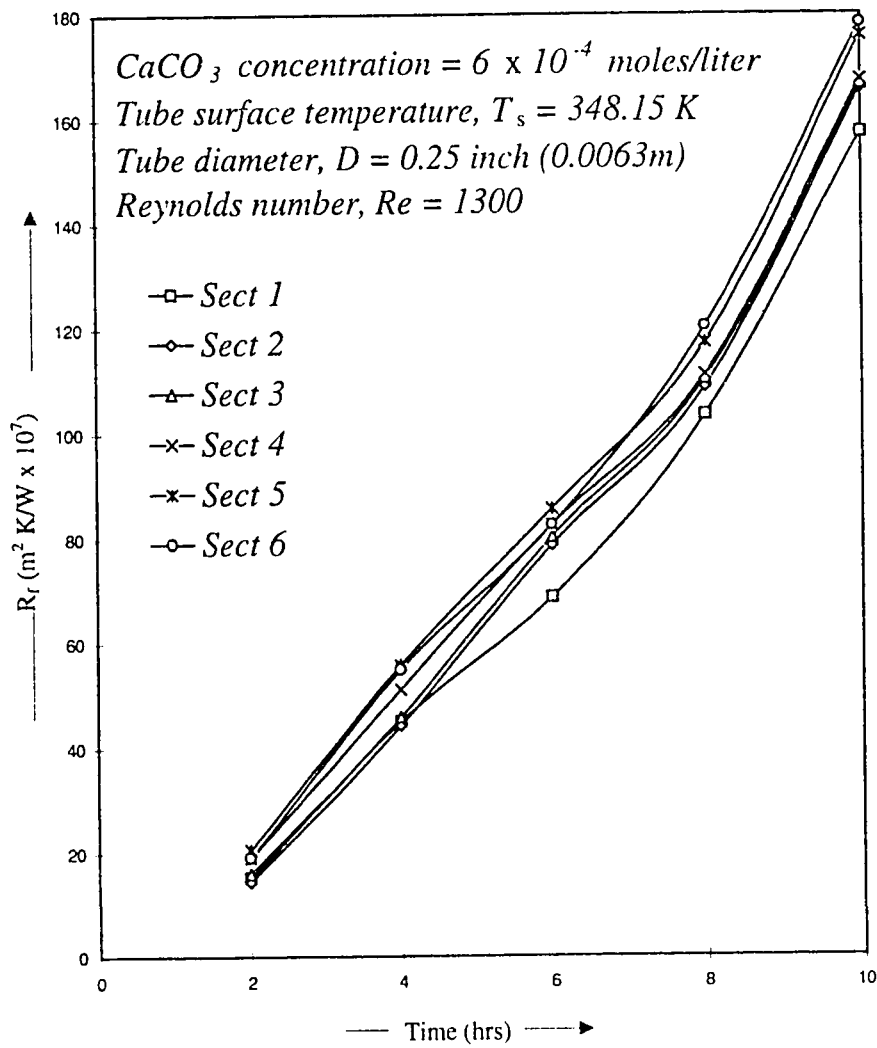
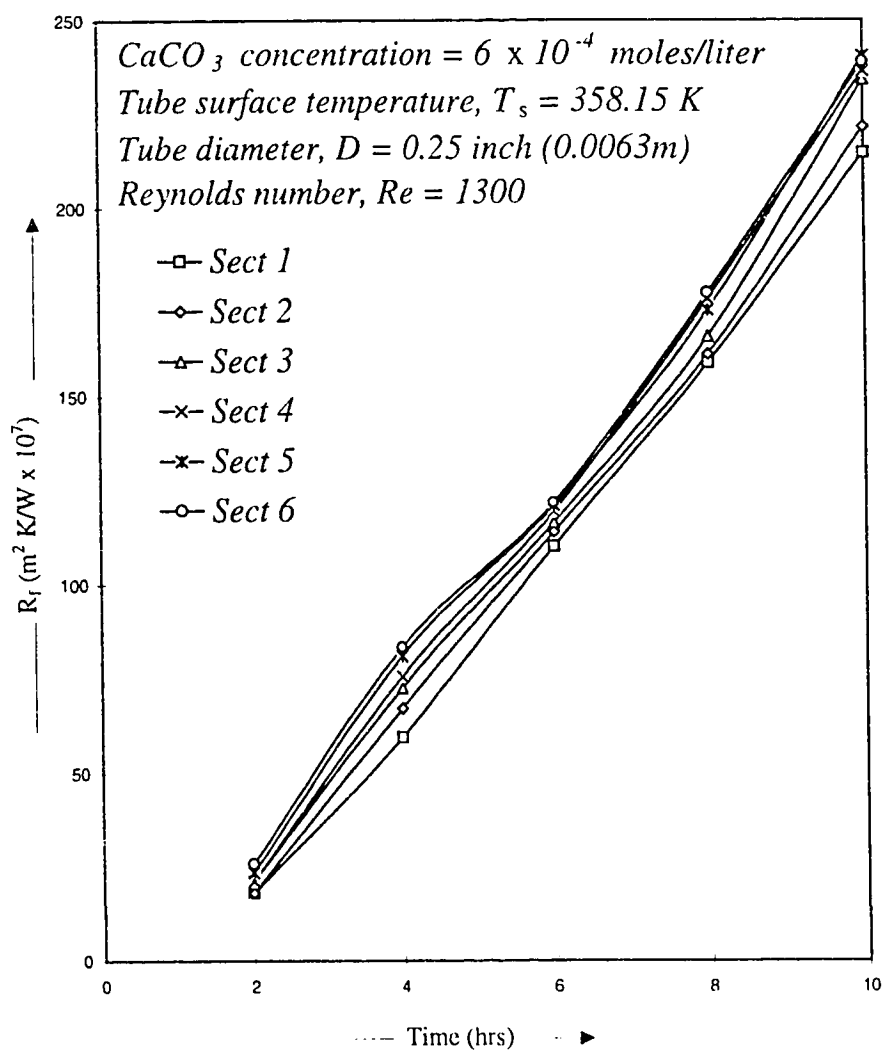
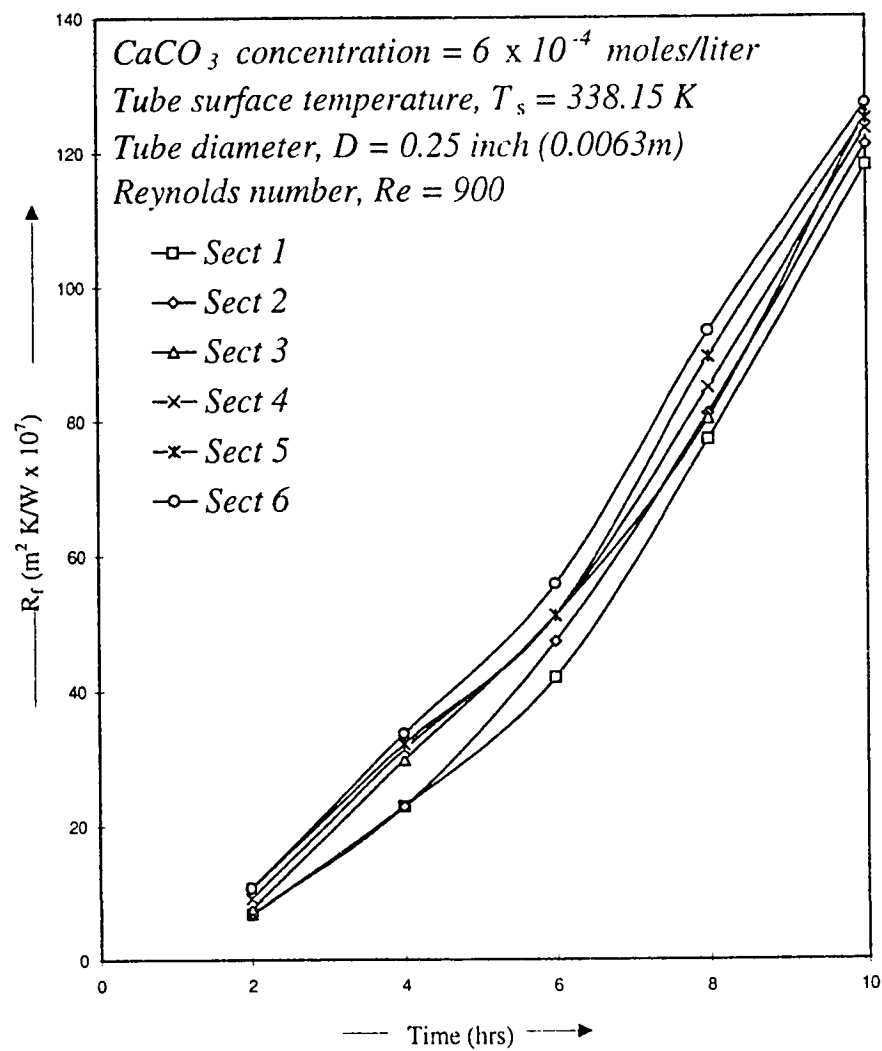
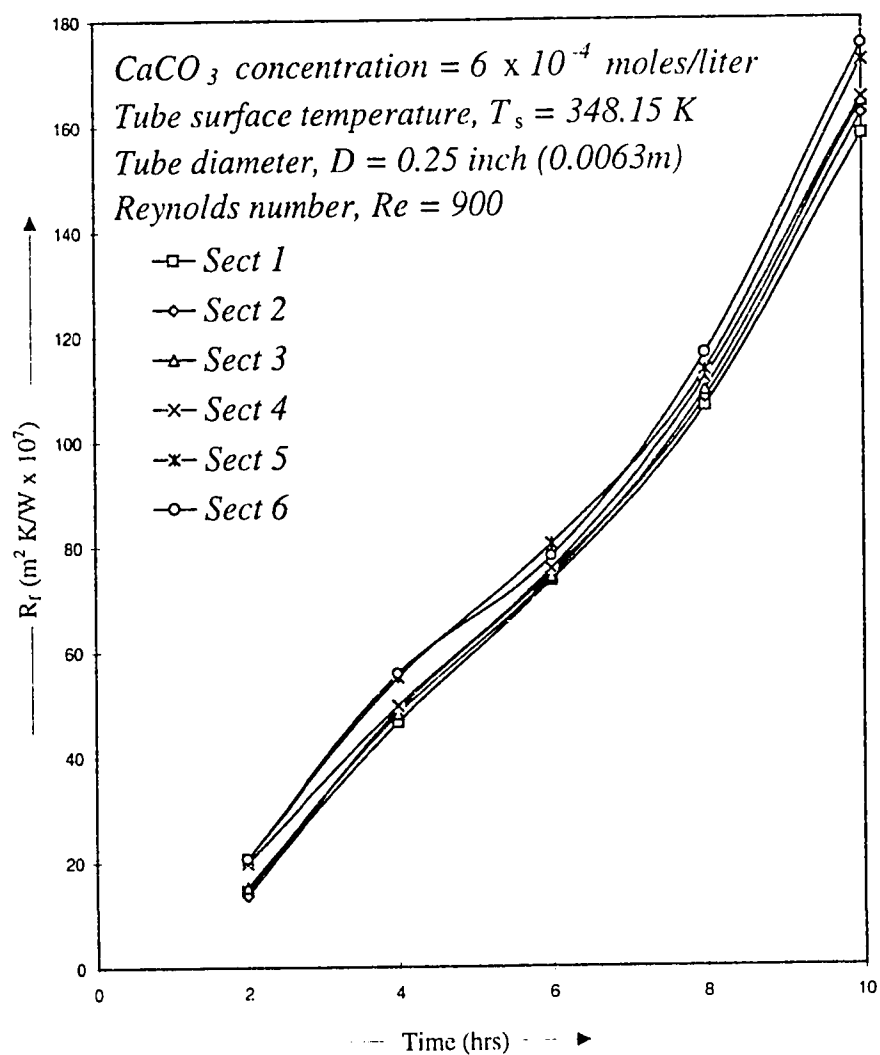
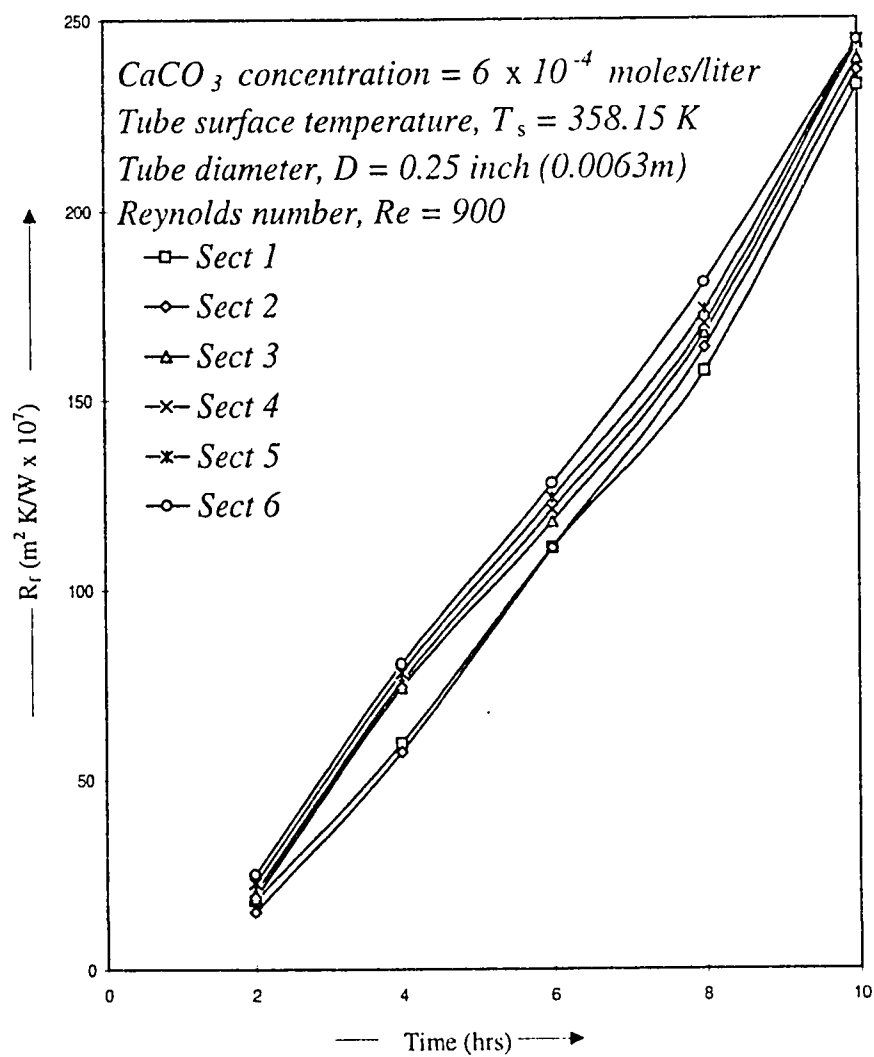


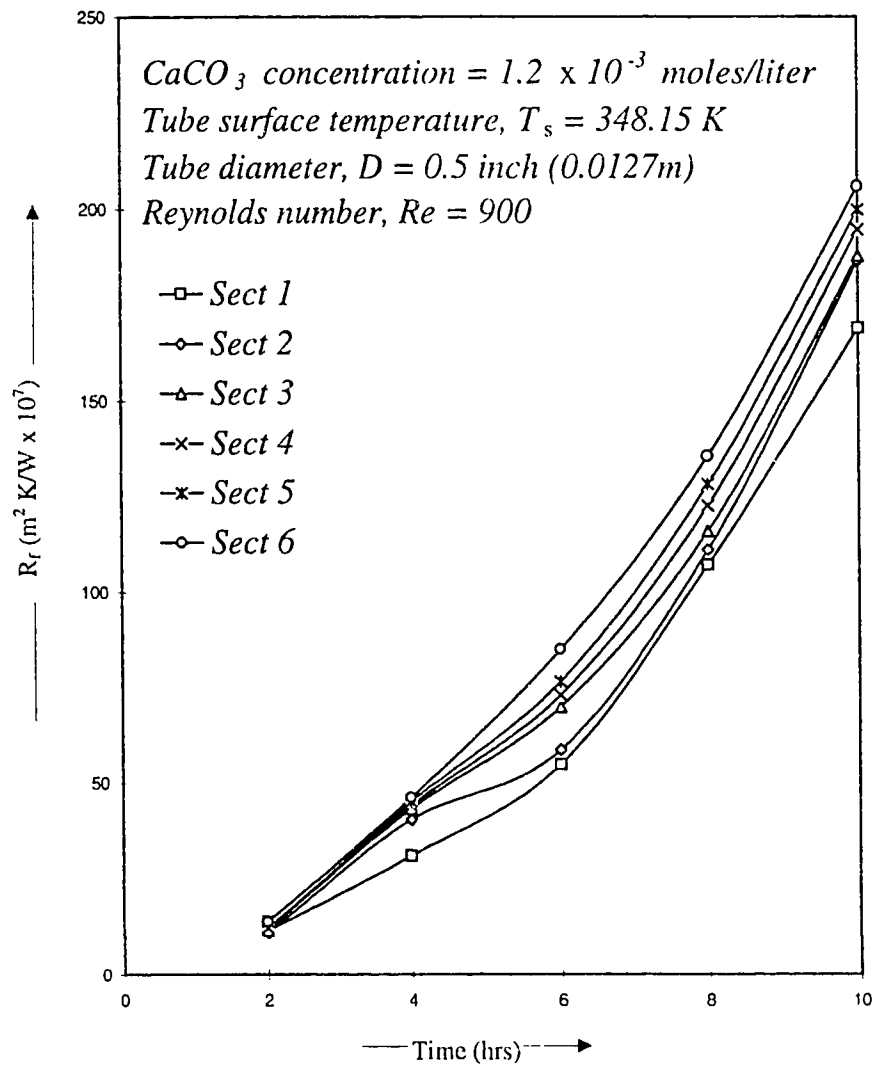
Figure E.23: R_f vs time of experiment No.23

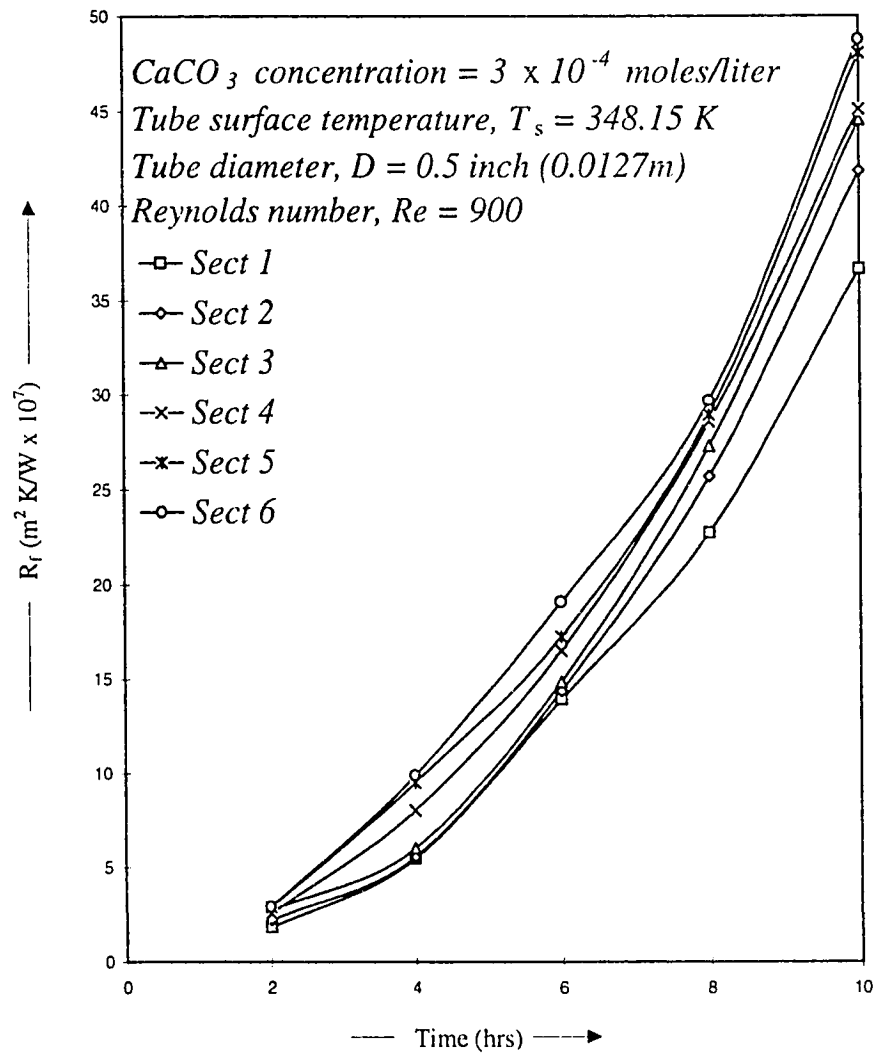
Figure E.24: R_f vs time of experiment No.24

Figure E.25: R_f vs time of experiment No.25

Figure E.26: R_f vs time of experiment No.26

Figure E.27: R_f vs time of experiment No.27

Figure E.28: R_f vs time of experiment No.28

Figure E.29: R_f vs time of experiment No.29

Appendix F

Sample Calculation

Calculations for Experiment number 1, section number 6 and mass gain measured after 10 hours of operation

r_2 = inner radius of the test section (m) = 0.004699

r_1 = average radius of the scale deposit (m)

$$r_1 = \sqrt{r_2^2 - \frac{\text{mass gain}}{\pi \rho l}} .$$

k = thermal conductivity of $CaCO_3$ (W/mk) = 2.2499

ρ = mass density of $CaCO_3$ kg/m^3 = 2700

l = length of the test section (m) = 0.1524

mass gain (kg) = 0.00013

Therefore

$$r_1 = \sqrt{0.004699^2 - \frac{0.00013}{\pi(2700)(0.1524)}} .$$

Thus

$$r_1 = 0.004688 \text{ m}$$

Logarithmic mean area was used to calculate the area of the scaling

$$A_{log} = \frac{A_o - A_i}{\ln \frac{r_2}{r_1}}$$

where

$$A_o = 2\pi r_2 l \text{ and } A_i = 2\pi r_1 l$$

$$R_f (m^2 K/W) = \frac{(A_{log})(\ln \frac{r_2}{r_1})}{2\pi k l}$$

After simplifying we get $R_f = \frac{r_2 - r_1}{k}$

$$R_f = \frac{0.004699 - 0.004688}{2.2499}$$

Thus

$$R_f = 4.76 * 10^{-6} (m^2 K/W)$$

Appendix G

Results of tube inner Surface Analysis

Table G.1: Results of surface analysis

Tube size (inch)	Average roughness (microinch)
1/2	100
3/8	97.5
1/4	60.0

Appendix H

Sensitivity Analysis

Table H.1: Results of sensitivity analysis showing percentage increase in R_f^*

t^*	$0.9Re^*$	$0.9D^*$	$1.1T_s^*$	combined effect
0.2	0.31%	28.12%	52.05%	98.44%
0.4	0.87%	22.39%	41.67%	78.10%
0.6	1.20%	19.16%	35.93%	67.18%
0.8	1.43%	16.92%	32.00%	59.85%
1	1.61%	15.21%	29.03%	54.38%

Appendix I

Results of SEM and EDX

Analysis

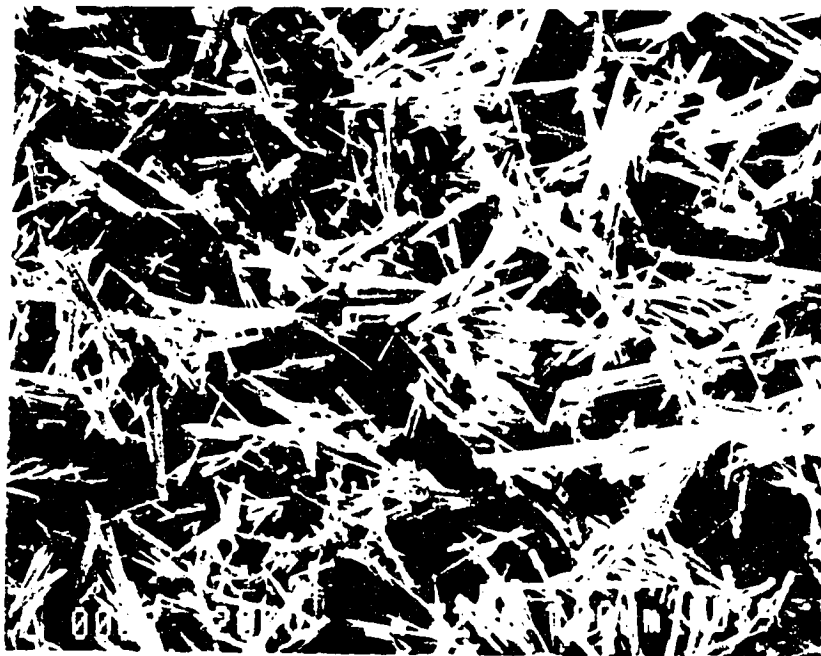


Figure I.1: Results of SEM analysis

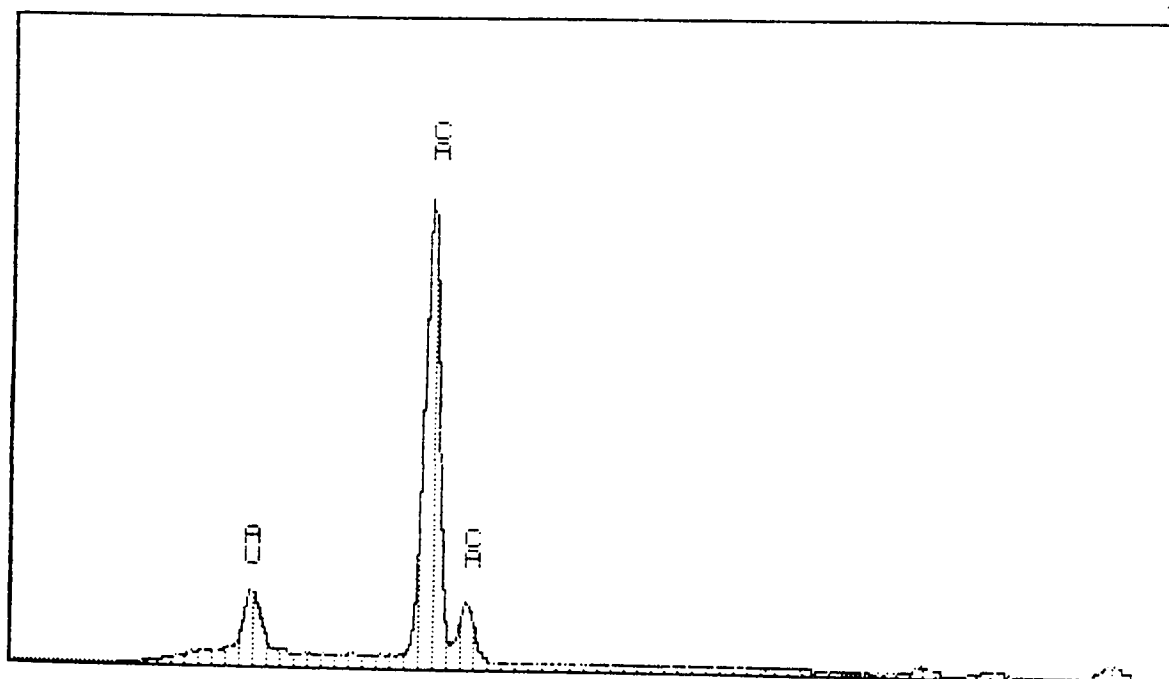


Figure I.2: Corresponding EDX plot

Vitae

- Mohammad Sultan Khan
- Born on February 07, 1967 in Lahore, Pakistan
- Received Bachelor of Science (**BS**) degree in Mechanical Engineering from **UET** University of Engineering and Technology, Lahore, Pakistan in December 1990
- Joined National Engineering Services Pakistan Pvt. Limited **NESPAK** (a Consultancy firm in Pakistan) as an Engineer in July 1991
- Joined the Department of Mechanical Engineering at King Fahd University of Petroleum and Minerals (**KFUPM**), Dhahran, Saudi Arabia as a Research Assistant in February 1994
- Received Master of Science (**MS**) degree in Mechanical Engineering from **KFUPM**, Saudi Arabia in May 1996.